

University of Alberta

INVESTIGATING THE LONG TERM IMPACT OF CHLORINE EXPOSURE ON HOLLOW
FIBRE MEMBRANES IN WATER TREATMENT

by

Steven J. Pickle



A thesis submitted to the Faculty of Graduate Studies and Research
in partial fulfillment of the requirements for the degree of

Master of Science

in

Environmental Engineering

Department of Civil and Environmental Engineering

Edmonton, Alberta
Spring 2007



Library and
Archives Canada

Bibliothèque et
Archives Canada

Published Heritage
Branch

Direction du
Patrimoine de l'édition

395 Wellington Street
Ottawa ON K1A 0N4
Canada

395, rue Wellington
Ottawa ON K1A 0N4
Canada

Your file *Votre référence*
ISBN: 978-0-494-30005-3
Our file *Notre référence*
ISBN: 978-0-494-30005-3

NOTICE:

The author has granted a non-exclusive license allowing Library and Archives Canada to reproduce, publish, archive, preserve, conserve, communicate to the public by telecommunication or on the Internet, loan, distribute and sell theses worldwide, for commercial or non-commercial purposes, in microform, paper, electronic and/or any other formats.

The author retains copyright ownership and moral rights in this thesis. Neither the thesis nor substantial extracts from it may be printed or otherwise reproduced without the author's permission.

AVIS:

L'auteur a accordé une licence non exclusive permettant à la Bibliothèque et Archives Canada de reproduire, publier, archiver, sauvegarder, conserver, transmettre au public par télécommunication ou par l'Internet, prêter, distribuer et vendre des thèses partout dans le monde, à des fins commerciales ou autres, sur support microforme, papier, électronique et/ou autres formats.

L'auteur conserve la propriété du droit d'auteur et des droits moraux qui protègent cette thèse. Ni la thèse ni des extraits substantiels de celle-ci ne doivent être imprimés ou autrement reproduits sans son autorisation.

In compliance with the Canadian Privacy Act some supporting forms may have been removed from this thesis.

Conformément à la loi canadienne sur la protection de la vie privée, quelques formulaires secondaires ont été enlevés de cette thèse.

While these forms may be included in the document page count, their removal does not represent any loss of content from the thesis.

Bien que ces formulaires aient inclus dans la pagination, il n'y aura aucun contenu manquant.


Canada

Abstract

The research explored long term membrane degradation in the context of a concentration-time relationship under varied pH conditions, using two different PVDF ultrafiltration hollow fibre membranes and sodium hypochlorite as a cleaning agent. One of the two membrane types had been modified in order to reduce its hydrophobicity. Membranes were characterized before and after treatment in order to identify changes in strength properties, hydrophobicity, and pore structure. Permeability, fouling tendency, and solute transport are also discussed and methodologies for their application are developed. The modified membrane was found to be more hydrophobic, brittle, weaker, and inelastic, quickly fracturing upon the application of stress. Chlorine was found to bear little consequence on the strength or pore structure of either membrane while showing a potential to increase hydrophobicity. Structural changes in both membranes were encountered after pressurizing the membranes to within normal ranges, leading to the conclusion that the membranes were operationally defective.

Key Words: microfiltration, ultrafiltration, hollow fibre, chlorine, membrane cleaning, fouling propensity, solute transport, hydrophobicity, strength, SEM

Acknowledgements

I am grateful for the assistance that Nick Churnuka, Maria Demeter, Garry Solonyenko, and my fellow colleagues provided me throughout my graduate experience. I would like to especially thank Dr. Daniel Smith, Dr. Rodney Guest, and Mr. Clark Svrcek for being my mentors and supplying the support that was necessary to complete my thesis. I would also like to express appreciation for the help that Dr. Ming Chen, Roy Gitzel, Dr. Jose Gonzales, Dr. Dimitre Karpuzov, and Dr. Jane Batcheller gave me in various aspects of my research.

The friends that I have made and had the opportunity to work with have both enriched my experience and my life, and for that I am grateful. More than anyone, I am indebted to my family and my future wife, Megan Ruth. For without their encouragement, understanding, and support, I would be absolutely nowhere.

Table of Contents

1	Introduction.....	1
1.1	Overview and Problem Statement	1
1.2	Research Hypotheses and Objectives	1
1.3	Research Approach	2
1.4	Thesis Layout.....	2
2	Background	4
2.1	Historical Membrane Usage	4
2.2	LT2ESWTR	5
3	Theory	6
3.1	Membrane Treatment.....	6
3.1.1	<i>General Concepts</i>	6
3.1.2	<i>Process Principles</i>	8
3.1.3	<i>Configurations</i>	10
3.1.4	<i>Operational Modes</i>	11
3.2	Membrane Properties	12
3.2.1	<i>Physical Properties</i>	12
3.2.2	<i>Polymer Materials</i>	13
3.2.3	<i>Symmetry</i>	15
3.3	Modelling Flux.....	15
3.3.1	<i>Ideal Flow</i>	15
3.3.2	<i>Mass Transport</i>	16
3.3.3	<i>Resistance in Series</i>	18
3.3.4	<i>Other Models</i>	20
3.3.5	<i>Temperature and Viscosity Effects</i>	21
4	Challenges in Membrane Treatment	22
4.1	Integrity.....	22
4.1.1	<i>Membrane Integrity Testing</i>	22

4.2	Fouling	24
4.2.1	<i>Fouling Types</i>	25
4.2.2	<i>Fouling Mechanisms</i>	26
4.2.3	<i>Concentration Polarization</i>	27
4.2.4	<i>Impact of Membrane Properties</i>	28
4.3	Long Term Performance	29
5	Cleaning Practices in Membrane Treatment	30
5.1	Membrane-Chlorine Interactions/Research	32
5.2	Impact of Cleaning on Membrane Properties and Life.....	34
5.3	Chlorine Properties	35
6	Membrane Characterization.....	37
6.1	Pore Properties	37
6.1.1	<i>Gas Transport</i>	37
6.1.2	<i>Thermoporometry</i>	38
6.1.3	<i>Microscopy</i>	38
6.1.4	<i>Solute Transport</i>	40
6.2	Fouling Propensity	44
6.2.1	<i>Flux Decline or Recovery</i>	44
6.2.2	<i>Resistance in Series</i>	46
6.2.3	<i>Flux Loss Ratios</i>	48
6.3	Hydrophobicity	49
6.4	Strength.....	50
6.5	Chemical Composition.....	51
7	Problems Encountered with Membrane Material.....	52
7.1	Identification of Problem	52
7.2	Experimental Investigation	53
8	Methodology Development.....	54
8.1	Choice of Membrane.....	54
8.2	Integrity.....	56

8.2.1	<i>Methodology</i>	56
8.2.2	<i>Reasoning</i>	56
8.3	Fouling Propensity	57
8.3.1	<i>Methodology</i>	57
8.3.2	<i>Reasoning</i>	60
8.4	Solute Retention.....	62
8.4.1	<i>Methodology</i>	62
8.4.2	<i>Reasoning</i>	63
8.5	Experimental Equipment	65
8.5.1	<i>Membrane Element and Module</i>	65
8.5.2	<i>Membrane Conditioning</i>	67
8.5.3	<i>Permeability and Fouling Apparatus</i>	68
8.5.4	<i>Equipment Considerations</i>	70
9	Materials and Methods	72
9.1	Overview.....	72
9.2	Chemical Exposure.....	72
9.2.1	<i>Ct Relationship</i>	72
9.2.2	<i>Buffers/pH</i>	73
9.2.3	<i>Chlorine Concentration</i>	74
9.3	Membranes.....	74
9.3.1	<i>Membrane Conditioning</i>	76
9.4	Characterization	78
9.4.1	<i>Hydrophobicity</i>	78
9.4.2	<i>Strength</i>	80
9.4.3	<i>Microscopy</i>	81
9.5	Statistics	82
9.5.1	<i>Factorial Design</i>	82
9.5.2	<i>Replication and Randomization</i>	83
9.5.3	<i>Data Treatment</i>	84
10	Experimental Results	85

10.1	Cumulative Concentration	85
10.2	Hydrophobicity	87
10.3	Strength.....	89
10.4	Microscopy	95
10.5	Membrane Problem Investigation.....	98
10.5.1	<i>Structure</i>	98
10.5.2	<i>Hydrophobicity and Strength</i>	100
11	Discussion of Results.....	102
11.1	Characterizations.....	103
11.1.1	<i>Hydrophobicity</i>	104
11.1.2	<i>Strength</i>	106
11.1.3	<i>Microscopy</i>	111
11.2	Ct Relationship.....	112
11.3	Experienced Flux Loss.....	114
11.4	Experimental Error.....	115
11.5	Statistics	118
11.5.1	<i>Variance Determination</i>	119
11.6	Research Significance	121
11.6.1	<i>Direct Implications</i>	121
11.7	Future Research	122
11.7.1	<i>Source Water and Fouling Conditions</i>	122
11.7.2	<i>Cleaning Regimes</i>	123
11.7.3	<i>Temperature</i>	123
11.7.4	<i>Hollow Fibre Vs. Flatsheet</i>	123
11.7.5	<i>Mechanical Stresses</i>	124
11.7.6	<i>Characterization</i>	124
12	Conclusions and Recommendations.....	125
12.1	Conclusions.....	125
12.2	Recommendations.....	126
	References.....	127

List of Tables

Table 1: Selected membrane water treatment installations.....	5
Table 2: Membrane terminology	8
Table 3: Configurations in membrane treatment	11
Table 4: Significant physical membrane properties.....	12
Table 5: MF/UF polymer properties (Cheryan, 1998; AWWA, 2005; USEPA, 2005)....	14
Table 6: Membrane manufacturer polymer usage (From AWWA, 2005).....	14
Table 7: Summary of primary tests used to determine membrane integrity.....	23
Table 8: Major classes of cleaning chemicals (From AWWA, 2005).....	30
Table 9: Effectiveness of cleaning strategies on fouling (From Liu et al., 2004).....	31
Table 10: Partial list of microscopic characterization research	39
Table 11: Partial list of solute transport research using PEMs	41
Table 12: Membrane characterization methods and analysis techniques	72
Table 13: Experimental treatments and associated information	73
Table 14: Recommended free chlorine dosages	73
Table 15: Buffer descriptions.....	74
Table 16: Membrane statistics	75
Table 17: Experimental factors and their levels	82
Table 18: $2^3 4^1$ Fractional factorial construction	83
Table 19: Experienced Ct values	85
Table 20: Significance of treatments on advancing angle (at a 95% confidence level) ...	89
Table 21: Significance of Run 2 strength parameters (at a 95% confidence level).....	91
Table 22: Significance of Run 2 strength parameters with modified 2-level factorial for each membrane type (at a 95% confidence level)	93

List of Figures

Figure 1: Increase in membrane plant prevalence between 1989 and 2003 (After Adham et al., 2005)	4
Figure 2: Rejection diagram for various membrane processes (After AWWA, 2005)	6
Figure 3: General membrane process	9
Figure 4: Thin film theory development.....	17
Figure 5: Fouling mechanisms of cake formation, pore plugging, and adsorption	27
Figure 6: Concentration polarization model (After Sablani et al., 2001)	28
Figure 7: Membrane materials resistance to chlorine (From Cheryan, 1998).....	33
Figure 8: Resistance mechanism definitions.....	46
Figure 9: General stress-strain curve	50
Figure 10: Series of flux measurements used in FLR methodology.....	58
Figure 11: Relationship between flux loss and (a) flux loss ratio values, and (b) resistance in series values (After Dal-Cin et al., 1996)	61
Figure 12: Single fibre membrane module (a) Schematic (b) Picture	66
Figure 13: Permeability/Fouling apparatus (a) Schematic (b) Picture.....	66
Figure 14: Apparatus for wetting single fibre elements.....	67
Figure 15: Permeability/fouling/solute transport apparatus schematic.....	68
Figure 16: LabView output screen.....	70
Figure 17: Membrane fibre (a) at low magnification, and (b) at high magnification.....	75
Figure 18: Multi-fibre membrane element used for wetting single fibres	76
Figure 19: Storage of the treatment baths	77
Figure 20: Storage of the 10,000 mg/L free chlorine, pH 6 treatments	77
Figure 21: FTA 200 with attached fibre section	79
Figure 22: FTA 200 software screenshot of hydrophobic fibre before calculation.....	79
Figure 23: FTA 200 software screenshot of hydrophilic fibre after calculation.....	80
Figure 24: Instron 4202 with 50 mm section of fibre	81
Figure 25: Cumulative exposure profile for 10,000 mg/L chlorine treatment (Run 2) ...	86
Figure 26: Cumulative exposure profile for 10,000 mg/L chlorine treatment (Run 2) ...	87
Figure 27: Advancing contact angle (Run 1).....	88

Figure 28: Advancing contact angle (Run 2)	88
Figure 29: Displacement at ultimate yield	90
Figure 30: Modulus of elasticity	90
Figure 31: Tensile strength at ultimate yield	91
Figure 32: Yield and ultimate strength comparison.....	92
Figure 33: Relative tensile strength at ultimate yield	94
Figure 34: Virgin membrane micrograph of the (a) top surface, and (b) bottom surface.	95
Figure 35: Virgin membrane micrograph of the (a) outer cross section (b) inner cross section	96
Figure 36: Anisotropic structure of membrane (a) peeled apart, and (b) dried in liquid nitrogen	96
Figure 37: Outside cross section of a modified membrane exposed to a chlorine concentration of (a) 1000 mg/L, (b) 10000 mg/L, and an unmodified membrane at (c) 1000 mg/L, and (d) 10,000 mg/L, all at a pH of 6.	97
Figure 38: Top view of an unmodified (a) unpressurized membrane and (b) pressurized membrane.....	98
Figure 39: Cross sectional view of an unmodified (a) unpressurized membrane and (b) pressurized membrane	99
Figure 40: Top view of an unmodified progressively pressurized membrane at (a) 30 minutes and (b) 4 hours.....	99
Figure 41: Flow rate reduction in pressurized modified and unmodified fibres.....	100
Figure 42: General stress strain relationship for the modified and unmodified membrane fibre.....	107
Figure 43: SEM micrographs of (a) modified, and (b) unmodified membrane rupture .	108
Figure 44: SEM micrographs of (a) modified, and (b) unmodified membrane rupture cross section	109
Figure 45: Appearance of an incompletely wetted membrane fibre.....	116
Figure 46: Distribution of chlorine residual sampling in treatments containing a concentration of 1000 mg/L at a pH of 6.....	117

List of Acronyms

ATR-FTIR	Attenuated total reflectance Fourier-transform infrared spectroscopy
AWWA	American Water Works Association
CA	Cellulose acetate
CIP	Clean in place
Ct	Concentration · time
DBP	Disinfection by-product
ESEM	Environmental scanning electron microscope
FESEM	Field emission scanning electron microscope
FLR	Flux loss ratio
HF	Hollow fibre
LT2ESWTR	Long Term 2 Enhanced Surface Water Treatment Rule
MF	Microfiltration
MIT	Membrane integrity test
MWCO	Molecular weight cutoff
NF	Nanofiltration
NMR	Nuclear magnetic resonance
NOM	Natural organic matter
OCl ⁻	Hypochlorite
PP	Polypropylene
PS	Polysulfone
PES	Polyethersulfone
PVDF	Polyvinylidene fluoride
RO	Reverse osmosis
TOC	Total organic carbon
TMP	Transmembrane pressure
UF	Ultrafiltration
USEPA	United States Environmental Protection Agency
SEM	Scanning electron microscope
TEM	Transmission electron microscope
XPS	X-ray photoelectron spectroscopy

List of Chemicals

CaCl ₂	Calcium chloride
DPD	N,N-diethyl-p-phenylenediamine
HCl	Hydrochloric acid
HOCl	Hypochlorous acid
K ₂ HPO ₄	Potassium phosphate monobasic
NaH ₂ PO ₄ ·7H ₂ O	Sodium phosphate dibasic heptahydrate
NaCl	Sodium chloride
NaHCO ₃	Sodium bicarbonate
NaOCl	Sodium hypochlorite
NaOH	Sodium hydroxide
OCl ⁻	Hypochlorite ion
Pure Water	Deionised water (> 15mΩ-cm)

List of Symbols

A	Area (m ²)
C _b	Bulk concentration (mg/L)
C _m	Membrane concentration (mg/L)
C _{obs}	Observed concentration (mg/L)
C _p	Permeate concentration (mg/L)
d	diameter (m)
D	Diffusivity constant
D _m	Relative flux loss ratio (%)
E (mod)	Modulus of elasticity
J	Flux (m/s)
J _{fs}	Fouling solution flux (m/s)
J _{pwb}	Pure water backwashed flux (m/s)
J _{pwf}	Pure water fouled flux (m/s)
J _{pwv}	Pure water virgin flux (m/s)
J _s	Solute flux (m/s)
J _v	Fluid flux (m/s)
k	Mass transfer coefficient
M	Molar mass (g/mol)
ΔP	Transmembrane pressure (kPa)
P _d	Downstream pressure (kPa)
P _p	Permeate pressure (kPa)
P _u	Upstream pressure (kPa)
Q _{total}	Total flow (m ³ /s)
R	Resistance (m ⁻¹)
R _{ab}	Absorbance resistance (m ⁻¹)
R _{ck}	Cake layer resistance (m ⁻¹)
R _{cp}	Concentration polarization resistance (m ⁻¹)
R _f	Fouling resistance (m ⁻¹)
R _{if}	Irreversible fouling resistance (m ⁻¹)
R _m	Intrinsic permeability membrane resistance (m ⁻¹)
R _M	Intrinsic operational membrane resistance (m ⁻¹)
R _n	Cumulative mechanistic resistance (m ⁻¹)
R _{obs}	Observed resistance (m ⁻¹)

R_{pp}	Pore plugging resistance (m^{-1})
R_{rf}	Reversible fouling resistance (m^{-1})
Re	Reynolds number
Sc	Schmidt number
Sh	Sherwood number
δ	Boundary layer thickness (m)
Δx	Pore length (m)
ε	Surface porosity
γ	Surface tension at air-liquid interface (N/m)
κ	Pore shape correction factor
Φ	Mass transfer constant
θ	Contact angle ($^{\circ}$)

1 Introduction

1.1 Overview and Problem Statement

The drinking water community is constantly attempting to improve the manner in which water is treated; aiming to produce high quality water in the most economically responsible manner. Challenges, including the emergence of pathogenic protozoa and the formation of disinfection byproducts, have pressed the industry to develop and implement alternative technologies. Membrane treatment, particularly low pressure microfiltration (MF) and ultrafiltration (UF) systems, has become more prevalent in the drinking water community over the last few decades. This increase has been due in part to the ease in which membrane systems can be operated, their ability to address new water treatment concerns such as *Cryptosporidium parvum*, and improving technology. However, in spite of the considerable growth of membrane usage in water treatment, membrane treatment is not without challenges that limit its potential growth. Fouling, integrity, and membrane life also pose significant challenges.

Chemical cleaning is used to address fouling that hydraulic cleaning cannot remove to restore membrane performance. Although chemical cleaning can be effective in addressing fouling, cumulative chemical exposure over a long period of time may result in changes in the membrane material and subsequent alterations in its water treatment capability, susceptibility to fouling, and longevity.

1.2 Research Hypotheses and Objectives

The aim of the research was to examine potential changes in hollow fibre membranes after long term chlorine (as hypochlorite) exposure to explore its impact on the physical properties of the membrane fibre as well as its fouling tendency over an operational lifetime within a concentration-time (Ct) framework. There is currently very little published research in the literature in this subject area, and to the author's knowledge, the concept of investigating the impact of membrane cleaning in a Ct framework is novel. Moreover, outside the recent work of Rouaix et al. (2006), there is no published research characterizing the impact of chemical cleaning on hollow fibre properties and performance. Therefore, the objectives were to:

1. identify a relationship between exposure to free chlorine and membrane performance,
2. characterize impacts of free chlorine exposure with regards to select water treatment properties as well as the difference between types of membranes, and
3. to review the existing and to develop methodologies to achieve the first two goals.

1.3 Research Approach

The research explored membrane degradation in the context of a Ct relationship using equivalent Ct values but varied times and concentrations. The chlorine exposure was investigated at different pH conditions using two different types of polyvinylidene fluoride (PVDF) UF hollow fibre membranes supplied by an industrial partner. Changes in the membrane fibres, as well as the differences between the two fibre types, were evaluated using electron microscopy in addition to hydrophobicity and strength testing. Although flux measurements, flux loss ratios, and solute transport analysis were intended to be carried out to further characterize the membranes, issues encountered with the membrane material prevented this from occurring. However, methodologies and experimental equipment were developed for these procedures and are included.

In reality, there are innumerable combinations of raw water quality and operating conditions that may lead to changes in the membrane material. Moreover, chemical and pressure exposure conditions experienced by membranes in operation are more complicated than those proposed in this research. However, fundamental work with controllable exposure conditions is a preliminary step in this research area. Future research could explore other factors including other cleaning chemicals and the impact of varying feed waters.

1.4 Thesis Layout

This thesis provides background and theory on low pressure treatment in water treatment as well as a review of the literature investigating chemical cleaning and its impacts on membranes. Traditionally, the materials and methods would follow, but due to unique circumstances of the present research, an alternate approach was taken. This was necessary due to the difficulties encountered with the membranes, which were

explored after the development of the characterization methodologies with the hope of resolving them during the course of treatment. The issues were not resolved, but the reasons behind them were discovered and a discussion of the encountered problems precede the actual laboratory methods

With this in mind, Sections 7 and 8 were included. The first section explores the experienced difficulties, and the second details the methodologies that were developed and not used. The experimental plan that was included follows in Section 9 and then the results of both the experimental plan and the investigation into the experienced issues are included in Section 10. Section 11, the discussion, explores the research project as a whole.

2 Background

2.1 Historical Membrane Usage

MF and UF are part of a suite of pressure driven processes that also includes reverse osmosis (RO) and nanofiltration (NF). RO and NF are well established technologies (AWWA, 2005) and have been used in the textile, pharmaceutical, medical, desalination, and food processing industries among others. Low pressure membranes have been used in wastewater treatment and industrial water treatment. However, the leap to economically treat drinking water was one that was only possible in the last two decades due to advances in technology and membrane materials.

As reviewed by Adham et al. (2005) and detailed in Figure 1, the number of worldwide membrane plants has substantially increased after 1989, to 213 and 450 plants in and outside of North America, respectively, as of 2003. 95% of the overall membrane treated water volume worldwide is done by water treatment plants having a capacity greater than 3.5×10^6 L/day. As of 2006, the largest membrane plant in North America is a UF membrane plant with a capacity of 265×10^6 L/day located in Minneapolis, USA. Other major worldwide water treatment plants and their associated treatment capacities and membrane manufacturers are listed in Table 1.

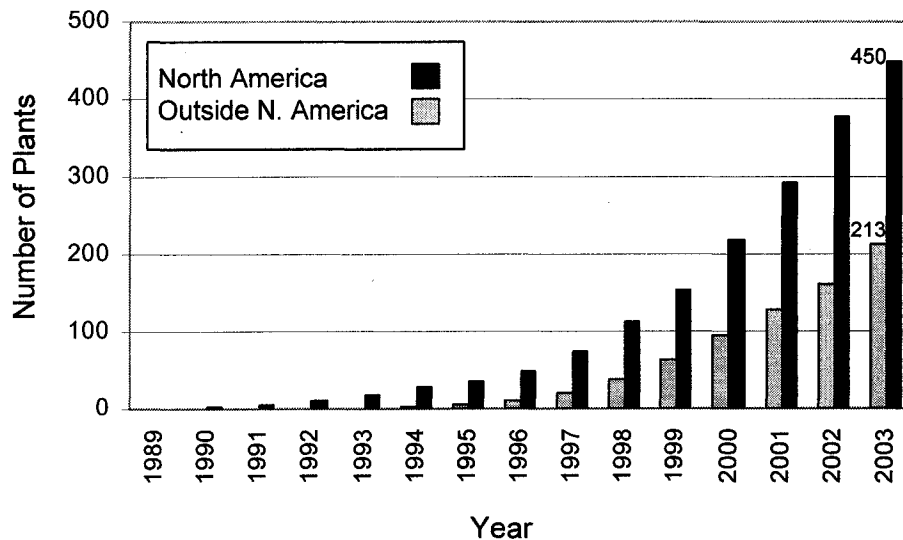


Figure 1: Increase in membrane plant prevalence between 1989 and 2003 (After Adham et al., 2005)

Table 1: Selected membrane water treatment installations

Location	Year	Manufacturer	Capacity (x 10 ⁻⁶ L/day)
Kamploops, BC	2005	GE Zenon	160
Bendigo, Aus	2002	UF Filter	126
Olivenhain, CA	2002	GE Zenon	94
Appleton, WI	2001	Koch	90
Bakersfield, CA	2003	Pall	75

The combined impact of decreasing capital costs and the increasing potential costs of meeting more demanding treatment standards with traditional filtration have fostered the growth of membrane treatment (Laine et al., 2000). Furthermore, as DBP regulations become more stringent, membranes and other technologies that reduce the necessary amounts of chlorine are becoming attractive as they rely less on disinfection processes for pathogen control. Also, the increase of tertiary wastewater treatment installations and the applicability of low pressure membranes in the area have further encouraged growth in the industry as a whole. As technology improves and the competitiveness of the supply industry grows, the economics of membrane filtration should continue to improve.

2.2 LT2ESWTR

The Long Term 2 Enhanced Surface Water Treatment Rule (LT2ESWTR) developed by the United States Environmental Protection Agency (USEPA) has driven interest in the use of membranes as a strategy for *Cryptosporidium parvum* and *Giardia lamblia* removal as well as disinfection by-product (DBP) reduction. The LT2ESWTR requires public water treatment systems to provide additional removal capability for *C. parvum* depending on the levels of protozoa in their source water. A ‘toolbox’ approach has been developed for utilities to provide options in addressing more stringent treatment requirements (AWWA, 2005). Due to the effectiveness of membranes in addressing *C. parvum* and the necessity for many utilities to address source water concerns, the LT2ESWTR has further increased the growth of membrane treatment technology in the United States. It has also inevitably impacted membrane growth in Canada as Canadian regulations will likely follow those in the United States in regards to *C. parvum*.

3 Theory

3.1 Membrane Treatment

3.1.1 General Concepts

Microfiltration and ultrafiltration are characterized by the ability to remove constituents above a particular size range primarily by size exclusion. Membranes are a selective barrier, allowing passage of some constituents while rejecting others (Cheryan, 1998). Although other removal mechanisms exist (such as adsorption and depth bed filtration), design is based on the removal capacity of the largest pore. Microfiltration pore sizes are generally between 0.1 and 0.2 μm whereas ultrafiltration pore sizes are between 0.01 and 0.05 μm with a cut-off as low as 0.005 μm . Figure 2 compares membrane pore sizes to the size of various source water constituents.

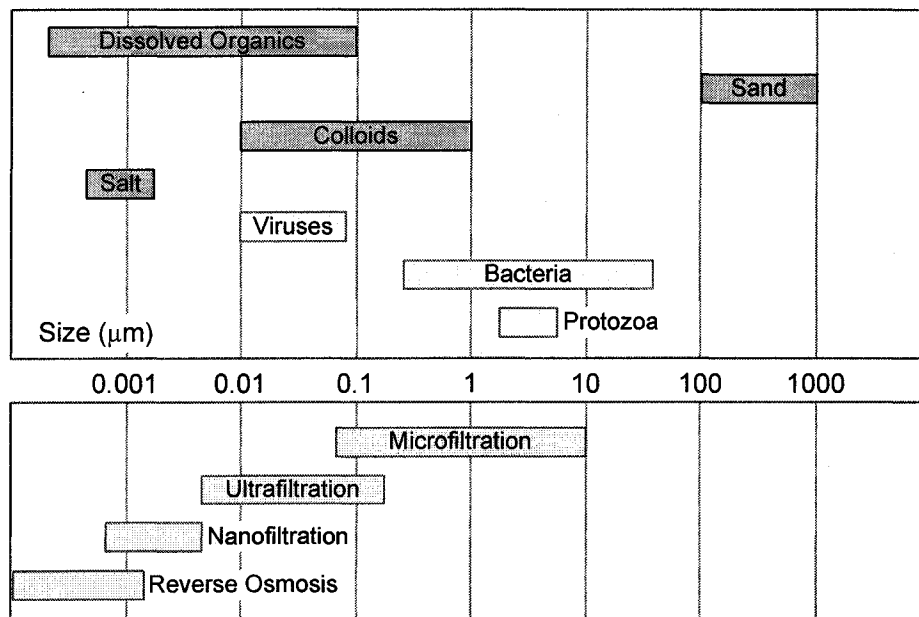


Figure 2: Rejection diagram for various membrane processes (After AWWA, 2005)

RO membranes have pore sizes smaller than 0.001 μm , whereas NF membranes contain pore sizes below 0.01 μm . RO is characterized by the ability to remove color and hardness causing materials, sulfates, nitrate, and sodium, whereas NF membranes are

capable of removing small molecules, some hardness, and viruses (Metcalf and Eddy, 2003). The smaller the pore sizes of a particular membrane are, the tighter it is considered. RO is therefore the 'tightest' membrane, and MF the 'loosest'. Both MF and UF are capable of removing protozoa and bacteria through size exclusion, and are capable of removing some viruses under certain conditions. Tighter UF membranes can physically remove most viruses whereas coagulation and other processes are necessary for partial virus removal in MF (Fiksdal and Leiknes, 2006).

Membrane treatment represents the major barrier to pathogens in a water treatment scenario. When membranes were initially introduced in water treatment, they were employed independent of pre-treatment steps including coagulation, flocculation, and sedimentation and used for low turbidity waters (Farahbakhsh et al., 2004). With the introduction of membranes into more challenging source waters and into existing plants, pre-treatment processes have shown to be necessary to reduce fouling as well as the precursors to disinfection by-products (Vickers et al., 1995). With membrane implementation with other unit processes, they become an alternative or a supplement to rapid sand filtration for most source water conditions.

Membranes offer numerous advantages over sand filtration; they provide an absolute versus probabilistic barrier, a smaller footprint, they are modular in configuration, and they are relatively easy to operate. Traditional water treatment is designed as a multi-barrier approach, where each unit process acts as a removal mechanism to pathogens, cumulatively delivering the appropriate level of treatment. Membranes differ from conventional filtration in that the barrier is absolute as opposed to probabilistic when integral. In rapid sand filtration for example, a certain percentage of particles over a certain size are removed by the gradations of filter media. As the filter run lengthens, there is a greater chance of breakthrough and a backwash must be initiated. Conversely, an integral membrane will remove particles larger than its largest pore (depending on the shape of the particle) and a percentage of particles smaller through other mechanisms such as adsorption, steric rejection, and depth filtration. Moreover, physiochemical processes, such as settling and coagulation, generally precede and are integral to sand filtration. As membrane treatment involves primarily size exclusion, it is not as dependent on processes preceding it, although they are often necessary for optimum

treatment (Farahbakhsh et al., 2004). As an absolute barrier, membranes also reduce the amount of chlorination necessary leading to subsequent reduction of disinfection by-products (USEPA, 2005). Disinfection by-products are further reduced with the removal of some dissolved organics under certain conditions and with tighter UF membranes (Vickers et al., 1995). Membranes, specifically hollow fibres, are also advantageous in that they occupy a smaller footprint due to their high surface area to volume ratio. This is due to the high surface area to volume ratio that exists in the hollow fibre configuration and because the fibres can be relatively densely packed in modules. Their modular nature allows for simple application to existing plants or staged growth in new plants.

Although the popularity of membranes continues to increase (Adham et al., 2005), issues including fouling, integrity, and membrane life and replacement still challenge the technology (discussed in Section 4).

3.1.2 Process Principles

MF and UF are governed by the same general principles and terminology. Common terms, listed and described in Table 2, are used in the proceeding discussion. Though not an exhaustive list, it covers the basic principles that will be subsequently discussed.

Table 2: Membrane terminology

Term	Description
Feed	Fluid entering the membrane module
Concentrate	Fluid rejected by the membrane
Permeate	Fluid passing through the membrane
Flux	Volume of fluid passed through a unit surface area of membrane
Specific flux	Standardized measure of permeability
Lumen	The inner bore of a hollow fibre
Element	Smallest structure of the membrane unit containing fibre(s)
Module	Membrane element plus all of the inlet and outlet structures
Molecular Weight Cutoff (MWCO)	The molecular weight representing the 90 th percentile of what the membrane rejects
Transmembrane Pressure	The difference between the pressure upstream and downstream of the membrane module
Driving Force	The pressure gradient providing the permeation energy

Membrane modules and elements are often described slightly differently, but for the purpose of this discussion a membrane module and element refer to the smallest structure containing the membrane material, and the structure containing the membrane element in addition to the inlet and outlet structures, respectively. This concept will be demonstrated in Section 8.5.

In its simplest form, a membrane system consists of four components: the membrane and the feed, permeate, and concentrate streams. As detailed in Figure 3, the feed and permeate streams are made up of the source solution and filtered solution, respectively. The concentrate stream contains what is rejected by the membrane and is either wasted, or partially recycled back to the feed stream or another membrane treatment stage.

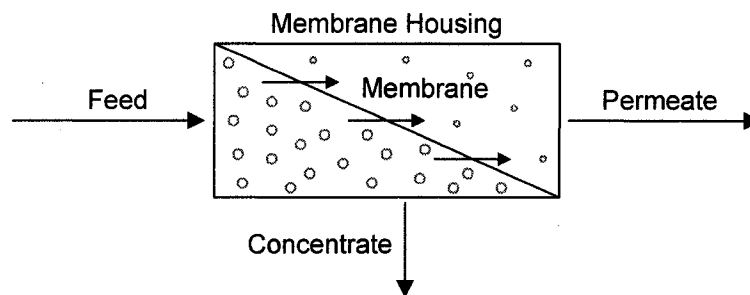


Figure 3: General membrane process

The production of water by a membrane is described by Darcy's Law (Bowen and Jenner, 1995), shown as Equation [1], where J represents membrane flux (m/s), ΔP the transmembrane pressure (Pa), μ the fluid viscosity (N·s/m²), and R_m the intrinsic membrane resistance (m⁻¹). Membrane flux is equal to the volume of produced permeate over the surface area of the membrane surface. Resistance, denoted by R , represents the impedance to flow through the membrane. It is in opposition to the driving force and is impacted by the membrane properties as well as the amount of fouling. Related to the resistance, is the specific flux shown in Equation [2]. In order to compare experimental results, the flux is often normalized by dividing the flux at a particular temperature, most often 20°C, by the transmembrane pressure. This is essentially a representation of the membrane intrinsic permeability (L_p) by eliminating the pressure term from Equation [1]. Alternatively, if experiments are not conducted at 20°C, a correction can be made by

multiplying the determined flux by the ratio of the fluid viscosity at the temperature tested over the fluid viscosity at 20°C (USEPA, 2005).

$$J = \frac{Q_{Total}}{A} = \frac{\Delta P}{\mu R_m} \quad 1$$

$$J_{Sp,20^\circ C} = L_p = \frac{J_{20^\circ C}}{\Delta P} \quad 2$$

The driving force that creates membrane flux is referred to the transmembrane pressure (TMP), shown in Equation [3], which describes the difference in pressure on either side of the membrane where P_u , P_d and P_p refer to the upstream, downstream, and permeate pressures, respectively. This pressure difference provides the energy to drive the filtration process.

$$\Delta P = \frac{P_u + P_d}{2} - P_p \quad 3$$

The molecular weight cutoff (MWCO) generally describes the 90th percentile of rejected molecules and is equivalent to the nominal pore size. The 90th percentile was chosen rather arbitrarily, but has been generally been accepted in the literature (Zydney and Xenopoulos, 2007).

3.1.3 Configurations

Membrane filtration makes use of either hollow fibres or flatsheet membranes. In an operational setting, flatsheet membranes are arranged in either a spiral wound or cartridge configuration. Spiral wound modules involve the membrane wrapped around a central collection tube where pleated flatsheets make up cartridges. Generally, the tighter membranes exclusively use flatsheet configurations whereas MF and UF can use either, but are often arranged in the hollow fibre configuration (USEPA, 2005). Tubular membranes have large inner diameters (10 to 25 mm) and are polymeric or ceramic. They are housed in stainless-steel or fibreglass tubular casing and are permeated inside to

outside (AWWA, 2005). The varying configurations in membrane filtration are detailed in Table 3.

Table 3: Configurations in membrane treatment

Configuration	Material	Notes
Hollow Fibre	Polymeric	Used in water treatment (MF/UF)
Flatsheet		
Spiral Wound	RO/NF	Used in water treatment (not MF/UF)
Cartridge	RO/NF	
Tubular	Polymeric, ceramic	Used in water treatment

Hollow fibre membranes are advantageous in that they are strong in both the radial and horizontal direction and because they occupy a smaller footprint than a flatsheet and tubular design for an equivalent production (AWWA, 2005).

3.1.4 Operational Modes

Membrane installations can either be operated in a deadend (deposition) or crossflow manner. Deadend filtration involves one feed inlet and one outlet with the reject being periodically emptied. In crossflow filtration, the feed stream runs parallel to the membrane, utilizing tangential scouring to reduce the accumulation of solids at the membrane surface. The feed flow that is not filtered is recycled back into the feed stream or wasted. Membranes are often operated somewhere in between these two modes, operating in a functional deadend mode but with a bleed stream to prevent excessive solids build up.

Other operational considerations include a driving force and flow direction. The driving force is generated either by applying a vacuum on the permeate side of the membrane or applying pressure on the feed side; both methods are used in water treatment. Hollow fibres can be operated in an inside/out or an outside/in mode. The direction chosen has implications on backwashing and carry different concerns in treatment. For example, a facility operating in an inside/out mode may run into lumen plugging problems if there are large particles present in the feed and one operating in an outside/in mode may have fouling problems due to reduced shear velocities within the lumen (AWWA, 2005).

Vacuum filtration is generally operated in a submerged membrane system where membranes are placed in an open tank of feed solution and operated in an outside to inside mode. Feed water is drawn into the fibre lumens and collected while the concentrate is either bled or wasted in batches. Alternatively, hollow fibres are housed in a pressurized module where they can be operated either inside out or outside in. Where pressurized membranes operate in a crossflow configuration, a submerged membrane system behaves closer to deadend filtration. Submerged filtration has been more recently developed and has been considered to require less maintenance with lower capital costs (Fane, 2005). In addition, the lower transmembrane pressures involved has been reported to lead to less severe fouling (Cote et al., 1998). Advantages of pressure systems over submerged have been said to include isolation from outside contamination, a smaller footprint, and the advantages of reduced fouling due to high fluid shearing velocities (Martinez, 2005).

3.2 Membrane Properties

3.2.1 Physical Properties

Physical properties of membranes are integral to operation. They determine performance characteristics and essentially determine rejection and fouling response. The most significant physical properties and their definitions are detailed in Table 4.

Table 4: Significant physical membrane properties

Configuration	Description
Pore Size	
Nominal	The pore diameter to which 90% of all pores are smaller
Absolute	The maximum pore diameter
Distribution	The full range of pore sizes
Hydrophobicity	Affinity to water (hydrophobic = water repelling)
Surface Roughness	Surface topography
Charge	Charge on membrane surface
Strength	Rigidity, brittleness, and resistance to bursting, collapse, and rupture

Pore sizes and their distribution are used to define the membrane. Due to the manufacturing process, pore size distributions exist. Membranes are described as having

a nominal and absolute cutoff value, relating to the pore sizes where 90% are smaller and 100% are smaller, respectively (USEPA, 2005). Pores are often simplified as being cylindrical and uniform. In reality, the membrane structure contains a distribution of pores of different shapes and sizes. Each 'effective pore' diameter actually represents an uneven flow path having the ability to reject a solute of the equivalent size.

Other properties include hydrophobicity, surface roughness, charge, and strength. The hydrophobicity (or hydrophilicity) of a membrane is a measure of its affinity for water, often described by contact angles. A large contact angle indicates a hydrophobic material whereas no contact angle represents a very hydrophilic material (Jucker and Clark, 1994). Hydrophobicity varies with the membrane material and is often modified in the manufacturing process to improve operational performance (Yu et al., 2005). Surface roughness and charge are surface properties and can have a significant impact on fouling. Strength of membrane fibres is generally represented by the modulus of elasticity (E), tensile strength, and resistance to elongation. The modulus of elasticity describes the rigidity in the elastic region, or the relationship between applied stress and the resulting deformation. The strength of the fibre refers to the maximum applied tensile stress at breakage, and elongation describes the brittleness of a membrane. Although membrane strength also can indicate its resistance to transmembrane pressure and bursting/collapsing resistance, it is generally not a concern in low pressure treatment.

3.2.2 Polymer Materials

Microfiltration and ultrafiltration membranes have been constructed out of wide number of polymers including cellulose acetate (CA), polysulfone (PS), polyethersulfone (PES), polypropylene (PP), polyacrylonitrile (PAN), and polyvinylidene fluoride (PVDF). Each material has varying properties with regard to hydrophobicity, charge, strength, and oxidant resistance, and therefore care must be taken when selecting the appropriate membrane material for a particular application. An ideal membrane will be resistant to a wide range of temperatures and pH, oxidation, and not be susceptible to fouling. Unfortunately, membranes less prone to fouling are generally more sensitive to operational conditions and oxidants (Ying et al., 2003). CA membranes are the most hydrophilic, but have very narrow pH and temperature ranges and are very sensitive to

oxidants. PP membranes have a greater temperature range, but are very hydrophobic. Alternatively, PS, PES, and PVDF are resistant to wide temperature and pH ranges, while being resistant to oxidants. For these reasons, they have become the most popular membranes in MF/UF. Table 5 details the advantages and disadvantages of various membrane materials with respect to their resistance to different operating conditions.

Table 5: MF/UF polymer properties (Cheryan, 1998; AWWA, 2005; USEPA, 2005)

Polymer	Acronym	Resistance			
		pH	Temperature	Oxidants	Fouling
Cellulose Acetate	CA	+	+	+	+++
Polysulfone	PS	+++	+++	+	+
Polyethersulfone	PES	+++	+++	++	++
Polypropylene	PP	+++	+	+	+
Polyacrylonitrile	PAN	+++			
Polyvinylidene fluoride	PVDF	+++	+++	+++	+(+++)*

⁺ Moderate ⁺⁺ Good ⁺⁺⁺ Excellent
 * when modified to be more hydrophilic

PVDF is considered the most oxidant resistant membrane, offering an advantage over the polysulfone group (Cheryan, 1998). It is also easily processed and its porosity is easily controlled (Ying et al., 2003). As will be discussed in Section 4.2.4, PVDF is post treated in order to reduce its hydrophobicity and lessen its propensity to foul. As can be seen in Table 5, post treated PVDF becomes a very desirable membrane material.

Table 6: Membrane manufacturer polymer usage (From AWWA, 2005)

Manufacturer	Pore Size	Polymer
GE Zenon Membrane Solutions	UF/MF	PVDF
US Filter Memcor	UF/MF	PVDF, PP
Norit Americas Inc.	UF	PES
Pall Corporation	UF/MF	PVDF, PAN, PES
Koch Membrane Systems	UF	PS
Hydranautics	UF	PES

Due to the effectiveness of the post-treatment and greater experience with the polymer, PVDF has become popular in water treatment membranes. At the present time, two major manufacturers use PVDF in their hollow fibre construction. Table 6 lists the

major membrane manufactures and the polymers that are used in their membranes. It should be noted that there are many smaller manufacturers that have, or are in the process of commercialized membranes.

3.2.3 Symmetry

Membranes can be either microporous or asymmetric in construction. Microporous membrane can be either isotropic or anisotropic; where isotropic membranes have a uniform pore structure, the pore size of anisotropic membranes differ through their depth and provide directional selectivity. Asymmetric membranes are characterized by a skin layer over a macrovoid pore structure. The structure in skinned asymmetric membranes provides strength for the active surface layer and provides little selectivity (Cheryan, 1998). Anisotropic membranes have been traditionally used for most commercial UF applications (Cha and Yang, 2007) because they offer less resistance than isotropic membranes (USEPA, 2005) and provide strength to the active layer (Boyd and Zydney, 1997). It should be noted that the definitions of symmetry vary between sources. Some, including Cheryan (1998) define symmetry as it was just described where others, including USEPA (2005) classify anisotropic and skinned membranes as asymmetric.

3.3 *Modelling Flux*

As previously discussed, MF and UF operate primarily on physical rejection based on the size of pores and their distribution. The proceeding discussion provides a brief overview of some of the models that have been used to describe flow through a membrane, which are important in understanding both the membrane process and membrane characterization. Moreover, knowledge of the relationships governing flux allows for informed decisions and appropriate action in the face of operational problems.

3.3.1 Ideal Flow

An appropriate starting point is the Hagen-Poiseuille relationship, describing an ideal membrane with uniformly distributed pores of the same size. The relationship is shown as Equation [4], where J is the membrane flux, ε is the surface porosity, d is the pore

diameter, ΔP is the transmembrane pressure, Δx is the length of the pore (or the thickness of the membrane's active layer), and μ is the permeating fluid viscosity (Cheryan, 1998).

$$J = \frac{\varepsilon d^2 \Delta P}{32 \Delta x \mu} \quad 4$$

Assumptions in its application include the presence of laminar and steady state flow through the membrane, the fluid is Newtonian, and the exit effects are negligible (Cheryan, 1998). The relationship shown in Equation [1] represents a simplification of Equation [4] where the resistance term incorporates the membrane properties shown in Equation [5].

$$\frac{1}{R} = \frac{\varepsilon d^2}{32 \Delta x} \quad 5$$

In the resulting model (Equation [1]) the flux through the membrane is dependent on transmembrane pressure and membrane resistance. When filtering pure water, where there are no feed solute effects, the membrane resistance is constant and the flux is entirely dependent on pressure.

3.3.2 Mass Transport

When operating membranes with a natural water source, constituents in the feed solution create a concentration gradient of solutes leading up to the membrane surface. This phenomenon, referred to as concentration polarization, creates a boundary layer where the concentration in the bulk feed begins to rise to a maximum solute concentration at the membrane surface.

The concept of concentration polarization in regards to fouling is discussed in Section 4.2.3, but its impact on modelling flow through the membrane is substantial and is accordingly discussed. Concentration polarization is shown schematically in Figure 4, where the concentrations relative to the permeate are shown in brackets and the boundary layer is represented as δ .

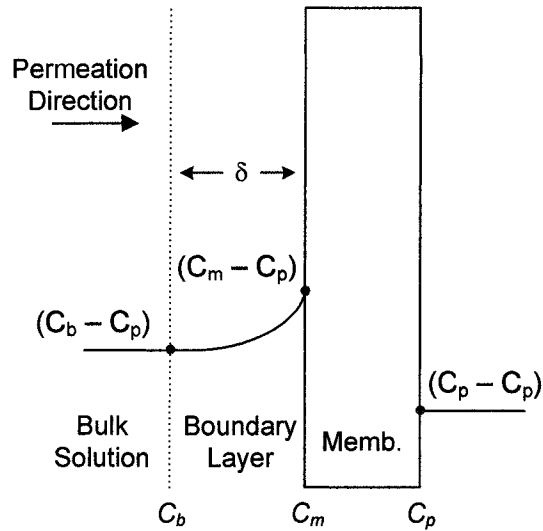


Figure 4: Thin film theory development

The governing relationship is comprised of diffusive flow of solutes away from the membrane, based on Fick's first law and shown in Equation [6], and convective transport of solutes to the membrane, shown in Equation [7]. J_s represents the solute flux, J_v the fluid flux, and D the diffusion coefficient. It is assumed that concentration gradients parallel to the membrane are negligible, the diffusion and concentration in the feed do not change over time, and that the membrane is operated in a crossflow manner (Bowen and Jenner, 1995; Cheryan, 1998).

$$J_s = -D \frac{\partial C}{\partial x} \quad 6$$

$$J_s = J_v C \quad 7$$

When steady state is reached, the convective and diffusive transport are equal, and a relationship can be developed between the concentration at the membrane surface and that in the bulk solution. Equating the convective and diffusive transport terms, and integrating across the boundary layer using the membrane and bulk solution concentrations relative to the permeate concentration yield the thin film relationship shown as Equation [8]. Equation [8] has also been referred to as the stagnant film model.

Substituting the mass transport coefficient, k , for D/δ yields the relationship shown as Equation [9].

$$J = \frac{D}{\delta} \ln \left(\frac{C_m - C_p}{C_b - C_p} \right) \quad 8$$

$$J = k \ln \left(\frac{C_m - C_p}{C_b - C_p} \right) \quad 9$$

At the condition represented in Equation [9], the concentration at the membrane wall can be related to the solution flux and the concentration of the bulk solution. It is important to note that the flux term was assumed to be constant in the integration leading to Equation [8]. Therefore, the relationship applies to a constant flux condition (Zydney, 1997).

The mass transport term often calculated using combinations of the Reynolds (Re), Schmidt (Sc), and Sherwood (Sh) numbers in the relationship shown in Equation [10] (Bowen and Jenner, 1995; Pradanos et al., 1995; Zydney, 1997; Cheryan, 1998).

$$Sh = \frac{k d_h}{D} = A(Re)^\alpha (Sc)^\beta \quad 10$$

The term d_h represents the hydraulic diameter, where A , α , and β are all constants that depend on the velocity and concentration profiles at the membrane surface. Alternatively, the mass transport term can be determined experimentally (Nakao and Kimura, 1981; Cleveland et al., 2002).

3.3.3 Resistance in Series

The two models discussed apply to two separate regions, namely, the pressure controlled and mass transport controlled regions. Moreover, the Hagen-Poiseuille based model is only applicable for filtering solutions where there are no solute impacts. To better address and model operational membranes, the resistance in series model is often used. In addition to considering the relationship between flux, intrinsic membrane

resistance, fluid viscosity, and transmembrane pressure, it also accommodates for the impacts of solutes in the feed stream. Resistance can be divided into three components, the resistance intrinsic to the membrane, R_M , the resistance attributed to fouling R_F , and the resistance due to concentration polarization, R_{CP} . The expanded model is shown as Equation [12].

$$J = \frac{\Delta P}{\mu(R_M + \sum R_n)} \quad 11$$

$$J = \frac{\Delta P}{\mu(R_M + R_F + R_{CP})} \quad 12$$

It is important to understand the concept of intrinsic resistance as it pertains to resistance in series measurement, denoted R_M , and to permeability, denoted R_m . The intrinsic membrane resistance is a genuine membrane parameter only when filtering pure water through a membrane as there are no other fouling mechanisms present, and for that reason it is used as a permeability measure. In the resistance in series model, it is a relative measure and is not an inherent characteristic. Nevertheless, it is useful in gauging the severity of other fouling mechanisms. If fouling accounts for a substantial flux loss, the intrinsic resistance will be low, and vice a versa if there is little fouling presence. The intrinsic membrane resistance is either large or small so to assign the appropriate weight to fouling mechanisms. For instance, if the flux is reduced to zero upon fouling and then completely regained after cleaning, the intrinsic membrane resistance will be zero and all of the fouling will be attributed to reversible fouling because, when compared to reversible fouling, the intrinsic membrane resistance is insignificant. Similarly, if there was no flux loss as the membrane fouls (impossible, but provides a good illustration), the intrinsic membrane resistance would constitute all of the overall resistance.

The resistance terms found in Equation [12] describe different things and establish themselves independently of each other. As previously mentioned, the intrinsic membrane resistance on its own is a good indicator of the performance of a membrane when the other resistances are insignificant, but cannot be used as an operational parameter because it changes based on the severity of the other two terms when present.

The resistance due to fouling is similar to the intrinsic resistance in that it is largely unaffected by operational parameters (Cheryan, 1998), depending on the physiochemical properties of both the membrane and the feed solution. The resistance due to concentration polarization on the other hand, is dependent in its creation on the make-up of the feed solution. Once developed, it is dependent solely on operational parameters; namely, the mass transport coefficient and the transmembrane pressure. The impact of fully developed concentration polarization on Equation [12] is shown in Equation [13] where ϕ is a constant representing the mass transport characteristics (Nabetani et al., 1990).

$$J = \frac{\Delta P}{\mu(R_M + R_F + \phi\Delta P)} \quad 13$$

It can therefore be seen that at low pressures, the resistance due to fouling and intrinsic to the membrane govern the flux, and at high pressures the mass transport characteristics govern the flux as Equation [13] approaches $1/\phi$. At this stage, an increase in pressure will only increase the thickness of the boundary layer and not the flux (Bowen and Jenner, 1995). Consequently, the only factors beyond the solute concentrations impacting flux are the concentration polarization parameters. Improved flux can only be achieved by increasing the mass transport constant, or effectively reducing the boundary layer thickness by means of higher cross flow velocities, greater membrane surface turbulence, or lower feed solute concentrations (Bowen and Jenner, 1995; Cheryan, 1998). This results in a model where flux is pressure dependent at low pressures and pressure independent at higher pressures, scenarios that are seen in operation.

3.3.4 Other Models

The osmotic pressure model has also been used to describe low pressure membrane processes (Ko and Pellegrino, 1992; Cheryan, 1998). Osmotic pressure effects are often considered negligible for MF and UF because the rejected solutes in the processes are too large to have appreciable osmotic impacts in most instances (Cheryan, 1998; Schafer et al., 2005). However, it has been suggested that high levels of concentration polarization

in ultrafiltration increase the solute concentration at the membrane surface to the point that osmotic effects are significant (Nabetani et al., 1990; Bowen and Jenner, 1995). Regardless, osmotic effects are not considered in this discussion and the reader is directed to Cheryan (1998), and Bowen and Jenner (1995) where osmotic impacts are thoroughly addressed. Osmotic pressure impacts are more substantial in the tighter RO and NF (USEPA, 2005).

The preceding discussion deals only with membranes operated in a crossflow manner. If operated in a deadend operational mode, cake filtration models would have to be used (Cheryan, 1998). A study by Iritani et al. (2002) discusses cake filtration models and references works of other authors who have explored these models and their applicability to low pressure membranes.

3.3.5 Temperature and Viscosity Effects

Seeing that chemical reaction rates double for every 10 degree temperature increase (Cheryan, 1998), temperature can play a large role in the interactions between chlorine, foulants, and the membrane material. Temperature also has a large impact on water viscosity and therefore, on water flux. Governed by the Arrhenius relationship, as the temperature goes up the viscosity goes down, resulting in increased permeate flux. This does not occur in all membrane filtration situations as increasing temperature also increases osmotic pressure counteracting the effect of decreased viscosity (Mohammadi and Esmaelifar, 2004). It should be noted that in the temperatures used in water filtration, the viscosity changes far outweigh any osmotic pressure impacts.

4 Challenges in Membrane Treatment

Although there are many advantages to membrane filtration when compared to traditional treatment, there remain challenges that have limited their growth and application. These concerns include operational factors such as fouling, integrity, and long term performance.

4.1 Integrity

Perhaps the most important issue is integrity. A non-integral membrane will not be effective as its primary removal mechanism is compromised. Membrane failure can arise during operation due to chemical attack, mechanical stress, or impact with abrasive materials (Garcia-Aleman and Lozier, 2005). Although manufacturing defects and faulty installation can also lead to integrity problems (Nederlof et al., 1997), there is a greater focus on operational integrity in the literature. Complicating the integrity concern is the difficulty in detecting integrity breaches online (Farahbakhsh et al., 2003). The testing currently necessary to meet the requirements of the LT2ESWTR requires a routine interruption in normal operation to demonstrate compliance (USEPA, 2005).

4.1.1 Membrane Integrity Testing

Membrane integrity can either be measured directly or indirectly. As reviewed by Farahbakhsh et al. (2003), direct measurement involves performing tests on the membranes themselves to find evidence of compromised fibres. Direct membrane integrity tests (MIT) can either be pressure based (measure pressure decay, vacuum hold, or diffusive airflow), or marker based (measure the removal capacity of a membrane after the influent is spiked with surrogate microorganisms or particles). Pressure based tests are based on bubble point theory that relates pore diameter and applied pressure. The bubble point refers to the pressure at which air can displace the liquid within the largest wetted pore of a membrane (Farahbakhsh et al., 2003).

The pressure decay test is the most widely used of the MITs and is performed by isolating and pressurizing either the permeate or feed side of the membrane and measuring the pressure drop across the membrane over a standard amount of time. Pressure will slowly decrease across an integral membrane and more rapidly in the

presence of non-integral fibres. Vacuum tests are similarly performed where a vacuum is drawn and the rate of pressure increase is measured (Farahbakhsh et al., 2003). In the diffusive airflow test, the inside of the lumen is isolated and pressurized to a constant pressure before the airflow rate is measured on the feed side of the membrane. Alternatively, the amount of water displaced by the diffused air can be measured and compared to integral displacement values (USEPA, 2005). Sonic testing can also be used to identify compromised fibres but is not widely employed. Challenge testing with pathogenic surrogates is also considered an MIT, but is not a routine procedure and generally only used in the commercial development stage, research, or to demonstrate compliance.

Indirect MITs utilize permeate parameters such as turbidity or particle counts to indicate the presence of non-integral fibres. Higher than normal turbidity or particle counts would indicate that the membrane has lost integrity. Direct tests are far more sensitive than indirect methods (Johnson, 2003) and offer the most accurate method for determining membrane integrity (USEPA, 2005). They also offer the benefit of isolating compromised fibres. Both direct and indirect MITs are summarized in Table 7.

Table 7: Summary of primary tests used to determine membrane integrity

Test Type	Name	Description
Direct	Pressure/Vacuum Decay	Wetted membrane module is pressurized on one side of the membrane (shell or lumen) and the pressure decay or vacuum hold is measured
	Diffusive Airflow	Wetted membrane fibres are held at a constant pressure and diffusive air flow through the pores is measured by air flow or water displacement
	Bubble Point	Line upstream of the membrane is pressurized below bubble point pressure resulting in bubbles developing from compromised fibres
	Marker Based	Pathogenic surrogate is spiked in the feed water and removal across membrane is measured
Indirect	Turbidity	Downstream turbidity is monitored for spikes
	Particle Counts	Downstream particle counting is monitored for spikes

The LT2ESWTR requirement for membrane integrity testing do not require the use of any particular direct MIT, but instead outlines standards of resolution, sensitivity, and frequency that have to be met by the chosen method. Resolution refers to the ability of a membrane to retain pathogens of a particular size, namely protozoa, and stipulates that a MIT must be able to detect an integrity breach of at least 3 μm . Sensitivity denotes the ability of a MIT to verify the log removal value credited to the process. If for example a utility needs an additional 2-log removal to meet LT2ESWTR requirements and intends to achieve this with membranes, the MIT must be able to show the membrane process to be integral to the extent that it achieves 2-log removal of particles greater than or equal to 3 μm . Finally, the MIT method chosen must have the ability to be performed once every 24 hours (USEPA, 2005). Indirect methods are inadequate for meeting the stipulations required under the LT2ESWTR primarily due to their lack of sensitivity, whereas challenge testing is inadequate due to a inability to meet the frequency requirement. The maximum removal credit given to membrane systems is the lower of the log removal demonstrated by a challenge study or that can be shown in a direct integrity test (USEPA, 2005).

4.2 Fouling

Fouling is caused by the build up of material on the surface of the membrane and within the pores, characterized by a deterioration in flux at a constant permeation pressure or an increase in transmembrane pressure at a constant flux (AWWA, 2005). It represents a second challenge encountered in membrane filtration and has been suggested as a factor preventing earlier growth of membrane technology (Cheryan, 1998). Membrane fouling is a phenomenon that is complex and heavily dependent on water composition, membrane type, and operating conditions, making it exceedingly difficult to predict (Laine et al., 2003). Much of the existing literature on the subject is contradictory, and points to various source water constituents and combinations thereof as the main source of fouling (Laine et al., 2003; Farahbakhsh et al., 2004; Katsoufidou et al., 2005). Fouling can be mitigated in numerous different ways. The feed water can be pre-treated, operational procedures can be designed to minimize fouling (i.e., backpulsing, increased crossflow velocities, air scouring), or chemical cleaning can be employed.

It is important to understand and address fouling to prevent additional costs associated with increased energy requirements, more cleaning chemical use (in either dose or frequency), maintenance, and reduced membrane life (Sablani et al., 2001; Kimura et al., 2004; Yeh and Wang, 2004; Schafer et al., 2005).

4.2.1 Fouling Types

Fouling is described most generally as either reversible or irreversible. Confusingly, the terms have two definitions depending on where one looks. In the first, reversible fouling differs from irreversible fouling in that it can be removed through hydraulic or chemical means. When irreversible fouling reaches an unacceptable level, the membranes must be replaced; in this case irreversible fouling is an age indicator. Alternatively, irreversible fouling has been considered removable through chemical cleaning while reversible fouling by physical cleaning methods. The second definition does not differentiate between fouling that can and cannot be removed through chemical cleaning.

Fouling can be organic, inorganic, or biological in nature, and is most often a combination of all types (Schafer et al., 2005). Organic foulants, primarily natural organic matter (NOM), is generally considered to be the principal cause of fouling (Fan et al., 2001; Howe and Clark, 2002; Laine et al., 2003; Farahbakhsh et al., 2004; Peng et al., 2004; Sundaramoorthy et al., 2005; Zularisam et al., 2006). NOM is made up of a suite of organics, primarily humic acids, and there is no consensus on the NOM fraction responsible for the majority of the fouling (Fan et al., 2001). Disagreement in the literature regarding NOM and fouling is indicative of the overall knowledge base in the area. Accordingly, pilot studies are necessary to determine how fouling is going to affect a specific membrane under a particular source water condition (Howe, 2001).

Inorganic fouling describes the build up of inorganics on the membrane surface and within the pores, and can refer to scaling or colloidal and particulate build-up. Scaling is caused most often by metal hydroxides. As they are not retained by MF and UF, scaling is only considered an issue in RO and NF, but do contribute to concentration polarization in low pressure systems (Liu et al., 2004). Particulate and colloidal foulants consist of inert, mineral material, although non-inorganics such as algae, bacteria, and some natural

organic matter (NOM) fit into its size category. Most particulate fouling is hydraulically reversible due to their relatively large size and inert nature (Liu et al., 2004).

Biological fouling refers to bacterial growth on the membrane surface and within its pores that results in biofilm formation. As the biofilm grows, extracellular polymeric substances created by the bacteria form a chlorine resistant gel. Biological fouling is dominated by the presence of bacteria and the conditions for bacterial growth including the availability of nutrients (Liu et al., 2004). This type of fouling is more prevalent in tertiary treatment of wastewater.

Divalent cations, particularly calcium, have been shown to increase the severity of fouling by intermolecular bridging between the negatively charged NOM and negatively charged membrane surfaces. The divalent ions neutralize the charge of the NOM thus allowing greater adsorption on the membranes surface (Jucker and Clark, 1994; Schafer et al., 2000; Saravia et al., 2006) and forming a more compact cake layer (Schafer et al., 2000; Li and Elimelech, 2004; Costa et al., 2006).

4.2.2 Fouling Mechanisms

Fouling is generally described by the mechanisms of adsorption, cake layer formation, and pore blocking. Adsorption takes place within the pores by particles smaller than the pore diameter as well as on the surface of the membrane while pore blocking occurs within the pores with larger diameter particles. Cake formation refers to the layer built up on the surface of the membrane through a combination of adsorption on the surface and the build up and compaction of particles that cannot fit into or through the pores (AWWA, 2005). Gel layer formation, created from the desolubilisation of organics at the membrane surface, is also considered by some authors for low pressure membranes (Nabetani et al., 1990; Sablani et al., 2001; Schafer et al., 2005), but can be considered as part of cake layer formation.

As discussed by Belfort et al. (1994), fouling occurs in stages, beginning with internal adsorption of solutes within the pores followed by a build up and densification of layers as filtering continues. This analysis corresponds with initial pore adsorption, followed by pore plugging, and ultimately cake layer formation, growth, and compaction. The severity of each separate mechanism depends on the nature and size of the solutes in

the feed water and their relationship with the membrane, as certain types having a higher affinity for adsorption and others for pore plugging (Schafer et al., 2005). The three primary mechanisms are shown in Figure 5. Although the three mechanisms are shown relatively independent in the figure, they interact with one another and take place at different times. Adsorption generally occurs first followed by pore plugging and cake layer formation.

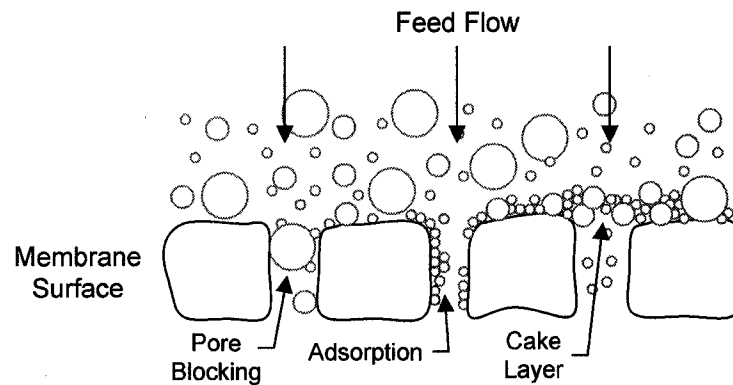


Figure 5: Fouling mechanisms of cake formation, pore plugging, and adsorption

4.2.3 Concentration Polarization

Although included in this section concentration polarization is not technically fouling, but has a similar impact on performance. Like fouling, concentration polarization reduces the membrane flux, but does so in a manner that is reversible (Sablani et al., 2001). As previously discussed, concentration polarization occurs as the solute concentration builds up at the membrane surface to a certain depth referred to as the boundary layer. A diagram depicting the phenomenon is shown in Figure 6. Concentration polarization results in reduced permeate flux due to the solute build up, and increased osmotic pressure at the upstream membrane surface as the less concentrated water downstream attempts to travel upstream. The effective transmembrane pressure is accordingly reduced (Belfort et al., 1994). Concentration polarization also prevents the flux from increasing with increased pressure above a critical pressure (Cleveland et al., 2002).

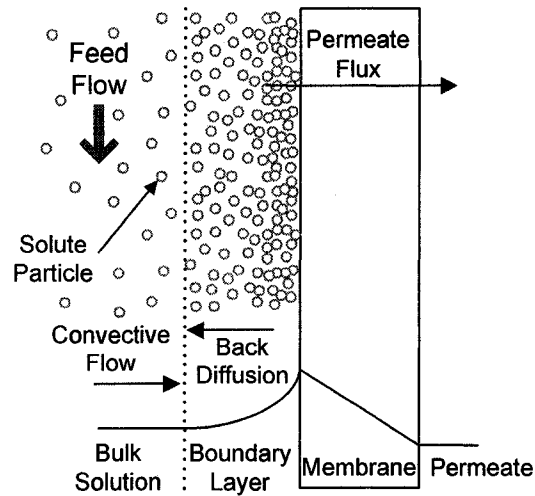


Figure 6: Concentration polarization model (After Sablani et al., 2001)

Where fouling is generally addressed with chemical cleaning, concentration polarization can be mitigated through operational conditions that reverse or reduce the concentration gradient or reduce the boundary layer. Such conditions include increased tangential velocities (shear) and air scouring. Concentration polarization can be temporarily eliminated by backwashing (Sablani et al., 2001). The former two techniques reduce the concentration gradient whereas the latter eliminates the gradient by reversing the direction of flow. The reversibility of concentration polarization differentiates it from fouling in that while reducing the membrane flux, it does not have the same long term impact on flux decline.

4.2.4 Impact of Membrane Properties

Factors that may play a role in membrane fouling include among others, the membrane material, and the charge and hydrophobicity of both the foulant and membrane (Cho et al., 2000; Howe, 2001). It has been shown that hydrophobic membranes are more susceptible to flux reduction when NOM is present in the feed (Jonsson and Jonsson, 1995). As NOM contains hydrophobic and hydrophilic components, the relationship between it and the membrane material is complex. For example, polypropylene (PP) membranes are more hydrophobic than polyethersulfone (PES) membranes. Howe and Clark (2002) found the greater hydrophobicity of a PP material allowed for a greater

retention of NOM than by the PES material and therefore increased fouling. It should be noted that while the link between absorptive fouling and hydrophobicity has been widely established, some authors have found no relationship between fouling susceptibility and hydrophobicity (Wienk et al., 1995; Tu et al., 2005).

A high surface roughness essentially traps foulants on the surface and reduces the effectiveness of the shear effect of the crossflow velocity. It has been shown to impact fouling significantly in RO membranes (Elimelech et al., 1997), but not to the same extent in low pressure systems (Khulbe and Matsuura, 2000) where the scale of the roughness is small relative to the solution components being filtered (Kilduff et al., 2005).

4.3 Long Term Performance

Although not generally considered a major challenge to membrane treatment, long term performance is an issue nevertheless. Over time and after continued irreversible fouling and repeated chemical cleanings, membrane performance declines. This is evidenced by a greater incidence of integrity problems and an increased cleaning frequency. Ultimately, performance concerns, caused by the challenges of fouling and integrity, will result in the need to replace the membranes. Because membrane replacement is one of the major capital costs associated with membrane treatment (Wiesner and Aptel, 1996), there is motivation to reduce the long term impact of fouling and cleaning.

5 Cleaning Practices in Membrane Treatment

Membrane cleaning is critical to effective operation. It is necessary to remove foulants and to reduce the transmembrane pressure to as near clean membrane levels as possible. Cleaning can be performed using either physical or chemical methods and must consider the interactions between the foulants, membranes, and cleaning agents (Li and Elimelech, 2004; Liu et al., 2004). Simple hydrodynamic methods can be used, such as backwashing or scouring, or chemicals can be employed to remove or assist in the removal of foulants. Hydrodynamic methods are considered routine and are periodically initiated during treatment. Chemical treatment is initiated less frequently, when physical methods no longer regain adequate flux.

Acids, caustics, oxidants, surfactants, or combinations thereof are used in a clean-in-place (CIP) process. CIPs involve taking the membranes out of operation and soaking them for a period of time. In some cases, lower concentrations of chlorine are circulated during a backwash to partially clean the membranes without having to take them offline (Belfort et al., 1994). The specific combination of chemicals is dependent on the type of fouling that occurs. For instance, acids may be used to address scaling concerns whereas caustics may be used for organic removal. Raising the temperature of the cleaning solution often improves the efficiency of the operation as does the use of softened water (AWWA, 2005). Major categories of membrane chemicals are detailed in Table 8. Chemicals would be rinsed out of the membrane before bringing back online.

Table 8: Major classes of cleaning chemicals (From AWWA, 2005)

Category	Primary Function	Common Chemicals
Acids	Solubilization	Citric acid, HCl
Oxidants	Oxidation, disinfection	NaOCl, H ₂ O ₂
Caustic	Hydrolysis, solubilization	NaOH
Surfactants	Emulsifying, dispersion, surface conditioning	Commercial compounds

Chemicals used in CIP operations aim to detach the foulants from the membrane by either dislodging them or breaking them down into removable products. For example, an increase in pH via caustic addition will increase the electrostatic repulsion thereby

removing foulants, where oxidants will break down organics into products with weaker bonds to the membrane material (Kuzmenko et al., 2005). Acids are effective in dissolving inorganic scaling on membranes and surfactants are used for difficult to dissolve or emulsify contaminants (Schafer et al., 2005) or when cleaning is limited to a small pH range (AWWA, 2005). Different cleaning agents are often used sequentially in order to obtain the most effective ‘cocktail’ of chemicals. The effectiveness of the various cleaning strategies on fouling is summarized in Table 9.

Table 9: Effectiveness of cleaning strategies on fouling (From Liu et al., 2004)

Fouling	Effectiveness of Cleaning Method			
	Hydraulic	Chlorine Circulation	Acidification	Clean in Place
Inorganic (scaling)	-	-	++	++
Inorganic (particulate)	++	-	-	++
Microbial	+	++	+	++
Organic	-	+	-	++

- Ineffective + Good ++ Excellent

The best method of membrane cleaning is fouling prevention, accomplished by controlling operational conditions, pre-treatment, and process design. High cross flow velocities, air scouring, and the reduction or selection of loading to the membrane surface all may reduce fouling and most often lengthen the filter runs before CIPs are necessary (Gijsbertsen-Abrahamse et al., 2006). Backwashing and backpulsing are also effective to loosen or remove reversible fouling and are used routinely in membrane operation before chemical cleaning is initiated.

A concern with chemical foulant removal is the interaction between the chemical and the membrane material, potentially leading to membrane damage (Farahbakhsh et al., 2004; Kuzmenko et al., 2005; Rouaix et al., 2006). This is important to varying degrees depending on the membranes and chemicals used as certain membrane materials are more susceptible to attack than others. For this reason, chlorine is generally only used as a primary cleaning agent for membranes made out of more resistant materials (AWWA, 2005).

5.1 Membrane-Chlorine Interactions/Research

With the exception of a recent publication by Rouaix et al. (2006), there has been little research published exploring the membrane-chlorine interaction in water treatment. Work has been done on the relationship between foulants and cleaning agents (Kim et al., 1993; Pontie et al., 1998; Zhu and Nystrom, 1998; Liikanen et al., 2002; Chen et al., 2003; Weis et al., 2003; Song et al., 2004), but few studies have focused on the interactions between the cleaning agent and the membrane material itself, although the problem has been identified (Vaisanen et al., 2002; Farahbakhsh et al., 2004; Kuzmenko et al., 2005). Those that do exist do not explore long term degradation or fully characterize the response of a membrane material to chemical exposure (Zhu and Nystrom, 1998; Vaisanen et al., 2002; Kuzmenko et al., 2005). The emphasis is on how best to recover flux and the mechanisms involved in long term degradation are not treated with the same urgency.

The research by Rouaix et al. (2006) was the first to explore the chlorine-membrane interaction in an accelerated aging study, although Wolff and Zydney (2004) performed a study of the same concept for hemodialyzers. In the work of Rouaix's group, PS membranes were exposed to relatively high levels of hypochlorite and its impact on the mechanical properties, permeability, and solute retention of the membrane was investigated. The same research group has since published more studies looking at the impact of chlorine on the PS/PES group of membranes (Gaudichet-Maurin and ThomINETTE, 2006; ThomINETTE et al., 2006). Another recent study by Kwon and Leckie (2006) explored the impact of chlorine exposure on PA membranes. PA membranes have also been investigated by Gabelich et al. (Gabelich et al., 2005), who characterized by their rejection properties and chemical structure. There have been other studies performed on the effect of hypochlorite on membrane properties, but the majority of the work focuses on the impact of hypochlorite during the manufacturing or conditioning processes (Wienk et al., 1995; Xu et al., 1999; Qin et al., 2005).

The interaction of chlorine and membranes was first investigated as RO membranes were being looked at for desalination, concentration of foodstuffs, and water reclamation. Vos et al. (1968) stored CA membranes in different chlorine solutions for varying amounts of time, finding that exposure to low concentrations of chlorine (as high as 51

mg/L) attacked the polymer material. This was expected as the organic CA is one of the most susceptible materials to oxidative attack and would therefore not be used in drinking water treatment. This was followed by research by Avlonitis et al. (1992) and Glater et al. (1994) examining chlorine degradation more directly, both using the more resistant synthetic PA membrane material. Actual mechanisms of degradation that alter the polymer chain are discussed. Avlonitis et al. (1992) used very similar techniques to those implemented in the present investigation.

As previously mentioned, different membrane materials are more or less susceptible to chlorine attack. Polymer materials generally can withstand relatively high chlorine concentrations for short periods of time, but the exposure concentration limit decreases with increased exposure time. Figure 7 demonstrates this concept, showing the various resistances to chlorine of major membrane materials over time. The material lines represent the product of concentration and time, or Ct, and demonstrate an increasing cumulative polymer resistance to chlorine as exposure times lengthen.

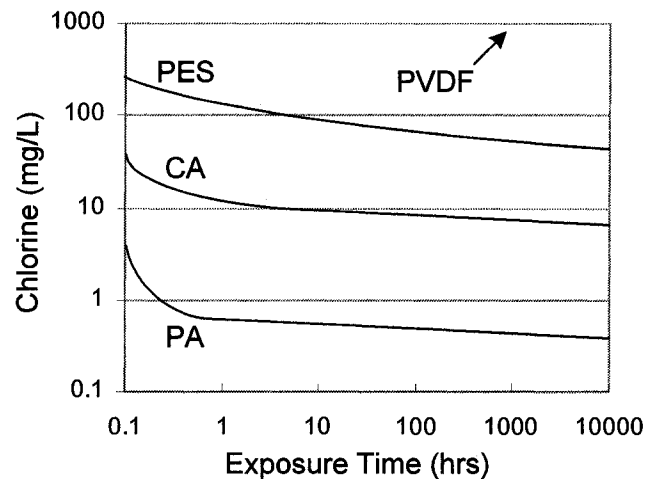


Figure 7: Membrane materials resistance to chlorine (From Cheryan, 1998)

To address the potentially damaging effect of chlorine contact, industry has created maximum exposure concentrations (MEC) as well as maximum cumulative concentration exposure (MCCE) times. MEC values indicate the maximum concentration that a membrane can be exposed to at any one period of time where MCCE values refer to the

cumulative exposure time as a product of the concentration and time of exposure, expressed as mg-hr/L (AWWA, 2005). In typical operation, membranes do not reach this ultimate exposure (Gijsbertsen-Abrahamse et al., 2006). PVDF is the most resistant membrane material to oxidative damage followed by sulfonated membranes (Cheryan, 1998); both materials have had MEC and MCCE values for chlorine assigned by membrane manufacturers. Chlorine exposure to membranes made out of polymers such as polypropylene (PP) or cellulose acetate (CA) is prohibited or low concentrations are suggested (AWWA, 2005).

5.2 Impact of Cleaning on Membrane Properties and Life

Although necessary periodically, chemical cleaning can lead to reduced membrane life (Liikanen et al., 2002; Kimura et al., 2004; Yeh and Wang, 2004; Kilduff et al., 2005; Kuzmenko et al., 2005) and necessitate membrane replacement. This leads to the conclusion that membrane properties are impacted throughout an operational lifetime, having a negative effect on performance. As PVDF membranes are rather new to water treatment, there is a deficiency of information on the mechanisms involved between chlorine and the polymer itself. Due to the high resistance to chlorine when compared to other membrane materials (Figure 7), the impact of chlorine is not merited the same importance. However, the presence of exposure limits in manufacturer's literature indicate the presence of long term impacts.

With respect to the impact of chlorine on membranes, research by Rouaix et al. (2006) found chlorine exposure embrittled PS, a claim also suggested by Gijsbertsen-Abrahamse et al. (2006). Although the reported literature studied PS membranes, similar impacts of chlorine exposure is possible in other polymer materials through other mechanisms, and may lead to integrity concerns. It has also been reported that pore sizes of membranes increase after oxidation (Combe et al., 1999; Park et al., 2005), potentially leading to the passage of larger solutes and pathogens. Other studies investigating membrane changes after exposure to hypochlorite as a conditioning step have shown an increase in flux due to the leaching of one of the polymer components of some sulfonated membranes (Qin et al., 2005; Kwon and Leckie, 2006; Rouaix et al., 2006). Pore enlargement of this nature depends on the make-up of the membrane and the additives

used, making the observation potentially inapplicable for membranes without the same additives. With the current body of knowledge, it is difficult to predict the effect of hypochlorite on PVDF membranes as they have been largely unstudied in the literature (Combe et al., 1999; Park et al., 2005).

There is little information in the literature on the impact of chlorine exposure on membrane hydrophobicity. Kuzmenko et al. (2005) and Zhu and Nystrom (1998) discuss the potential impact of chemical cleaning on fouling susceptibility. As fouling is dependent on the membrane properties (charge and hydrophobicity among others), any change in the membrane due to chemical cleaning may affect its fouling properties and potentially make it more or less susceptible to fouling. Although PVDF benefits from a resistance to oxidation, it has been considered more susceptible to adsorptive fouling due to its higher hydrophobicity (Cornelissen et al., 1998). The two most resilient membranes to chlorine exposure, PS and PVDF, are also the most hydrophobic membrane materials and therefore are potentially more susceptible to fouling. Other materials, including CA, PES, and PS, may be more favourable from a fouling perspective, but are more vulnerable to oxidative attack (Cornelissen et al., 1998; Ying et al., 2003). To avoid this trade off, PVDF is often post-treated in order to decrease hydrophobicity and improve its fouling characteristics.

5.3 Chlorine Properties

Chlorine undergoes three reactions in water: oxidation, substitution, and microorganism destruction. Oxidation occurs when the oxidizing agent, in this case chlorine, reduces (takes an electron) another species in solution (Connel, 1996). Oxidation is the primary concern in membrane life as the polymer material is vulnerable to attack. Substitution occurs in the formation of chloramines and is not important in the present reaction. Microorganism reduction involves the disruption of pathogen lifecycles and is similarly not important.

When dissolved in water, chlorine undergoes hydrolysis as it combines with water to form hypochlorous acid (HOCl). Ionization subsequently occurs where hypochlorous acid dissociates to form an equilibrium with the hypochlorite ion (OCl⁻). The pH level plays an important role in its impact in water treatment as it determines the amount of

hypochlorite and hypochlorous acid present. The total free chlorine is made up of the cumulative quantity of hypochlorite and hypochlorous acid and therefore does not change as the pH varies. However, the distribution of the two chlorine species changes as the hypochlorite concentration increases and hypochlorous acid concentration decreases with rising pH values. Hypochlorous acid has a greater oxidizing capacity than hypochlorite at the same concentration (Metcalf and Eddy, 2003) and therefore acidic chlorine solutions are likely more damaging to polymers than basic ones. The pK of hypochlorous acid is approximately 7.6 at 20°C yielding a solution of primarily hypochlorite at pH levels above 9 and of primarily hypochlorous acid at pH levels below 6 (Metcalf and Eddy, 2003).

6 Membrane Characterization

Membrane characterization has been widely performed for numerous reasons. It has been used to evaluate the impact of cleaning (Kuzmenko et al., 2005; Kwon and Leckie, 2006; Rouaix et al., 2006), the effect of different foulants (Yuan and Zydney, 2000), and fibre construction and conditioning methods (Wolff and Zydney, 2004; Qin et al., 2005). In each case, membranes are characterized before and after a particular treatment or procedure to better understand its impact. Characterization methods can be separated into two major categories, material and operational. Material characterization refers to morphological changes, accumulation of species, or leaching of membrane components, while operational characterization describes empirical changes in operational characteristics such as increased fouling propensity or reduced flux. Operational characterization includes pore property and fouling propensity investigations where material characterization includes hydrophobicity, strength, and chemical composition among others.

6.1 Pore Properties

There are varying methods of characterizing membrane pore sizes found in the literature but currently no standard method has been developed (USEPA, 2005). As reviewed by Nakao (1994) and Zhao et al. (2000), methods used in low pressure filtration include solute retention, gas transport theory, thermoporometry, and microscopy. Although gas transport, atomic force microscopy (AFM), and scanning electron microscopy (SEM) have been used successfully to characterize pore properties (Chan and Chen, 2004), solute retention appears to be the most effective and widely used. Unlike other characterization methods, solute transport studies are performed under operational conditions and allow the measurement of functional pore sizes and therefore provide a direct measurement of rejection properties.

6.1.1 Gas Transport

Gas transport evaluates pore sizes by evaluating the pressure and gas transport relationships through a membrane (Nakao, 1994) and is fundamental in evaluating the integrity of membranes. Methods of determining pore size characteristics by gas transport

including bubble pressure, gas permeability, and permoporometry. As was previously discussed, bubble point theory can identify the size of the largest pore within a membrane based on the diffusion of air through a wetted pore. These methods are not commonly used for pore size characterization and only work well in integrity analysis because of the large diameter of a potential breach that the methodology is designed to detect. Although not as popular as other techniques, gas transport theory has been used in the literature to determine pore size characteristics (Wang et al., 1999; Kong and Li, 2001; Khayet et al., 2002b; Khayet et al., 2002a).

6.1.2 Thermoporometry

Thermoporometry is a technique that uses the thermodynamics of a solution in determining pore sizes. It was first applied to ultrafiltration membranes by Smolders and Vugteveen (1985) and Zemen et al. (1985) and has since been used by Kim et al. (1994) among others for pore size characterizations. Thermoporometry does not have the recent support in the literature of other methods and is therefore not discussed in detail. A review of the analysis involved and its use in the literature is found in Nakao et al. (1994).

6.1.3 Microscopy

Microscopic methods using SEM, transmission electron microscopy (TEM), field emission scanning electron microscopy (FESEM), environmental scanning electron microscopy (ESEM), and AFM have been used in the characterization of membranes and been reviewed by Nakao et al. (1994) and Zhao et al. (2000). Microscopic methods can provide visual information about pore size, structure, and density to varying degrees of success. A partial list of characterization research for each of the microscopic methods is listed in Table 10 with the associated authors.

SEM and TEM both utilize electron beams akin to an optical beam in light microscopes; how the electrons interact with the sample dictate the produced image. TEM involves measuring the intensity of electrons transmitted through an entombed ultra-thin sample and provides a higher special resolution. SEM operates by measuring the intensity of secondary and backscattered electrons excited from the primary electron

beam and emitted from a three dimensional sample that is coated with a conducting material. Both techniques operate in a high vacuum (Clarke and Eberhardt, 2002). ESEM differs from SEM in that a high vacuum is not necessary. As a result, samples can be imaged without extensive preparation (Howe, 2001). FESEM differs from SEM in that it has lower accelerating voltages and therefore does less damage to the sample (Zhao et al., 2000). AFM is a wholly different concept, involving a stylus at the end of a cantilever that scans the surface of a sample, producing a three dimensional topographical image by measuring the deflections of the cantilever. It was first used in membrane characterization in 1988, and has since become a popular tool that can be used on both wet and dry samples (Khulbe and Matsuura, 2000).

Table 10: Partial list of microscopic characterization research

Method	Author(s)	Year
SEM	Latt and Kobayashi	(2006)
	Nghiem and Schafer	(2006)
	Lee et al.	(2004)
	Fritzsche et al.	(1992a)
TEM	Sheldon et al.	(1991)
ESEM	Koh et al.	(2005)
	Howe	(2001)
FESEM	Kim et al.	(1990)
AFM	Barzin et al.	(2004)
	Chan and Chen	(2004)
	Lee et al.	(2004)
	Khayet et al.	(2002a)
	Khulbe and Matsuura	(2000)
	Combe et al.	(1999)
	Singh et al.	(1998)
Fritzsche et al.	(1992a; 1992b)	

One of the difficulties in using microscopic methods is the challenge of preparing a sample in a way that does not significantly damage the membrane or introduce artifacts. The energy used in electron microscopy may damage the membrane surface while any cutting motion may add striations or compress the structure. The ESEM is advantageous in that it permits the imaging of samples in their original state, alleviating the potential

damage and introduced artifacts of sample preparation. It also has the benefit of allowing samples to be tested wet. Howe et al. (2001) have produced images with high resolution without sputtering using an ESEM. Although theoretically possible, Howe (2001) could not find a preparation techniques to image a hydrated membrane that provided adequate image resolution, and there are no effective methods described in the literature. Chan and Chan (2004) also concluded that, although ESEM offers a unique advantage, the obtainable resolutions did not compare with SEM. Although allowing for higher resolution than SEM or FESEM, TEM is not frequently used in characterization studies (Sheldon, 1991). Destructive and laborious preparation techniques in addition to the inability to obtain pore structure and depth information make it less attractive than other techniques.

AFM has become popular in the literature, offering the advantage of direct analysis, wet or dry, with non-destructive preparation. Where SEM can distort perceived depth in an image that have high surface gradients, AFM gives physical topographical imagery. AFM is not without its problems, namely the potential obscuring of depth by 'overhanging' structures and a lower spatial resolution than SEM (Clarke and Eberhardt, 2002). AFM and SEM have been directly compared by Fritzsche et al. (1992a), who found the sputtering preparation technique used in SEM obscured details and give the perception of smaller pores. AFM was therefore determined to be more suited to pore size determination. Singh et al. (1998) also compared AFM and SEM and found pore sizes calculated with AFM were 3.5 times greater than those calculated with SEM and were better fitted to the pore size distribution chosen.

6.1.4 Solute Transport

Solute retention characterization involves filtering solutes of different molecular weights and determining the pore properties based on what is retained and what passes through the membrane. The rejection properties are determined by measuring the concentration of the various sizes in the bulk and permeate solutions. Experimental data are subsequently applied to mass transport models and an assumed pore size distribution. Methods to obtain the rejection and hydrodynamic methods vary as do the models that the data are applied to and the solutes used.

Selected molecules for solute transport experimentation must be soluble and of a known size. Research of this nature was first performed using dextran by Nobrega et al. (1989), but polyethylene glycols (PEGs) and oxides (PEOs), and proteins have also been used. PEGs and PEOs, collectively termed polyethylene molecules (PEMs), appear to have replaced dextran as the solute of choice. Both dextran and PEMs have little interaction with the membrane material and therefore their removal better approximate size exclusion than proteins, providing a better representation of physical membrane properties. Moreover, a wide range of sizes are available for both groups. The primary difference between the dextran and PEMs is how they make up a solution; where dextran is a poly-dispersed solute, polyethylene is available in discrete sizes. As a result, dextran solutes are filtered as one solution as different sized PEMs are filtered separately. Table 11 lists authors who have used the various solute materials for solute transport studies. A more detailed description of PEM solute transport studies can be found in Appendix D.

Table 11: Partial list of solute transport research using PEMs

Solute	Author(s)	Year
PEMs	Causserand et al.	(2004)
	Khayet et al.	(2002a)
	Cleveland et al.	(2002)
	Schlichter et al.	(2000)
	Singh et al.	(1998)
	Meireles et al.	(1995)
	Pradanos et al.	(1995)
Dextran	Zydney and Xenopoulos	(PROOF)
	Meireles et al.	(1995)
	Nobrega et al.	(1989)
Protein	Meireles et al.	(1995)

The shape of the chosen solutes can vary a great deal, and two molecules of the same molecular weight may be rejected differently. Furthermore, the shape of the molecule may be impacted by factors such as ionic strength, interactions with other solutes, and shear forces at the membrane surface. For these reasons, molecular weights are not the best representation of rejection (Cheryan, 1998). To overcome this potential difficulty, hydrodynamic radii can be used as a size parameter opposed to MWCO (Meireles et al.,

1995). As defined by Singh et al. (1998) and shown in Equation [14] and [15], the hydrodynamic radius can be calculated for PEGs and PEOs, respectively, as a function of the molecular mass using the Stokes-Einstein equation and properties of the solutes.

$$r(\mu m) = 16.73 \times 10^{-6} M^{0.557} \quad 14$$

$$r(\mu m) = 10.44 \times 10^{-6} M^{0.587} \quad 15$$

Concentration polarization complicates efforts to characterize solute rejection. It is not possible to measure the solute concentration at the membrane surface (C_m) as only the bulk solution (C_b) and permeate (C_p) concentrations are measurable. Rejection of solutes as a membrane property cannot be determined directly from these two values, as the concentration difference between the feed solution and the membrane surface results in an observed rejection lower than what is actually being rejected at the membrane surface. For this reason, it is important to understand the mass transfer that is occurring. Although there are several models used in describing solute transport, including the resistance and osmotic pressure models (Nabetani et al., 1990; Cheryan, 1998), the thin film model, used to describe concentration polarization and described earlier, is generally used (Kim et al., 1994; Pradanos et al., 1995; Combe et al., 1999; Platt et al., 2002; Causserand et al., 2004; Zydney and Xenopoulos). The thin film theory relationship is shown as Equation [9].

Solute data is defined by membrane rejection; the observed rejection (R_{obs}) and the real rejection (R) are shown in Equation [16] and Equation [17], respectively. Substituting Equations [16] and [17] into Equation [9], yields the thin film rejection relationship of Equation [18]. The relationship of Equation [18] allows the calculation of the real rejection using flux and observed rejection data.

$$R_{obs} = 1 - \frac{C_p}{C_{obs}} \quad 16$$

$$R = 1 - \frac{C_p}{C_m} \quad 17$$

$$\ln\left(\frac{1-R_{obs}}{R_{obs}}\right) = \left(\frac{J}{k}\right) + \ln\left(\frac{1-R}{R}\right) \quad 18$$

The real rejection value has been determined in various ways in the literature. Some authors (Schlichter et al., 2000; Rana et al., 2005) have adjusted k to a level where they felt the impact of concentration polarization was negated. The thin film relationship was therefore not necessary, and rejection was determined based on observed feed concentrations. Nakao and Kimura (1981) found that the real rejection term changed with changing pressures, and that varying the velocity of the feed stream thereby varying the mass transport coefficient was more accurate in determining the real rejection. Their method was subsequently adopted by Cleveland et al. (2002) among others. Other authors have calculated k by using a combination of crossflow velocities, solute diffusivities, and dimensional analysis (Kim et al., 1994; Pradanos et al., 1995; Platt et al., 2002), or by other means (Liu et al., 1991; Zydney and Xenopoulos), from which R was determined. A third method used in the literature (Combe et al., 1999; Causserand et al., 2004) involves graphing Equation [18] in the form $y=mx+b$ with the R_{obs} and J terms as y and x respectively. In this manner, k can be determined as the slope and R_m from the intercept. A number of assumptions have to be made in using this technique, namely that the mass transport and diffusion coefficients are constant at a fixed flow rate, as is the real rejection term being determined. The latter condition meaning that the relationship between C_p and C_m in Equation [17] is constant (Pradanos et al., 1995).

Once the solute molecule is chosen and the mass transport at the membrane surface has been considered, a rejection curve can be obtained based on the size of solutes and the experimental data collected. The pore size distribution now may be considered using the obtained rejection curve (Aimar et al., 1990). From the rejection curves, a nominal solute cutoff size can be approximated, but a pore size distribution cannot be obtained. If a pore size distribution is desired, assumptions have to be made about a shape of their distribution so that the experimental solute information can be transformed into a distribution. Generally, the log normal distribution is chosen (Zydney et al., 1994; Derjani-Bayeh and Rodgers, 2002), but other distributions have been employed. Derjani-

Bayeh and Rodgers (2002) provide an overview of pore size distribution models in ultrafiltration, and those which have been used in the literature.

When setting up an experimental design, it is important to consider whether absolute values of pore sizes and distributions are needed, or if relative differences are the ultimate goal. If a membrane construction technique or a particular treatment effect is being evaluated, the determination of a pore size distribution may not be necessary. A comparison of the rejection profiles provides the necessary comparative information. For instance, Causserand et al. (2004) fully characterized a virgin membrane with respect to solute transport and pore size characterization. Chemical aging was subsequently investigated using an abbreviated experimental procedure that only used one size of PEG filtered at one flux.

6.2 *Fouling Propensity*

In the examination of fouling propensity or fouling susceptibility, researchers have used a number of different methods. Most studies use empirical flux measurements to gauge fouling propensity by determining the pure water flux and either (a) how much flux is lost after fouling, or (b) what the difference between the pure water flux of a virgin membrane and of one that has been fouled. Alternatively, flux modelling can be used, employing the resistance in series model that has been previously described. A third method involves a modification of the resistance in series model entailing what are referred to as flux loss ratios (FLRs). Although other methods exist, such as microscopy and spectroscopy, they will not be discussed.

6.2.1 Flux Decline or Recovery

Flux decline or recovery studies are a more empirical approach to fouling propensity, as they examine the impacts of fouling on flux as an indication of fouling propensity. It partially disregards the aforementioned fouling mechanisms and treats the fouling process as a black box, meaning that only the end results are examined. The work is performed as either a flux decline study, where the loss of flux under particular conditions are measured, or a flux recovery study, where flux is measured before and after fouling using pure water. Batsch et al. (2005) states that flux has traditionally been the best way to

evaluate membrane fouling. Moreover, comparing pure water fluxes before and after fouling treatment allows for reproducibility in experimentation.

A good example of flux decline research is a study by Lee et al. (2004). The flux decline of membranes that had undergone fouling by NOM are measured and relative flux losses are used to determine which membrane demonstrated the highest degree of fouling propensity. Alternatively, a good example of flux recovery work is research by Bottino et al. (2000). Flux recovery is examined using a flux recovery ratio (*FRR*) shown in Equation [19], where J_{fs} represents the pure water flux after fouling and J_{pwf} represents the pure water flux of a virgin membrane. The authors associate a higher relative flux recovery ratio with a lower fouling propensity.

$$FRR = \left(\frac{J_{fs}}{J_{pwf}} \right) \times 100\% \quad 19$$

Yu et al. (2006) employed the same relationship when studying antifouling characteristics in PP membranes, as did Lindau and Jonsson (1999) when investigating adsorptive fouling of PVDF membranes. Generally, no cleaning takes place between flux measurements with the only change being the replacement of the fouling solution with pure water.

Cleaning studies have also used flux recovery as an indication of cleaning effectiveness by measuring flux before and after cleaning (Zhu and Nystrom, 1998; Kuzmenko et al., 2005). In these studies, the flux recovery concept is applied to measurements before and after cleaning. For example, Kuzmenko (2005) examined fouling propensity by measuring the pure water flux through a virgin membrane and membranes that have been cleaned in different ways.

Flux recovery is popular due to its efficiency; a large amount of information that can be obtained from a limited and convenient amount of experimental effort. Moreover, due to the non-invasiveness of these types of tests, they can be applied to pilot scale operations as demonstrated by Kimurea et al. (2004) among others.

6.2.2 Resistance in Series

Fouling propensity is often described in the literature by the resistance in series model, used by Yeh and Wang (2004) and Lin et al. (2005) among others. This model, shown as Equation [9], is derived from the Darcy's law relationship (Bowen and Jenner, 1995) shown in Equation [1]. When investigating fouling propensity, the additive membrane resistances, R_n play an important role. As mentioned by Schafer et al. (2005), R_n varies in the literature and largely depends on the mechanisms that are deemed important, which are included in the summed value. Additive membrane resistances may include pore plugging, adsorption, cake and gel layer formation, and concentration polarization. These resistances can be summarized as those relating to fouling (R_F) and concentration polarization (R_{CP}) or alternatively, as reversible (R_{rf}) and irreversible (R_{if}) fouling, and concentration polarization. In the previous discussion on the resistance in series model, R_F and R_{CP} were considered. As demonstrated in Figure 8, combining the additive resistances with R_M , constitutes the total membrane resistance (R_T). R_T is theoretically the same regardless of how R_n is defined, with only the experimentation methods and classification that differ.

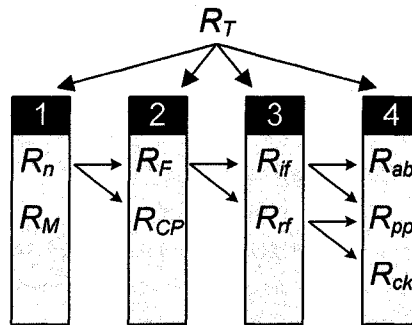


Figure 8: Resistance mechanism definitions

As shown in Figure 8, R_T can be broken up into four categories represented by the three separate columns. The first two columns describe its components as found in Equation [9] and [10], as R_M and R_n , or as R_M , R_F , and R_{CP} . The third and fourth columns describe a more mechanistic categorization, with R_F being broke up into R_{if} and R_{rf} , which are further classified as R_{ab} , R_{pp} , and R_{ck} . As concentration polarization is treated

differently as described in Section 3.4, it always is considered a separate term. R_{pp} is included in both the breakdown of R_{if} and R_{rf} because it is considered to be partly irreversible and partly reversible, whereas R_{ck} is considered completely reversible and R_{ab} completely irreversible. These divisions are general and by no means apply to every situation, but provide a basis from which to understand a broader picture of fouling than possible with one fouling resistance term.

Calculating the resistance values involves measuring fluxes under different operating conditions and using them to successively calculate all of the terms in the denominator of Equation [10]. To provide an example, the mechanisms of Equation [10], namely R_M and R_{CP} can be evaluated by obtaining the following fluxes in an experimental program (Dalcin et al., 1996):

- the pure water flux, J_{pww} ,
- and the fouling solution flux, J_{fs} ,
- the pure water fouled flux, J_{pwf} .

The pure water fouled and fouling solution terms refer to the fluxes obtained by filtering pure water through a fouled membrane, and by filtering a particular fouling solution through a fouled membrane, respectively. The difference between J_{fs} and J_{pww} represents the total flux loss and the differences between the other flux terms and the J_{pww} are compared to this overall term. Other flux terms may be considered depending on the mechanisms chosen to investigate.

The R_M is calculated first using Equation [1] and the pure water flux. Subsequently, the R_F is determined using the ratio of the pure water flux for a virgin membrane and when the membrane is fouled using Equation [21], developed from Equation [20]. Similarly, the resistance due to concentration polarization is determined. In order to compute it, R_F must be known and fouling solution flux must be known. The calculation for R_{CP} is shown as Equation [22].

$$\frac{J_{pww}}{J_{pwf}} = \frac{R_M + R_F}{R_M} = 1 + \frac{R_F}{R_M} \quad 20$$

$$R_F = \left(\frac{J_{pww}}{J_{pwf}} - 1 \right) R_M \quad 21$$

$$R_{CP} = \left(\frac{J_{pww}}{J_{fs}} - 1 \right) R_M - R_F \quad 22$$

Depending on the mechanisms that are being investigated, this procedure can be used to identify the other resistance terms included in Figure 8 as long as the flux terms that are obtained relate to those particular fouling mechanisms.

6.2.3 Flux Loss Ratios

Flux loss ratios (FLRs) were developed more recently by Dalcin et al. (1996) as an alternative to resistance in series modelling. Rather than evaluating resistance terms in the resistance in series equation, the flux loss associated with each mechanism relative to the overall flux loss is determined. The FLR method apportions the overall flux loss between the different fouling mechanisms and concentration polarization. Flux loss ratios are mathematically related to membrane resistances, but allow a direct comparison between flux loss and the associated fouling mechanism responsible for that flux loss. As such, they are not a replacement for membrane resistances, merely an alternative mathematical measure that allow the contributions from the different fouling mechanisms to be clearly evaluated.

The FLR method can be designed to investigate different flux reduction mechanisms similar to the resistance in series method. Using the same experimental fluxes as the preceding section, the calculations are similar. Rather than calculating R_F in Equation [21], the overall mechanistic resistance term, R_n , is determined as in Equation [23]. The total resistance is determined by the addition of R_n and R_M as in Equation [24].

$$R_n = \left(\frac{J_{pww}}{J_{fs}} - 1 \right) R_M \quad 23$$

$$R_T = R_n + R_M \quad 24$$

The overall mechanistic resistance term represents the difference between the highest flux, $J_{p_{wv}}$, and the lowest flux, J_{fs} . The FLRs are subsequently calculated as percentages of the overall flux loss and resistance term, detailed in Equations [25], [26], and [27].

$$D_M = \frac{R_M}{R_T} \times \frac{J_{p_{wv}} - J_{fs}}{J_{p_{wv}} - J_{fs}} \times 100\% \quad 25$$

$$D_F = \frac{R_n}{R_T} \times \frac{J_{p_{wv}} - J_{p_{wf}}}{J_{p_{wv}} - J_{fs}} \times 100\% \quad 26$$

$$D_{CP} = \frac{R_n}{R_T} \times \frac{J_{p_{wf}} - J_{fs}}{J_{p_{wv}} - J_{fs}} \times 100\% \quad 27$$

The intrinsic membrane resistance, the fouling resistance, as well as the percentage of reversible and irreversible fouling are evaluated using this methodology. Although the FLR and resistance values are not absolute and will change under different transmembrane pressures and fouling conditions, they are sufficient for comparative purposes between membranes or treatments.

6.3 Hydrophobicity

The measurement of hydrophobicity using contact angles is well established for flat sheet membranes with the sessile drop or captive bubble methods (Zhang et al., 1989; Zhang and Hallstrom, 1990). Although these methods are applicable and easily performed on flat sheet membranes, measurement of contact angles on hollow fibres is not as simple and not often performed directly in the literature. The small surface available on the circumference of a hollow fibre makes placing drops or retaining bubbles difficult, though it has been done (Tan et al., 2006).

A method more suited to hollow fibres involves measuring the capillary rise on a fibre dipped into a fluid of known properties and subsequently calculating the contact angle. The rise of the fluid on the fibre is photographed and the angles measured between the solution and the membrane are calculated into a contact angle. Gu et al. (1997) thoroughly discusses the theory of the procedure and compares it to traditional contact

angle measurements using small diameter glass cylinders. To the authors knowledge, this method has not been used in hollow fibre membrane research.

6.4 Strength

Mechanical strength of membrane fibres is generally represented by the modulus of elasticity (E), tensile strength, and elongation at ultimate yield. Points of interest relating to stress strain relationship inherent to a material are indicated on Figure 9.

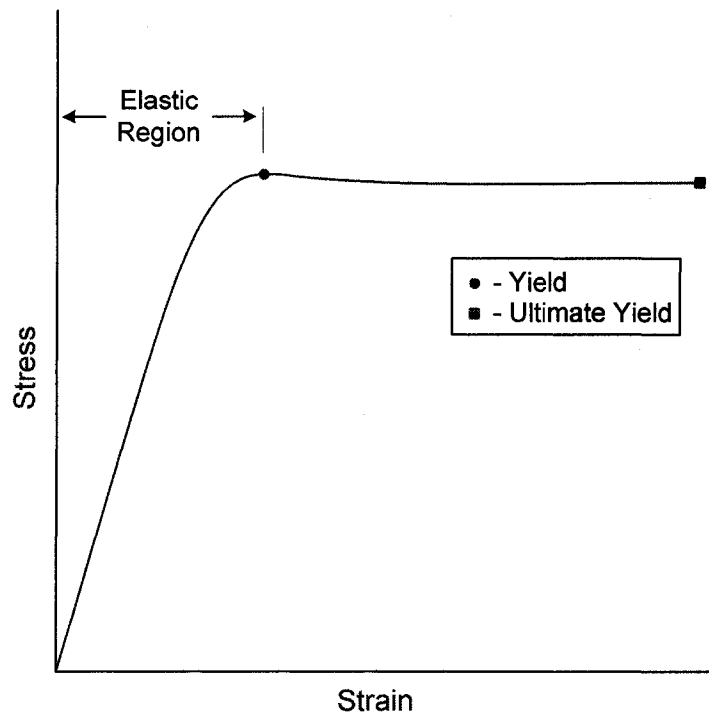


Figure 9: General stress-strain curve

Yield refers to the point where any further membrane deformation is irreversible. In the region before yield, designated the elastic region, the fibre would rebound to its original form. The level of elasticity in this region, or the tensile rigidity is denoted by the modulus of elasticity. It is a measure of how much axial deformation occurs per unit stress. After yield, a greater amount of elongation occurs for the same unit stress that was applied in the elastic region. Ultimate yield is analogous to rupture. Conversely,

brittleness is a property that relates the amount of deformation or elongation before rupture under a particular stress condition.

The mechanical strength of membrane fibres has been investigated in the literature (Qin and Chung, 1999; Xu et al., 1999; Nghiem and Schafer, 2006; Rouaix et al., 2006) by slowly stressing the membrane and measuring the elongation and stress of the fibre at failure as well as the modulus of elasticity. There is no available literature that was found investigating the radial (bursting) strength nor the shear strength of membrane fibres.

6.5 Chemical Composition

Changes in chemical composition can be investigated by attenuated total reflectance Fourier-transform infrared spectroscopy (ATR-FTIR) and X-ray photoelectron spectroscopy (XPS) in order to determine the functional groups and elemental make-up of the membranes. ATR-FTIR and XPS have been used extensively in membrane characterization including work by Fontyn (1987), Oldani and Schock (1989), Chan and Chen (2004), and Shon et al. (2004), among others. These techniques have been used primarily to characterize chemical changes in the production processes, but have also been used to identify foulant make-up and the impact of operational activities.

7 Problems Encountered with Membrane Material

When initiating the first step in the analysis, measuring membrane permeability, it was discovered that the membrane fibre quickly and dramatically lost flux. What occurred at pressures of 30 kPa and more dramatically at higher pressures up to 75 kPa, was unknown, but rendered the membrane irreversibly damaged and incapable of permeating pure water let alone carrying out fouling and solute experimentation. Due to these issues, neither permeability, solute retention nor fouling propensity investigations were performed. In spite of the difficulties, methods were nevertheless developed and are a critical part of the research. Whereas Section 9 discussed the methodologies that were actually used, the following section describes the problems that were encountered, and the subsequent section (Section 8) discusses the methodologies chosen for permeability, fouling propensity, and solute retention that were not executed in the present research.

7.1 Identification of Problem

Initially, it was not understood why the membrane flux was decreasing, but a number of hypotheses were made. The flux loss was considered potentially attributable to either air binding within the pores, fouling, faulty element or procedural construction, or structural damage to the membrane. Each of these could have potentially caused the flux to decrease and in severe instances, present the problem that was encountered. As similar flux loss was experienced with membranes from different treatments including untreated membranes, the chlorine exposure did not cause the problems experienced.

A number of procedures were undertaken to explore each hypothesis. Air binding was not considered a factor after backwashing and rinsing with 100% ethanol did not improve flux. Fouling was initially thought to be unlikely as no build-up of material was visually evident, and only pure water (resistance of $>15 \text{ m}\Omega$) was used in permeability testing. Nevertheless, the membrane module and all of the associated tubing was thoroughly cleaned and an alternative pure water source was used with no impact. Backwashing a membrane that had lost its flux with 500 mg/L hypochlorite was also undertaken to no improvement in flux. After a thorough investigation of the equipment and procedures was completed and multiple membrane elements were tested, problems with the equipment were ruled out. Structural damage was the only hypothesized option

remaining. The pressurized membranes were therefore investigated with microscopy with the hope of identifying structural damage.

7.2 Experimental Investigation

In order to fully understand the impact the flux loss and potential structural damage was having on the membrane fibre, an amended experimental program was initiated that explored the hydrophobicity and strength changes associated with the pressurizing of the membrane fibre. Whereas the microscopy was used in identification of the problem, characterizing the properties of the membrane would allow the operational ramifications to be better understood.

Virgin membrane fibres were pressurized at 50 kPa for approximately four hours, in which time the flow rate through the single fibre went from above 10 mL/min to below 2 mL/min in all of the samples. They were considered adequately pressurized after a minimum of three hours and when the flux began to stabilize. The membrane fibres were subsequently cut from the membrane elements and prepared for both strength and hydrophobicity testing. Four elements of both types of fibre were pressurized so to obtain 5 strength samples and 3 hydrophobicity samples. The results of this experimentation are presented in Section 10.5.

8 Methodology Development

One of the objectives of the present research was to develop methodologies to examine the impact of a particular treatment to hollow fibre membranes. In light of the problems experienced with the membrane fibres, the focus shifted from developing methods for use in the present experimentation to providing a starting point for future research.

As membrane use in large scale drinking water production is relatively new, standard methods that are used for more established technologies do not exist. Moreover, most membrane research has been developed for the more traditional flatsheet configuration as opposed to hollow fibres. It also appears that most technology development and testing has been performed privately, resulting in a dearth of information in the public literature. Membrane cleaning in particular, has been largely unexplored and most information available on its effect on membrane materials remains confidential due to the proprietary nature of membrane development.

Bearing all of this in mind, it was necessary to review existing techniques for the characterization of both hollow fibre and flatsheet membranes in the areas that the present research investigates, namely hydrophobicity, solute retention, fouling propensity, and strength. By no means do these areas encompass all of the characterization techniques used in membrane characterization, but they were selected for their applicability to different membranes and the broad picture that they paint of the impact of chlorine cleaning on membrane fibres. Where the techniques used for strength and hydrophobicity testing are detailed in Section 9, permeability, solute retention, and fouling propensity are included in this section.

8.1 *Choice of Membrane*

Much of the research on membranes has been performed on flat sheet membranes. This is principally due to the establishment of flat sheet membranes, and correspondingly, how established the characterization techniques are. Hollow fibres are relatively new and have only recently been used on a large scale. A secondary factor to the lack of research using hollow fibres is the difficulty their geometry pose to some techniques. This is

especially true in hydrophobicity work, but also true for some microscopy and strength testing.

Perhaps the most difficult obstacle is performing bench scale studies when standard small scale operational process units are unavailable and difficult to construct. Flatsheet style membranes are easier to produce and use in bench scale testing as methodologies are far more developed than they are for hollow fibre membranes and flatsheets are commercially available. As a result, research in membranes has traditionally been performed with flatsheet membranes. Standard equipment for flatsheet study has been accepted and used, namely the SEPA (GE Osmonics) cells (Youm and Kim, 1991; Cleveland et al., 2002; Tarabara et al., 2002; Mosqueda-Jimenez et al., 2004), the Amicon (Amicon Corp.) cells (Meireles et al., 1995; Yuan and Zydney, 1999; Causserand et al., 2002; Mosqueda-Jimenez et al., 2004), and the Minitan (Millipore) unit (Zydney and Xenopoulos, 2007). This is not the case for hollow fibres, resulting in each research group constructing their own devices or using supplier specific equipment.

Consequently, it has not been uncommon to assume equivalent material performance and carry out hollow fibre research on flatsheet membranes. Studies by Katsoufidou et al. (2005), Schlichter et al. (2000), Yu et al. (2006), and Dal-Cin et al. (1996) have used flat sheet membranes as part of a hollow fibre study and assumed that the mechanisms involved are the same. For instance, Dal-Cin et al. (1996) used flatsheet membranes to investigate adsorptive fouling in hollow fibres and Lee et al. (2005) used flatsheet membranes to investigate changes in hydrophobicity of a hollow fibre of the same material. Although the fundamental mechanisms are considered the same (Liu et al., 1991), the flow geometries, mass transport, and internal stresses found in operation are different (Liu et al., 1991; Smith et al., 2006), potentially impacting the applicability of the results.

Research with hollow fibres has become more popular. Fouling studies have been performed by Yeh and Wang (2004), Carroll et al. (2001), Lin et al (2005), Kaiya et al. (1996), and Katsoufidou et al. (2005). Hydrodynamic work has been performed by Berube and Lei (2006), where membrane properties have been investigated by Casseraund et al. (2004). Research by Kim and DiGiano (2006ba; 2006ab) used a two-fibre module to investigate secondary wastewater fouling and used a single fibre module

to study critical flux in two separate studies. Genkin et al. (2006) also used a two-fibre module, but to investigate the impact of vibration on critical flux. Hollow fibre studies have also been carried out by Ghosh (2006), Wicaksana et al. (2006), Nghiem and Schafer (2006) and single fibre work has been carried out by Chang et al. (2006) among others. In almost every study, the experimental set-up was unique. There have also been cases where membrane manufacturers supply membrane filtration units (Wang et al., 1999; Oschmann et al., 2005).

Hollow fibres were chosen over flatsheet membranes in the present research to assist in the development of methodologies and to better understand the impact of the research conditions with the flow geometries and structure of a hollow fibre. Although thousands of fibres constitute a commercial membrane module, a one-fibre design was used in the approach of the present research. The one-fibre module allows the membrane material to be investigated in an isolated condition. Research of this nature would not be possible with multiple fibre modules and large sample sizes as material impacts would be diluted and interactions between membrane fibres (integral and non-integral) may be introduced.

8.2 *Integrity*

8.2.1 Methodology

Pressure decay testing is conducted in accordance to ASTM 6908-03 to ensure the membrane modules are integral before and after exposure to the varying chlorine conditions. This is done by pressurizing and isolating the lumen using air from a compressor throttled to 86 kPa, and measuring the pressure decay. The initial pressure of the lumen is recorded as it is isolated, and measured continuously for 10 minutes. If no air bubbles are seen and if the decay is within a predetermined range, the membrane is considered integral. The pressure decay of 10 virgin membranes are measured and the confidence interval obtained is used to establish a baseline.

8.2.2 Reasoning

As described in Section 4, before any testing of hollow fibres can occur operationally the integrity of the membranes must be verified. The integrity test is performed using pressure that allows the detection of a 3 μm pore, roughly equivalent to the size of a *C.*

parvum oocyst. A pressure of 86 kPa was chosen based on achieving the critical pressure necessary to identify pores of 3 μm based on the bubble point relationship shown in Equation [28], where γ (N/m) represents the surface tension at the air-membrane interface, θ ($^\circ$) the contact angle, d (μm) the pore diameter, and κ , the unitless pore shape correction factor. The surface tension of water at 5 $^\circ\text{C}$, a κ value of 1, and a contact angle of 30 $^\circ$ were chosen as conservative values in determining the critical pressure. A correction factor on one assumes a perfectly cylindrical pore and maximizes the critical pressure (USEPA, 2005).

$$P = \frac{4 \cdot \kappa \cdot \gamma \cdot \cos(\theta)}{d} \quad 28$$

Defects in construction or poor seals in the membrane module can be identified with escaping air bubbles indicating bulk air flow through the membrane. Although testing at 86 kPa does not identify integrity breaches smaller than 3 μm , far larger than the absolute pore size of the tested membranes, it can test integrity to a sufficient standard for the purposes of the research and in accordance with industry standards.

8.3 Fouling Propensity

8.3.1 Methodology

In order to identify changes in the membrane's tendency to foul, flux loss ratios (FLRs), originally developed by Dal-Cin et al. (1996), are used. As previously discussed, FLRs are an alternative method to resistance in series models to evaluate the contributions to flux decline from different fouling mechanisms including the intrinsic membrane resistance. Fluxes were measured in a series of stages in a manner similar to Ko and Pellegrino (1992), so to understand the impact of the various fouling mechanisms.

Permeability is first measured by permeating pure water at three incremental pressures: 25, 50, and 75 kPa. The intrinsic membrane resistance, or R_M , is found using this relationship where the constant $1/R$ is used to represent the permeability of the membrane. The lower the resistance offered by the membrane, the lower the R value is,

and the greater the permeability is. Permeation occurs for a minimum of 0.5 hours before a flux is recorded so to allow the flux to stabilize.

Fluxes are subsequently determined for a virgin, fouled and backwashed membrane to obtain the following values:

- the pure water virgin flux, J_{pww} ,
- the fouling solution flux, J_{fs} ,
- the pure water fouled flux, J_{pwf} ,
- and the pure water backwashed flux, J_{pwb} .

The pure water flux through a virgin membrane is measured first. The membrane is then fouled and the flux of the fouling solution through the fouled membrane is measured. After draining off the fouling solution and thoroughly rinsing the membrane, the pure water flux through the fouled membrane is measured. A backwash is then initiated, followed by a flux measurement of pure water through the backwashed membrane. These steps are demonstrated in Figure 10.

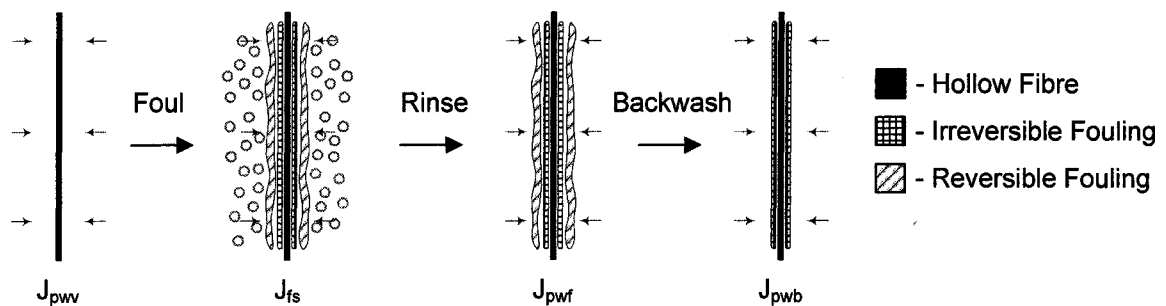


Figure 10: Series of flux measurements used in FLR methodology

At each flux measurement, the flux is first stabilized for a minimum of 0.5 hours and then measured. Theoretically, the lowest flux should be obtained for J_{fs} , followed by J_{pwf} , and J_{pwb} , and J_{pww} . The difference between J_{fs} and J_{pww} represents the total flux loss for the experimental regime and the differences between the others represent the relative contributions of reversible and irreversible fouling, as well as concentration polarization. The flux loss between J_{pww} and J_{fs} indicates the total flux loss due to the addition of all of

the membrane resistances, the flux loss between J_{pwf} and J_{pww} can be attributed to pore blocking and adsorption by the foulant, and the difference between J_{pwf} and J_{pwb} represents the flux loss associated with reversible fouling. Finally, the difference between J_{fs} and J_{pwf} demonstrates the flux loss associated with concentration polarization.

These differences are illustrated in the flux loss ratios for reversible fouling, irreversible fouling, and concentration polarization shown in Equations [29], [30], and [31], respectively. The mechanistic resistance and the relative flux loss ratio terms for the intrinsic membrane resistance are calculated using Equations [21], and [23], respectively.

$$D_{RF} = \frac{R_n}{R_T} \times \frac{J_{pwb} - J_{pwf}}{J_{pww} - J_{fs}} \quad 29$$

$$D_{IF} = \frac{R_n}{R_T} \times \frac{J_{pww} - J_{pwb}}{J_{pww} - J_{fs}} \quad 30$$

$$D_{CP} = \frac{R_n}{R_T} \times \frac{J_{pwf} - J_{fs}}{J_{pww} - J_{fs}} \quad 31$$

Although the FLR and resistance values are not absolute and will change under different transmembrane pressures and fouling conditions, the present research was concerned with comparative differences for which the described methodology is sufficient. A worksheet over viewing the calculations and a methodology protocol is included in Appendix E.

A supplemented synthetic NOM solution is used as the fouling solution, made up of:

- 10 mg/L humic acid solution, with
- 4 mM CaCl₂,
- 20 mM NaCl, and
- 1mM NaHCO₃, all dissolved in
- pure water (> 15 MΩ-cm).

A 500 mg/L free chlorine solution was used for backwashing, performed inside to outside at 60 kPa using an air-pressurized backwash tank. All fluxes are stabilized for 0.5 hours before measurement and the membrane is flushed with 5 L of pure water after both fouling and backwashing before subsequent fluxes are obtained.

8.3.2 Reasoning

Numerous authors have explored 'anti-fouling' properties of membranes through recovered flux. As the primary parameter of interest, flux data provide empirical information of value but fails to give information on mechanisms of fouling. One of the inherent difficulties in using flux recovery or membrane resistance as an indicator of fouling extent is the relative nature of the measurement. A more severely fouled membrane will experience greater flux recovery and potentially disproportionate amount of a particular type of cleaning efficiency will be demonstrated (Munoz-Aguado et al., 1996).

What is different with the present research, is that rather than simply identifying whether the fouling characteristics have improved, the methodology chosen characterizes how the fouling properties have changed through the investigation of individual fouling mechanisms. Opposed to looking solely at flux recovery or flux loss, the relative contributions of reversible and irreversible fouling are quantified relative to the overall flux loss after a particular treatment. It is a much more illustrative methodology that allows for a more detailed understanding of changes in the membrane over time or after particular treatments, such as cleaning or a modification of the polymer make-up.

The resistance in series methodology has also been used in the literature, and unlike the flux recovery studies, it does allow for an investigation of the individual mechanisms. However, it is biased towards a particular type of fouling based on assumptions that have to be made in its calculation. Inherent in the inverse relationship of the series model, a small amount of initial fouling will result in a large flux loss. Demonstrated by Dal-Cin et al. (1996), one type of fouling resistance must be determined first and therefore the resistance representing this initial drop will be underestimated. This creates a problem in that the resistance that is underestimated is always the one that is calculated first, usually adsorptive fouling. Although the overall resistance relationship is inverse, the

contributions to flux loss constituting the overall resistance should not be inversely proportioned.

The FLR method removes the mathematical bias associated with the resistance in series model by apportioning contributions of the flux loss between the mechanism and the overall flux loss to the different fouling mechanisms. Flux loss ratios are mathematically related to membrane resistance, but allow a direct comparison between flux loss and the associated fouling mechanism responsible for that particular flux loss. As such, they are not a replacement for membrane resistances but merely an alternative mathematical measure that allow mechanistic contributions to be clearly evaluated.

An illustration of the difference in the two methods is shown in Figure 11. The linear relationship found with FLRs and the inverse relationship found with the resistance in series model are shown. Previously defined flux values are shown across from their associated flux loss and resistance values in Figure 11(a) and Figure 11(b), respectively. It can be easily seen that equal flux losses for each fouling mechanism will equate to equal flux loss ratios. This is not the case for the resistance in series model, as the resistance due to reversible fouling and concentration polarization is increasingly greater than the resistance due to irreversible fouling even though its addition resulted in the same relative flux loss as the other mechanisms. The flux is most severely impacted by an initial increase in resistance where further rises in resistance have an increasingly smaller impact.

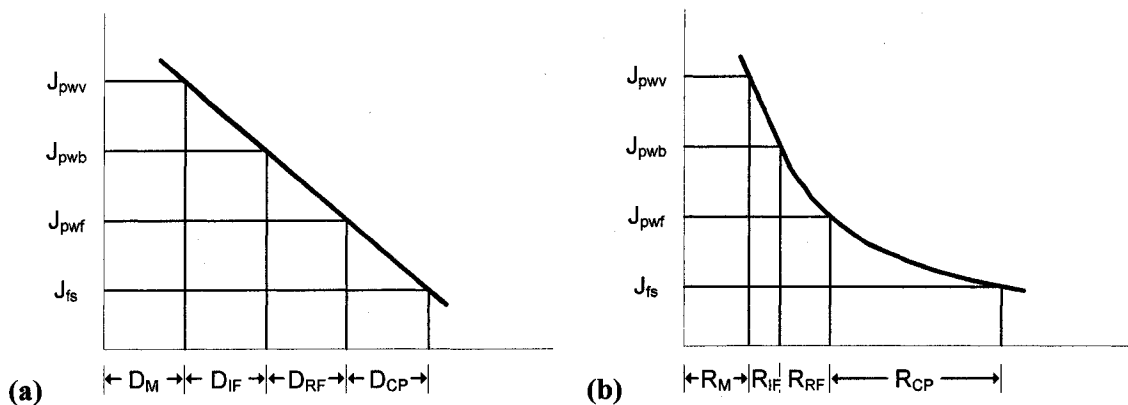


Figure 11: Relationship between flux loss and (a) flux loss ratio values, and (b) resistance in series values (After Dal-Cin et al., 1996)

So when the flux loss contributions of each mechanism are the same, the FLR values are also the same. For instance, if the flux loss was almost entirely due to irreversible fouling, the FLR values would reflect it while the resistance in series values would still underestimate the irreversible contribution. Although FLRs will change under different conditions, the present research was concerned with comparative differences for which the described methodology is sufficient. More extensive examples can be found in Dalcin et al. (1996).

A foulant solution is chosen that is both consistent with what may be found in source waters and that significantly fouls the membrane. As previously discussed, there is a substantial amount of interest in NOM as a foulant, and accordingly, it is chosen for the fouling solution. Moreover, information using a NOM solution is widely applicable as it is found in most source waters. Humic acid constitute a large portion of NOM and have been identified as the fraction most associated with fouling. Hence, it has been used in numerous fouling studies (Schafer et al., 2000; Yuan and Zydney, 2000; Costa et al., 2006). Calcium has been shown to add to the severity of NOM fouling (Costa et al., 2006), and is therefore also added to the solution. Using a solution that has a higher capacity to foul allows for changes in membrane properties to be more easily identified. Sodium chloride and bicarbonate were added to adjust the ionic strength and pH. Calcium, sodium chloride, and bicarbonate values were based on research performed by Tiller and O'Melia (1993).

8.4 Solute Retention

8.4.1 Methodology

Solutions of PEGs and PEOs ranging between 35,000 g/mol to 400,000 g/mol are used in concentrations of 200 mg/L. Single sized solute solutions are separately filtered through the hollow fibre membranes at pressures of 25, 50, and 75 kPa while at room temperature. Crossflow filtration is employed using a flow rate of 2 L/min with a recycle line back to the feed tank. The largest solute sizes are filtered first followed progressively by smaller solutes in an attempt to avoid cross contamination of samples. It is hoped that the larger solutes are more easily cleaned between runs, where pure water is used to thoroughly rinse the membrane element and module. The concentrations of the solute

solutions in both the feed and permeate at the different TMPs are measured using total organic carbon (TOC) analysis. Einstein-Stokes diameters are calculated from equations detailed by Singh et al. (1998) and shown in Equations [14] and [15].

Using the PEM concentration data from TOC analysis in the feed and permeate, observed rejections can be determined for each solute at every pressure increment. These values inputted into the thin film relationship shown in Equation [18] in the form $y = m \cdot x + b$ demonstrated in Equations [32], [33], [34], and [35].

$$y = \ln\left(\frac{1 + R_{obs}}{R_{obs}}\right) \quad 32$$

$$m = \frac{1}{k} \quad 33$$

$$x = J \quad 34$$

$$b = \ln\left(\frac{1 + R}{R}\right) \quad 35$$

By using linear regression, the slopes and intercepts are determined, followed by the rejection at the membrane surface and the mass transport constants for each pressure and solute condition. The method assumes linearity, and if a linear relationship is not obtained when graphing the data the method cannot be used. The observed and actual rejections can be subsequently compared by choosing a flux at which all of the PEM observed rejection curves fall on. Actual membrane rejection occurring at the membrane surface does not change with pressure, but the observed rejection does. A method protocol and a worksheet overviewing the calculations is included in Appendix C.

8.4.2 Reasoning

Solute transport was chosen over the other reviewed methods because it is the only operational framework available for determining pore size parameters. The other approaches involve either visual inspection or procedures either not normal for the membrane. Additionally, tracer retention has proven to be more accurate than AFM in

determining membrane characteristics as they relate to actual filtering capability (Causserand et al., 2004). Kim et al. (1994) and Ren et al. (2006) also concluded that the solute transport methods were the best tool for defining rejection properties. Once chosen, decisions have to be made within the solute transport framework. These included the choice of tracer, how to treat solute size, how to interpret the data, and how to apply the experimental data to pore characteristics.

PEGs are the most common solute used for this type of application because they have little interactions with the membrane material and therefore their removal best approximates steric rejection based on size. PEOs have not been used as extensively, but have proven effective in work done by Singh et al. (1998) and Meireles et al. (1995). Generally, PEGs are all that are needed as most solute transport data in the literature has involved tighter membranes than those used in the present study. A range of solute sizes that includes molecules representing both 0% and 100% retention are necessary in solute characterizations (Cheryan, 1998). In order to have the appropriate range of solute sizes to characterize membranes with average pore sizes in the 0.1 μm range, the larger PEOs are necessary and were therefore introduced in the methodology.

Tam and Tremblay (1991) compared the mono- and poly-dispersed methods using both PEMs and dextran, and found that the poly-dispersed methodology underestimated pore sizes due to the interaction of the different sized solutes. However, most poly-dispersed work is done with dextran molecules and not PEMs. Nevertheless, the concern of interaction between solutes remains an issue. Dextrans are used in poly-dispersed work in part due to the liquid chromatography analysis used for quantification, which facilitates the use of different sized solutes. This leads to an additional advantage of PEMs; the analysis can be performed using TOC analysis as opposed to the more time consuming chromatography (Causserand et al., 2004).

Hydrodynamic volumes opposed to molecular weights are used as they mitigate the problem of molecular shape. Calculating sizes using hydrodynamic volumes has shown to be applicable to spherical, coiled, and rod-like polymers (Meireles et al., 1995) and has been used in numerous studies (Liu et al., 1991; Singh et al., 1998; Khayet et al., 2002a). Hydrodynamic radii are also called Stokes-Einstein radii based on the equation that describes them. An illustration of the problem with molecular weight as a size parameter

can be demonstrated by a spherical and rod shaped particle. Although both may potentially have identical molecular weights, they will be filtered differently. Rejection of the rod shaped molecule would differ depending on its orientation. Hydrodynamic volumes resolve this issue by ascribing equivalent volumes based on the volume they occupy.

The amount of solutes tested and the pressures used are less than others have used in the literature. As the aim of this study was to comparatively characterize membranes after different chlorine exposures, obtaining an accurate MWCO or pore size distribution was not considered essential. In the present methodology, the actual pore sizes were not deemed important as the research is only interested in the relative differences between the treatment outcomes and aims to show a measurable effect of free chlorine exposure. Changes in the rejection profile from one membrane treatment to another would indicate the change that has potentially take place.

Kim et al. (1994) and Ren et al. (2006) suggest that oversimplified mathematical assumptions used in the solute methodology may give misleading results. While this may be true, the most important issue when comparing the same membranes exposed to operational stresses is to easily obtain a representative parameter that has the capability of detecting pore size changes. As this is the goal of the present research, and as an operational opposed to a visual indicator was desired, the solute transport methodology was chosen.

8.5 *Experimental Equipment*

8.5.1 Membrane Element and Module

Membrane elements contain one hollow fibre approximately 160 mm in length and 1.4 mm in diameter, yielding a filtering area of approximately $7.04 \times 10^{-4} \text{ m}^2$. The element, shown in Figure 12, contains a single fibre sealed at the bottom and open at the top. Permeate is collected in the inside of the fibre in an outside to inside operational mode. The fibre is sealed with slow curing epoxy at the top and the bottom of 19 mm diameter schedule 40 polyvinyl chloride (PVC) fittings. A push connect fitting at the top of the element allows for connection to the permeate collection and backwashing

systems. Stress on the fibre is eliminated by a glass stiffening rod incorporated into the fittings.

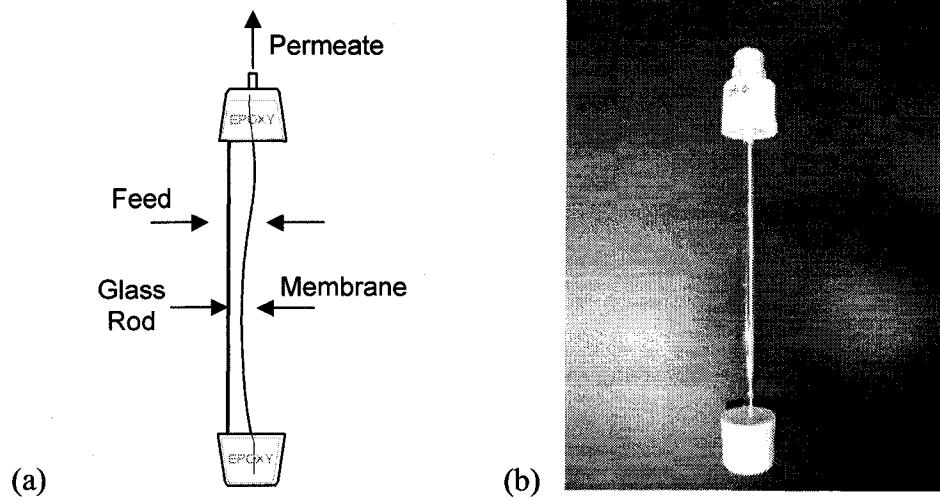


Figure 12: Single fibre membrane module (a) Schematic (b) Picture

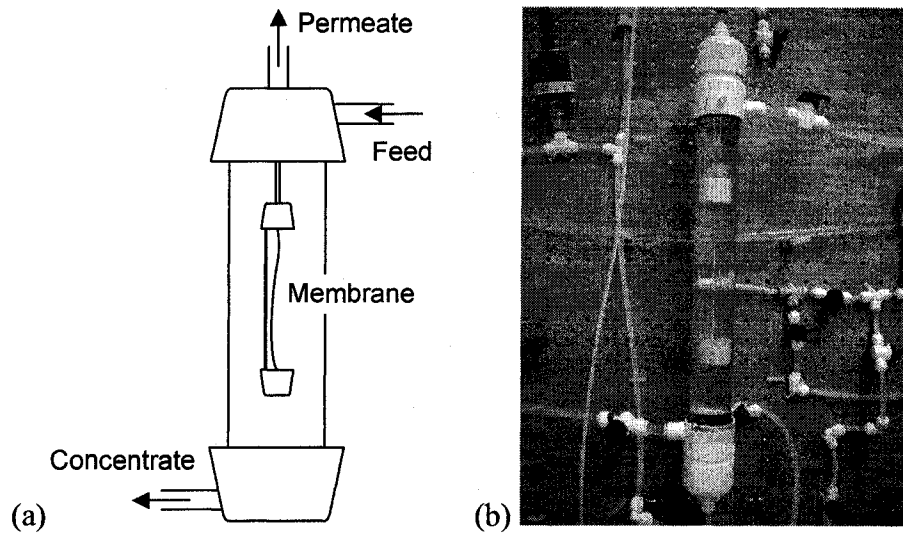


Figure 13: Permeability/Fouling apparatus (a) Schematic (b) Picture

The membrane housing, shown in Figure 13, is made out of 38 mm Schedule 40 PVC fittings and 38 mm diameter Schedule 40 clear PVC pipe. A feed line enters the

housing and both permeate and recycle lines exit the housing. The membrane element is 'hung' from a push fitting glued into the underside of the membrane housing cap by a piece of tubing attaches to the element and carries the permeate out of the module. The module operates in a crossflow configuration with the concentrate being either wasted or recycled back to the feed tank from the bottom of the module. The details of the membrane element construction are included in Appendix A.

8.5.2 Membrane Conditioning

Before treatment exposures occurs, membrane fibres are wetted with a 50% (v/v) ethanol/water solution until the membranes are visually wet. This involves running the ethanol solution through the membrane in an inside to outside manner at a pressure of 70 kPa for approximately 10 minutes. The membrane fibre is subsequently rinsed with pure water at the same pressure for approximately 15 minutes. The saturated fibre has an appearance similar to wetted paper with free flowing fluid over the entire outside surface area. Identification can therefore be easily made. After wetting, the membrane elements are transferred to a slightly chlorinated (<1 mg/L) pure water storage solution until treatment occurs.

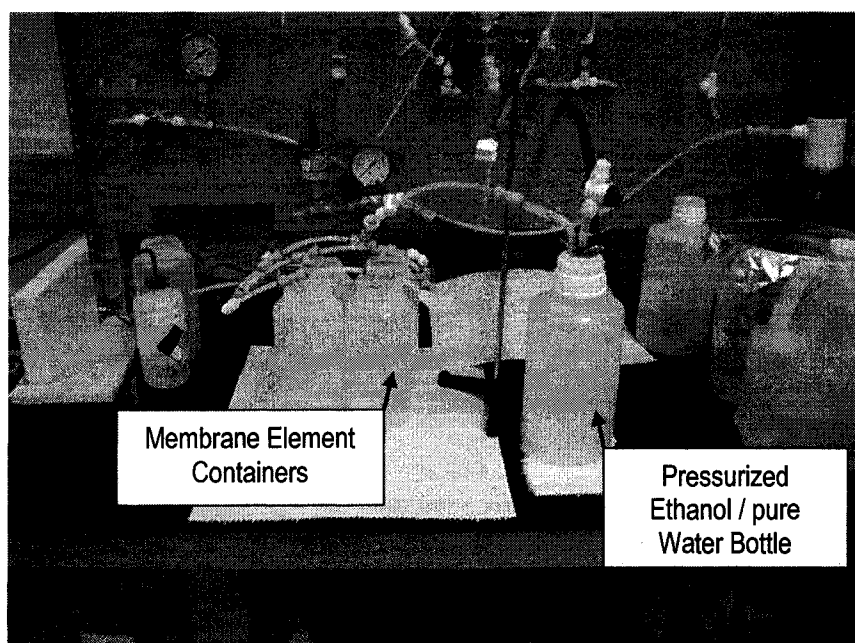
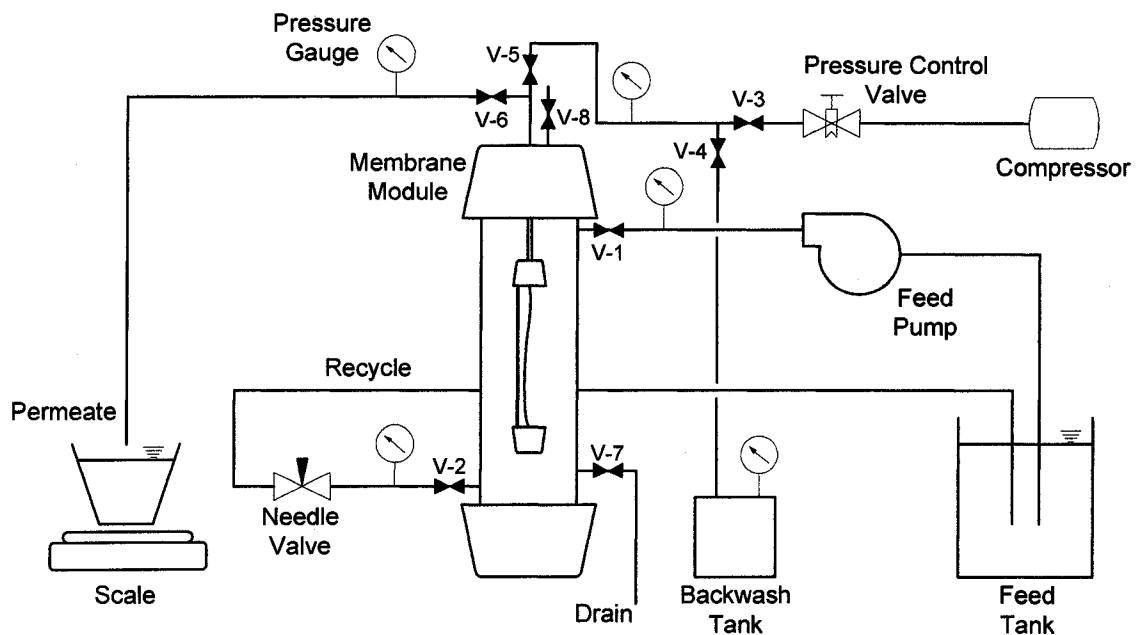


Figure 14: Apparatus for wetting single fibre elements

Figure 14 shows the apparatus that is used to wet the membrane elements. A bottle containing the ethanol solution is pressurized by a throttled laboratory air supply and connected to the top fitting of up to four membrane elements, each in an open container where the ethanol is collected. In the rinsing stage, the ethanol bottle is replaced with a bottle of pure water and the outside of the membrane elements are thoroughly rinsed.

8.5.3 Permeability and Fouling Apparatus

Integrity, permeability, solute transport characteristics, and flux loss ratios can be determined using one experimental apparatus, a schematic of which is shown in Figure 15. The valving for the various operations are included below the figure.



Operation	Description
Integrity	Valves 3 and 5 are initially open with Valves 1, 2, 4, 6, 7 and 8 closed. Valve 3 is closed after the lumen has been pressurized
Permeability / Fouling / Solute Transport	Valves 5, 7 and 8 are closed while Valves 1, 2, and 6 are open with the permeate flux measured using a scale.
Backwashing	Valves 1, 2, 3, 6 and 8 are closed while Valves 4, 5, and 7 are open.

Figure 15: Permeability/fouling/solute transport apparatus schematic

The testing apparatus is designed so that testing of the different applications can be made by simply changing the input or flow path. Integrity is evaluated by pressurizing and isolating the lumen before measuring the pressure decay. The compressor is used for a pressurized air supply, which is throttled down before pressurizing the membrane lumen. The presence of air bubbles indicates the presence of gross integrity breaches or loose connections, whereas the pressure decay data can be used to identify smaller breaches. Permeability, flux loss ratio measurements, and solute transport work can be performed using crossflow filtration with unpermeated feed being recycled back into the feed tank. Backwashes are initiated by pressurizing a backwash feed tank with throttled in-house air pressure and feeding the isolated lumen. Both the permeation and backwash flow are measured by the mass of fluid collected on the scale, either through the permeate line or the backwash drain. Pressure transducers upstream and downstream of the membrane module, and on the permeate stream track the TMP and measure the pressure decay. It can be operated in either vacuum or pressure mode, acting as a pressurized membrane vessel or submerged membrane tank. In the pressure scenario, the transmembrane pressure is developed by a needle valve downstream of the membrane casing and measured as the difference between the average pressure upstream and downstream the element, and that of the lumen, which is close to atmospheric. This procedure is demonstrated as Equation [3]. In the vacuum mode, not shown in the schematic, a valve on top of the membrane casing is opened to the atmosphere and the transmembrane pressure is developed by a gear pump located where the needle valve on the present diagram is located. A negative pressure is developed inside the lumen and the transmembrane pressure is the pressure difference between the vacuum inside the lumen and the average hydrostatic pressure in the membrane casing.

Pressure transducers (Cole Parmer) and push-connect fittings (John Guest) are used in construction, as is a 600 RPM positive displacement pump drive (Masterflex) with high performance Easyload II (Masterflex) pump heads and two pulsation dampeners (Masterflex). Low spallation Norprene (Masterflex) tubing was used in the pump head and generic 3/8" flexible tubing was used for the rest of the feed and recycle lines.

LabView software was used, and a program was written to log the experimental data. Outputs from the scale, pressure transducers, and the pump drive are inputted into the

program, allowing the pressures and flow rates to be measured and logged in real time. From these values, the membrane flux and transmembrane pressure to be calculated. A screenshot of the LabView output screen is shown in Figure 16. All the data is logged into an Microsoft Excel spreadsheet at an interval inputted into the interface.

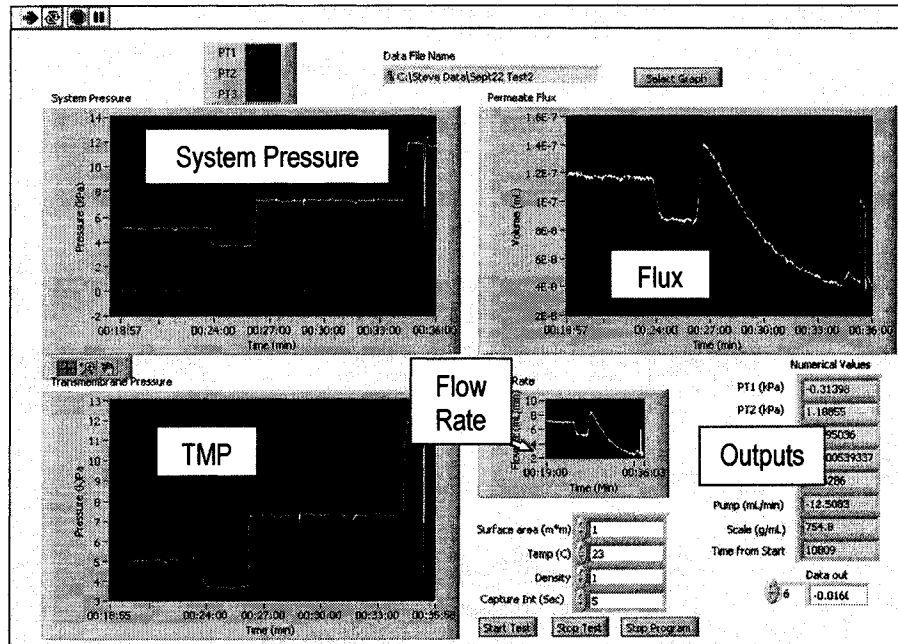


Figure 16: LabView output screen

8.5.4 Equipment Considerations

In development of the element presented for this research, a number of challenges had to be overcome. A suitable epoxy had to be found, there had to be a way to eliminate stress on the fibre itself, the element had to be easily taken in and out of the module, and its construction must be simple and economical enough to facilitate the construction of large numbers. Through various design phases, the element shown in Figure 12 achieved all of these goals.

Although efforts to minimize construction impacts on the membrane material itself, it could not be entirely avoided. Perhaps the issue that poses the most potential impact on the membrane was the heat of curing of the epoxy used to secure the fibre. As detailed in Appendix A, a quick set, viscous epoxy (Holdtite Macroplex) was used to attach the

membrane fibre into the top cap. This was necessary so that the epoxy did not run through the push-connect fitting and render itself unusable. This epoxy was originally intended to fill the cap and form a flush surface, but because of the substantial heat released when curing, this option was unfavourable. To overcome this, the more viscous epoxy was used to cover the push-connect fitting, which was then covered with a 24 hr curing (Nu-Lustre-55) epoxy that became the top surface that would be exposed to operational conditions. Where no push-connect fitting was used on the bottom cap, only the slower setting epoxy was used. Although the heat involved was far less than the other epoxy, there still exists the potential of membrane fibre damage, reducing its effective surface area.

9 Materials and Methods

9.1 Overview

Contact with free chlorine was tested in such a manner as to represent lifetime exposure with the resulting changes in the membranes characterized. Free chlorine concentrations of 0, 1000, and 10,000 mg/L were tested at pH levels of 6 and 9. Exposure times were adjusted based on the concentrations used to yield a cumulative Ct of 1,500,000 mg·hr/L. Surface characteristics, hydrophobicity and fibre strength characteristics were investigated using various techniques as detailed in Table 12.

Table 12: Membrane characterization methods and analysis techniques

Test	Analysis and Associated Equipment
Microscopy	Forensic analysis – Hitachi 4500 SEM
Hydrophobicity	Contact angle using capillary technique – FTA 200
Strength	Strength testing – Instron 553

Contact angles were determined to identify changes in hydrophobicity and tensile testing was used to evaluate strength properties. Both the advancing and receding contact angles were measured in the hydrophobicity work and the ultimate membrane tensile strength, the deformation at yield, and the modulus of elasticity were measured for the strength testing. Scanning electron microscopy was used to investigate changes in the surface and cross sectional membrane morphology. Membrane elements were constructed to run permeability, fouling propensity and solute transport testing. As was discussed in Section 8, this was not possible due to problems encountered with the membrane material.

9.2 Chemical Exposure

9.2.1 Ct Relationship

Chemical concentrations were chosen to significantly stress the membrane fibre while being within a reasonable range. The concentration as well as the associated exposure times are detailed in Table 13. The product of the exposure hours and concentration levels are equivalent to a Ct value of 1,500,000 mg·hr/L.

Table 13: Experimental treatments and associated information

	Free Chlorine in mg/L (Ct = 1,500,000 mg·hr/L)		
Concentration (mg/L)	0	1,000	10,000
Exposure Time (days)	6, 63	63	6

Based on manufacturers recommendations found in the AWWA MF and UF Membrane Manual (2005), typical cleaning exposure with chlorine for PVDF membranes does not exceed 5000 mg/L for instantaneous exposure. These concentrations will vary between membrane materials, manufacturers, and for the particular water quality being treated as can be partially seen in Table 14. The chlorine concentration of 10,000 mg/L will likely cause severe stress on the membrane material and allow the research to identify gross changes in membrane structure and properties whereas 1000 mg/L represents a more likely cleaning concentration exposure, but still far above the normal continuous dose.

Table 14: Recommended free chlorine dosages

Company	Exposure Concentration (mg·hr/L)		
	Continuous	Instantaneous	Cumulative
Pall Corporation	20	5000	n/a
GE Zenon	n/a	1000	500,000
US Filter Memcor	n/a	1000	n/a

9.2.2 Buffers/pH

Phosphate buffers were chosen to control the pH because they are inorganic materials that will not be oxidized by the chlorine. Moreover, phosphate was unique in that it allowed the same species to be used for both buffer solutions thereby negating potential buffer impacts on the polymer-chlorine interaction. A combination of potassium phosphate (K_2HPO_4) and sodium hydroxide (NaOH) was used for the pH 9 solution where a solution of sodium phosphate and potassium phosphate (NaH_2PO_4) was used for the pH 6 solution. Buffer descriptions can be found in Table 15.

Table 15: Buffer descriptions

Treatment	Primary Constituent	Other
pH 6 – 10,000 mg/L	0.5M K ₂ HPO ₄	1M HCl
pH 9 – 10,000 mg/L	0.25M NaH ₂ PO ₄ ·7H ₂ O	2M NaOH
pH 6 – 1000 mg/L	0.5M K ₂ HPO ₄	0.25M NaH ₂ PO ₄ ·7H ₂ O
pH 9 – 1000 mg/L	0.25M NaH ₂ PO ₄ ·7H ₂ O	0.5M K ₂ HPO ₄
pH 6 – 0 mg/L	0.5M K ₂ HPO ₄	0.25M NaH ₂ PO ₄ ·7H ₂ O
pH 9 – 0 mg/L	0.25M NaH ₂ PO ₄ ·7H ₂ O	2M NaOH

9.2.3 Chlorine Concentration

Chlorine concentrations were maintained through routinely performing chlorine residual analysis using the DPD (N,N-diethyl-p-phenylenediamine) Colorimetric Method (Eaton et al., 2000) using a UV Spectrometer (Pharmaci Biotech) and measuring absorbance at a wavelength of 515 nm. Due to the higher reactivity of chlorine at a lower pH, the concentration of the pH 6 solutions had to be more frequently adjusted. At the 1000 mg/L level, pH 6 solutions were checked twice weekly while the pH 9 solutions were checked roughly once every two weeks. Appropriate volumes of sodium hypochlorite (both diluted and at full strength) were added to maintain an averaged target concentration. At the 10,000 mg/L concentration level, the pH 6 solutions were completely replaced daily and the pH 9 solution concentration was checked approximately every three days. Because of the decay over time, the 1000 mg/L and 10,000 mg/L chlorine concentration solutions at the pH 6 level were mixed to approximately 1200 mg/L and 12,000 mg/L of free chlorine, respectively, and readjusted over time so that the average concentration would approximate the target. A tabulation of the concentrations of the treatment paths over the course of the exposures is included in Appendix F.

9.3 Membranes

PVDF hollow fibre membranes were supplied by an industrial partner. They are asymmetric and were designed to be operated outside to inside with operational pressures between 50 and 100 kPa (for constant operation) to a maximum of 200 kPa. The average

pore size is approximately 0.1 μm with a maximum pore size of approximately 0.250 μm . Two different types of membranes were provided, one was a natural PVDF fibre and the other was surface modified so to decrease its hydrophobicity and improve its operational characteristics. The two membrane types were coded A and B, for the modified and unmodified fibres, respectively. The pore sizes differ for the surface modified and unmodified membranes as described, with their respective diameters, in Table 16. The modified membrane was slightly larger in diameter and contained a larger average and maximum pore size. Low and high magnification cross sections of the unmodified membrane fibre are shown in Figure 17. Figure 17(b) depicts the cross section at the outer membrane surface. The membrane surface is in the background whereas the cross section is in the foreground.

Table 16: Membrane statistics

Statistic	Modified (A)	Unmodified (B)
Outer Diameter (mm)	1.385	1.356
Inner Diameter (mm)	0.882	0.858
Average Pore Size (μm)	0.136	0.104
Maximum Pore Size (μm)	0.272	0.214

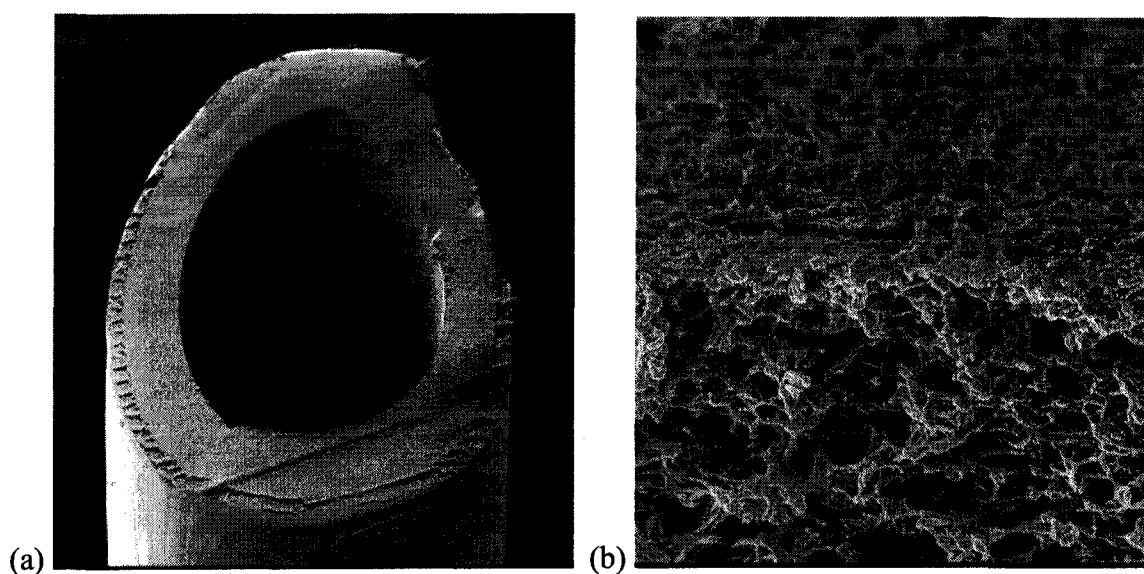


Figure 17: Membrane fibre (a) at low magnification, and (b) at high magnification

It is apparent from the micrographs that the membrane fibre is anisotropic and the pores sizes are made up of the tortuous path of polymer. Two distinct layers can be seen on the membrane fibre in Figure 17(a), made more obvious from the artifacts created when slicing the fibre.

The membranes were supplied in four continuous, separate threads of 50 m each before they were cut into experimental lengths in the laboratory. They were shipped and stored dry until treatment occurred at which time they were wetted and stored wet.

9.3.1 Membrane Conditioning

The fibres used for the strength and hydrophobicity work are wetted in a similar, yet not identical manner to the single fibre elements described in Section 8.5.2. They were treated as single, loose fibres and not in elements like those prepared for the solute and fouling work. In order to facilitate the wetting of the loose fibre membranes, they were built into a multi-fibre membrane element shown in Figure 18, details of which are included in Appendix A.

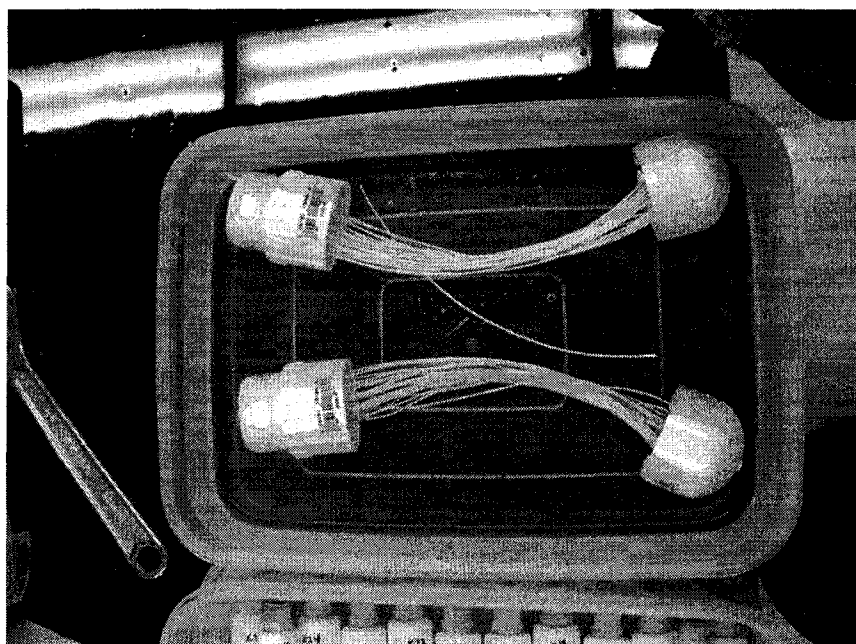


Figure 18: Multi-fibre membrane element used for wetting single fibres

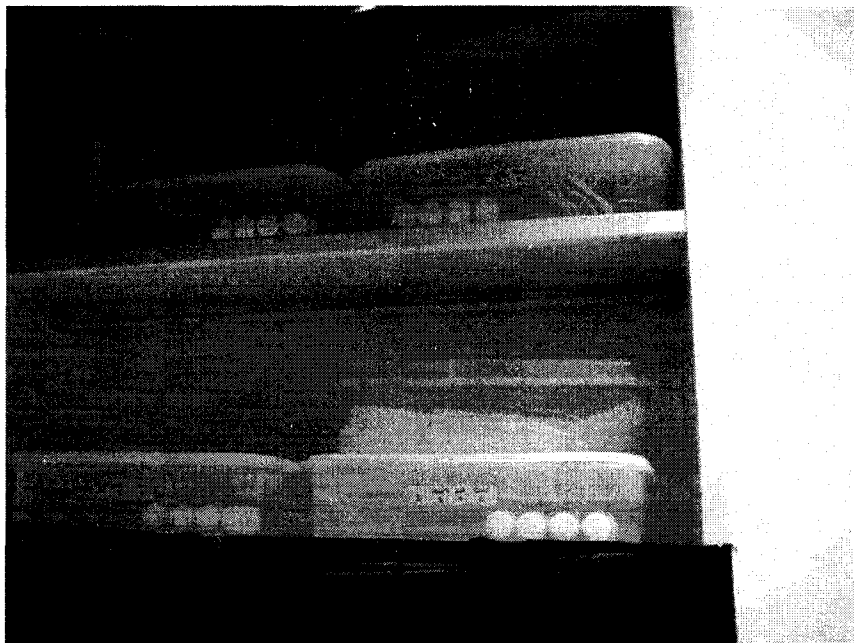


Figure 19: Storage of the treatment baths

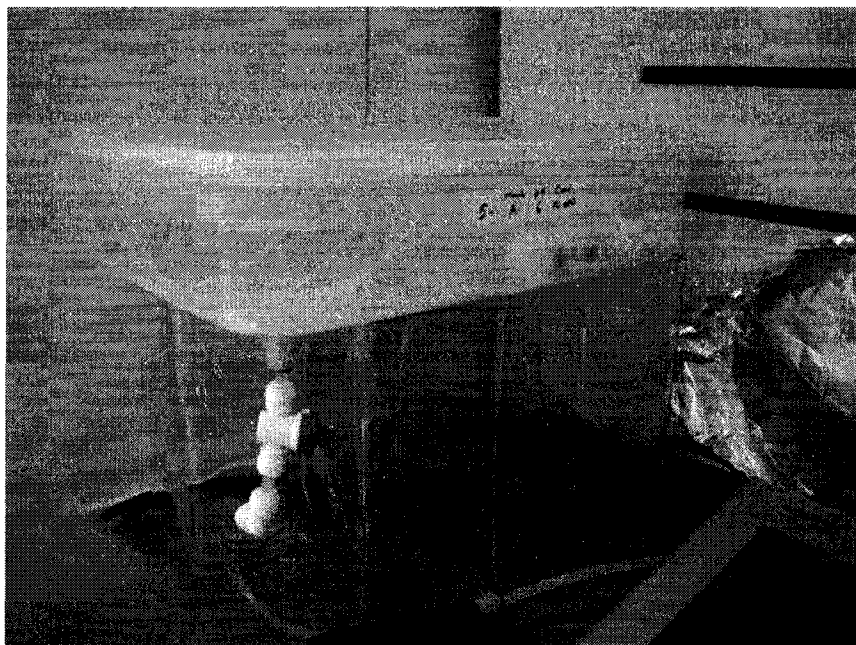


Figure 20: Storage of the 10,000 mg/L free chlorine, pH 6 treatments

Wetting occurred from the inside to the outside at a pressure of 70 kPA, but occurred for a longer period of time due to the volume of fibres that were being wetted. After wetting, the fibres were cut from the element and stored as single fibres before being

exposed to treatments. Exposures occurred at a thermostat controlled temperature of 21°C.

The majority of the solutions were stored in a bookshelf, shown in Figure 19, where they covered to prevent ultraviolet light from more rapidly decaying the chlorine residual. Due to the safety concern posed by the evolution of chlorine gas from the 10,000 mg/L, pH 6 solution, it was stored in a fume hood. Preparation and residual adjustments were carried out in the same fume hood. Drains were installed at the bottom of the containers, shown in Figure 20, to reduce the potential for exposure during the daily emptying and refilling the treatments. Treatments in the fume hood were also covered to prevent ultraviolet chlorine residual decay.

9.4 Characterization

9.4.1 Hydrophobicity

Hydrophobicity measurements were made with a First Ten Angstroms (FTA) 200 instrument and the assistance of the Alberta Centre for Surface Science and Engineering, housed at the University of Alberta. The capillary rise method was used where fibre sections were dipped into a Petri dish containing pure water and a photo was taken of the capillary rise of the pure water up the fibre. Photos and subsequent contact angles were taken as the fibre entered the water and as it exited to obtain both advancing and receding angles, respectively. 20 mm sections of fibre samples were cut with a scalpel and placed on a 21.5 gauge luer fitted onto a syringe. The syringe moved up and down at a rate of 0.091 mm/s and the advancing contact angle was made after it had travelled 3 mm into the solution. The fibre was further immersed by 2 mm before being pulled back out to the same point the first measurement was taken and the receding contact angle was measured. A picture of the FTA 200 is shown in Figure 21.

The software used data points, manually inputted, that identified the extremes of the capillary rise up the fibre and calculated the contact angle. Screen shots of the software output for a hydrophobic and hydrophilic membrane are shown in Figure 22 and Figure 23, respectively. Figure 22 shows the software output after a photo has been taken and Figure 23 shows the output after the data points are entered and the contact angle is

calculated. A zoom feature, shown to the left of the fibre in Figure 23, allows for accurate data point entry.

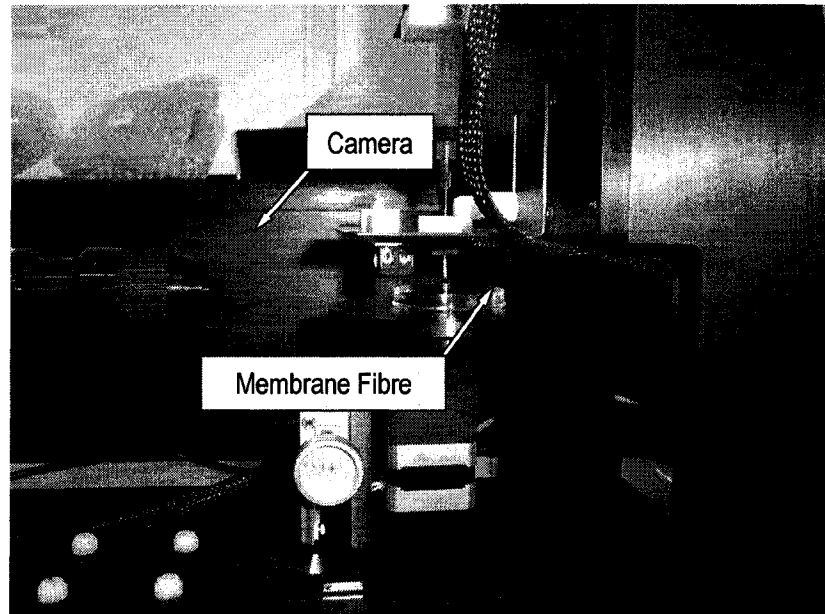


Figure 21: FTA 200 with attached fibre section

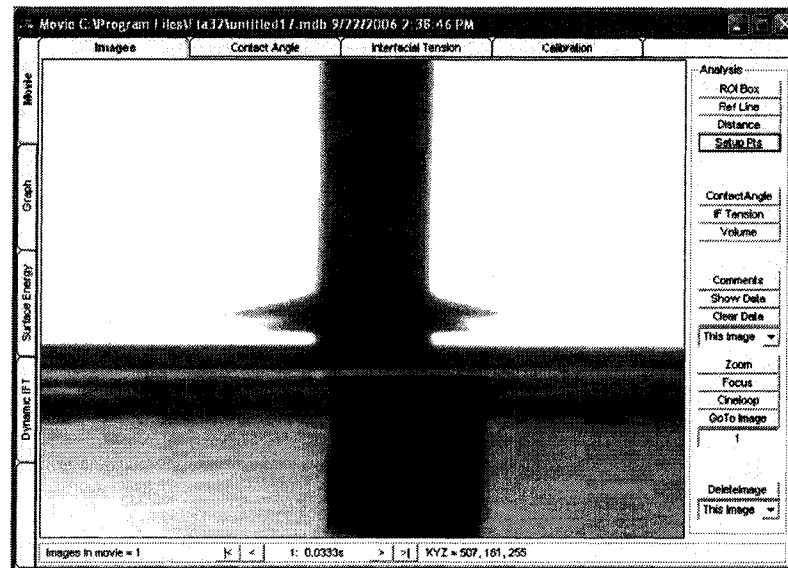


Figure 22: FTA 200 software screenshot of hydrophobic fibre before calculation

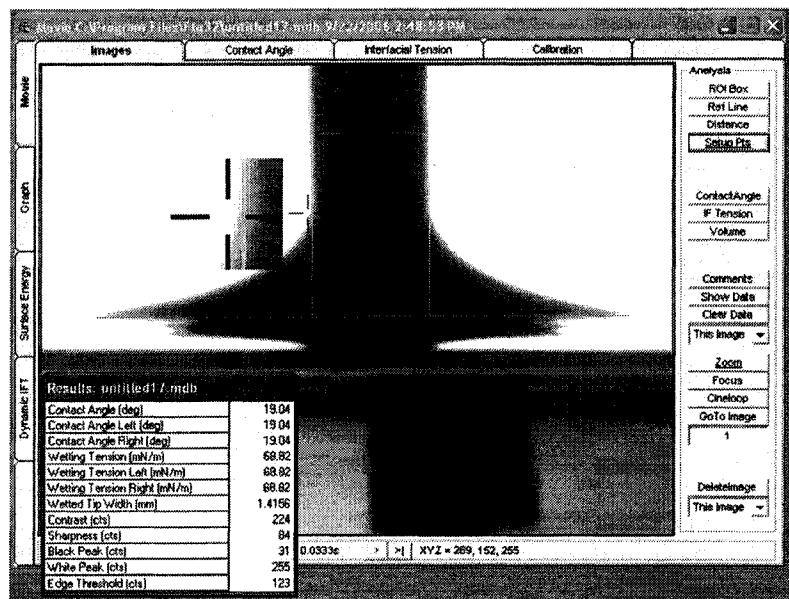


Figure 23: FTA 200 software screenshot of hydrophilic fibre after calculation

The software stills in the preceding figures show the shadow of capillary action up the outside surface of a membrane fibre that has been dipped into a solution of pure water. The higher the solution climbs, the more hydrophilic the membrane fibre is and the lower the contact angle will be. The method can show a contact angle of up to 90° at which point there will be no shadow visible and a right angle will be formed between the membrane and solution surface. Greater hydrophobicity is possible, evidenced by a depression in the water surrounding the fibre, but cannot be calculated using this software.

9.4.2 Strength

Strength testing were performed with an Instron 500 (Canton, MA) tensile testing machine, housed in the Protective Clothing Research Facility of the Department of Human Ecology and shown in Figure 24. Figure 24(b) depicts the testing of a unmodified membrane fibre. A modified standard for testing polymer strands was used (ASTM D 265301). A 100 N load cell was used in conjunction with a crosshead speed of 25 mm/min, a clamp pressure of 105 kPa, and a sample length of 50 mm. For all testing, the temperature was 21°C and the relative humidity was 65%. The membrane fibre is held in the clamps by a cork spacer, and the load cell pulls the fibre in tension at a constant speed

until the fibre snaps. For each sample, the modulus of elasticity, the ultimate and yield tensile stress (N), and the elongation (mm) of the fibre was measured.

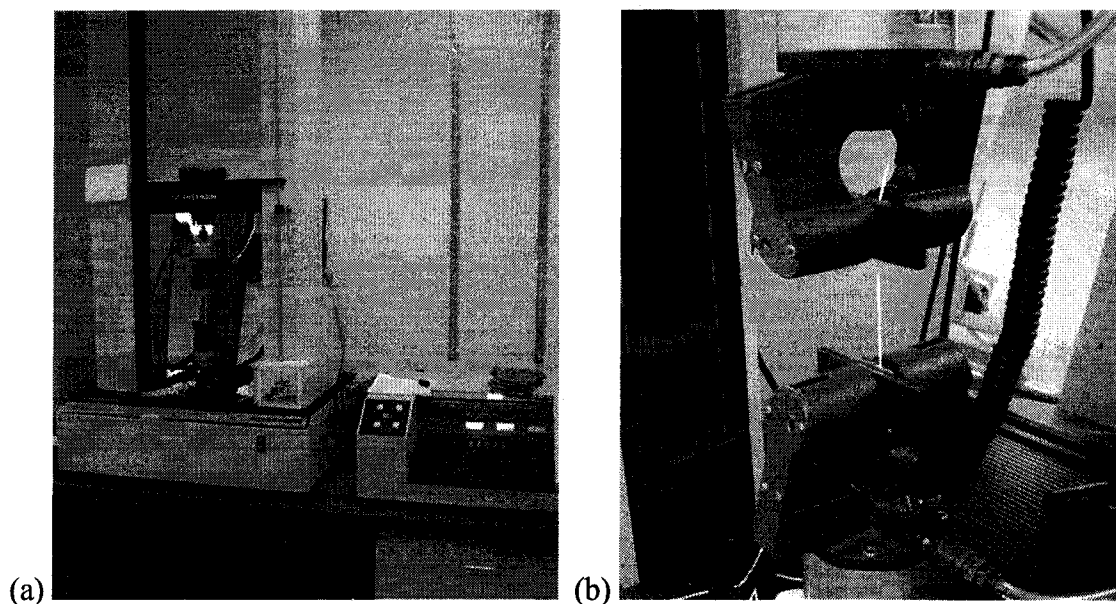


Figure 24: Instron 4202 with 50 mm section of fibre

9.4.3 Microscopy

Microscopy was completed with a Hitachi S-2500 model SEM. Samples were prepared in one of three ways: the first had the membrane fibre air dried and then cut in either a cross sectional or longitudinal section with a scalpel, the second had the fibre air dried and peeled apart into small sections with tweezers under a light microscope, and the third involved liquid nitrogen freezing. Samples were briefly immersed in water, placed in liquid nitrogen for 30 seconds, and fractioned into sections on a cold stage. These pieces were further sectioned using tweezers under a light microscope. In all cases, the prepared sections were placed onto a sample stub surfaced with a clear adhesive before getting gold sputtered by an Edwards Sputter Coater S150B. Images of the inner and outer surface edges, the entire cross section, and the exterior and interior walls were taken for the various treatments of membranes. A number of sections for each experimental and condition and fibre orientation were prepared. Each micrograph was verified with another fibre section to ensure it was representative.

9.5 Statistics

9.5.1 Factorial Design

A mixed two-level and three-level (2^23^1) full factorial statistical design was used containing a total of 12 runs. A factorial design allows for numerous factors to be investigated at different levels while maximizing the amount of information available with the chosen experimental workload. The independent impact of the selected factors as well as the interactions between all of the factors can be determined. Factorial designs offer the advantage of being simple in concept and easy to analyze (Berthouex and Brown, 2002). Both the modified and unmodified membrane fibres were tested at pH levels of 6 and 9 and chlorine concentrations of 0, 1000, and 10,000 mg/L as free chlorine shown in Table 17.

Table 17: Experimental factors and their levels

Factor	Levels
A. Membrane Type	Modified, Unmodified
B. pH	6, 9
C. Chlorine Concentration	0, 1000, 10,000 mg/L

Table 18 shows the coding used in the factorial design and the subsequent variance and regression analysis, as well as the corresponding factor levels. The ‘-’, ‘0’, and ‘+’ symbols refer to the low, middle, and high treatment levels, respectively. Analysis of variance (ANOVA), is a statistical test that compares the variability between treatments to that found within treatments. Significance of the main effects and interactions are determined by incorporating a probably distribution, usually the F or t probability distribution. The present research used a F -distribution for the ANOVA and the t -distribution for paired comparisons. Tukey’s paired comparisons were also used in some of the analysis

Assumptions were made in the execution of the ANOVA including the independence of variables, normality, and constant variance. Residual analysis was performed to ensure that the assumptions appeared correct. The statistical program SAS was used to determine significance; a confidence level of 95% was used.

Table 18: $2^3 4^1$ Fractional factorial construction

Run	Factor Levels			Coded Factors		
	A	B	C	A	B	C
1	A	6	0	-	-	-
2	B	6	0	+	-	-
3	A	9	0	-	+	-
4	B	9	0	+	+	-
5	A	6	1000	-	-	0
6	B	6	1000	+	-	0
7	A	9	1000	-	+	0
8	B	9	1000	+	+	0
9	A	6	10000	-	-	+
10	B	6	10000	+	-	+
11	A	9	10000	-	+	+
12	B	9	10000	+	+	+

9.5.2 Replication and Randomization

All of the analysis was replicated within the treatment as well as between the treatments. Every test condition in the 12-run design had a minimum of five fibre replicates with two tests per membrane fibre. The suite of 12 runs was carried out a second time to achieve between treatments replication with the same strength and hydrophobicity testing schedule used. The two suites of experimentation are hereafter referred to as 'Run 1' and 'Run 2'.

Numerous, but varied numbers of samples from both runs were used in the microscopy analysis. Sections were prepared and placed on a SEM stub from where an appropriate section was found with the SEM while looking at a number of different areas to ensure a representative sample.

Randomization was integrated as much as possible into the experimental design, preparation, and execution so as to ensure variable independence and allow the use of statistical analysis. This was carried out by

- cutting fibre from membrane spools and then randomly placed in fittings,

- constructing elements in batches and then randomly assigned treatments,
- similarly distributing free fibres for strength and hydrophobicity testing, and
- conducted analysis randomly among treatments.

9.5.3 Data Treatment

The Q-test (with 90% confidence) was performed on the hydrophobicity and strength testing to identify and remove outlying data. The Q-test is a statistical test that deals with small sample sizes and identifies potential outliers, shown in Equation [36].

$$Q_n = \frac{|x_a - x_b|}{\Delta x_{\max}} \quad 36$$

Up to 10 replicates are arranged in order and the difference between the suspected outlier and the next closest value are divided into the difference between the highest and lowest values. If the dividend is above the value indicated in the Q-test table (not included) the value is rejected. Caution must be taken in implementing this procedure so not to exclude potentially telling data points. Only one point can be eliminated from a particular data set.

10 Experimental Results

10.1 Cumulative Concentration

The cumulative exposure, or Ct, of the treatments was designed to be 1,500,000 mg·hr/L. The actual Ct for the various treatments (excluding the controls) was between 1,512,100 and 1,634,270 mg·hr/L, all above the target. Table 19 details the Ct values experienced by each of the treatments for both of the runs.

Table 19: Experienced Ct values

Run	Mem. Type	pH	[Cl ⁻] (mg/L Free)	Mean Ct Value (mg·h/L)		Chlorine Concentration Range (mg/L)	
				1	2	1	2
1	A	6	1000	1,538,831	1,523,894	817 to 1107	786 to 1143
2	B	6	1000	1,569,937	1,512,100	800 to 1270	786 to 1209
3	A	9	1000	1,557,148	1,525,610	827 to 1094	939 to 1115
4	B	9	1000	1,566,302	1,518,669	752 to 1120	871 to 1094
5	A	6	10,000	1,578,743	1,578,330	6700 to 13,200	6600 to 13,200
6	B	6	10,000	1,577,550		6600 to 13,000	
7	A	9	10,000	1,591,200	1,634,270	10,300 to 12,800	9190 to 10,500
8	B	9	10,000	1,576,800		10,100 to 12,800	

The cumulative Ct for each exposure condition is included as well as the corresponding maximum and minimum chlorine concentration experienced during the treatment. A more rapid chlorine residual decay occurred in the pH 6 treatments and consequently, the residual had to be tested and adjusted more frequently and the ranges are correspondingly larger. This effect was more severe at the higher chlorine concentration. None of the Ct values deviate from the goal of 1,500,000 mg·hr/L more than 10%, and more importantly, all of the Ct values are within 5% of their combined mean. The controls had a design Ct value of zero, but were non-zero due to the chlorine residual maintained in the treatment to prevent biological growth. The residual was kept below 1 mg/L yielding a maximum potential residual of less than 75 mg/L or 0.005% of the designed Ct for the non-controls.

The treatments were monitored at regular intervals, the length of which depended on the concentration of the chlorine in the treatment. As shown in Table 19, the chlorine concentration ranged between approximately 800 and 1200 mg/L for the 1000 mg/L treatments, and 6000 and 13,000 mg/L for the 10,000 mg/L treatments. Figure 25 and Figure 26 show the change in chlorine residual for both concentration levels at pH values of 6 and 9, corresponding to the treatments of Run 2. A chlorine residual adjustment is easily seen in the figures as a spike in concentration. Again, the greater decay experienced at pH 6 and at the 10,000 mg/L concentration levels is demonstrated. The pH, buffered with phosphate systems, remained fairly constant throughout the treatments and did not vary more than ± 0.5 . The pH 9 treatments were more stable than the pH 6 solutions and did not need to be adjusted. The remainder of the chlorine concentration profiles of the different treatments are included in Appendix F.

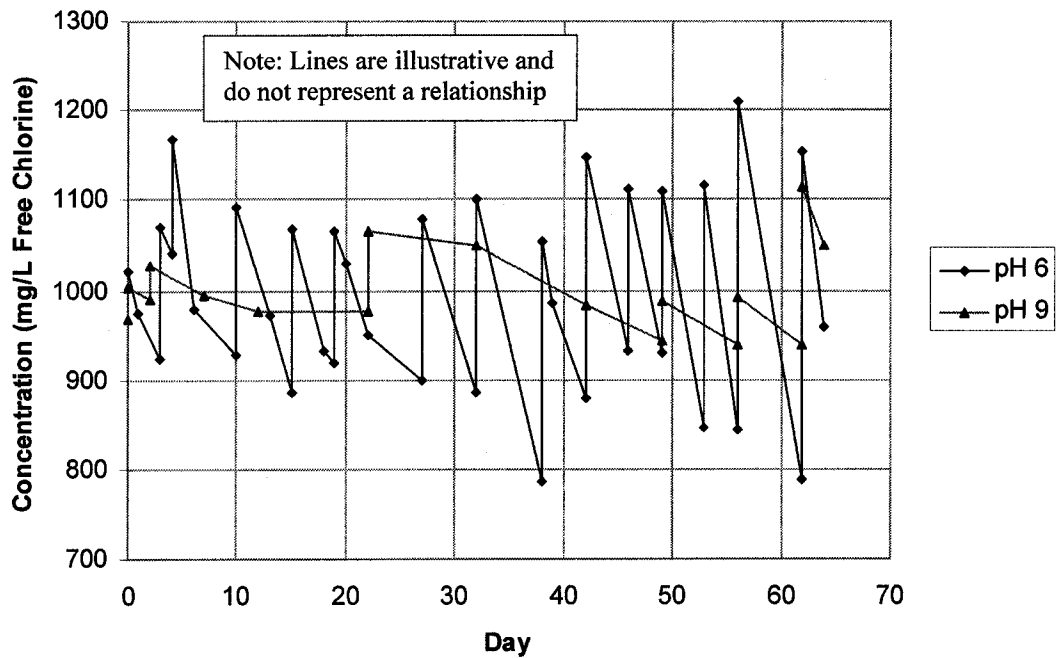


Figure 25: Cumulative exposure profile for 10,000 mg/L chlorine treatment (Run 2)

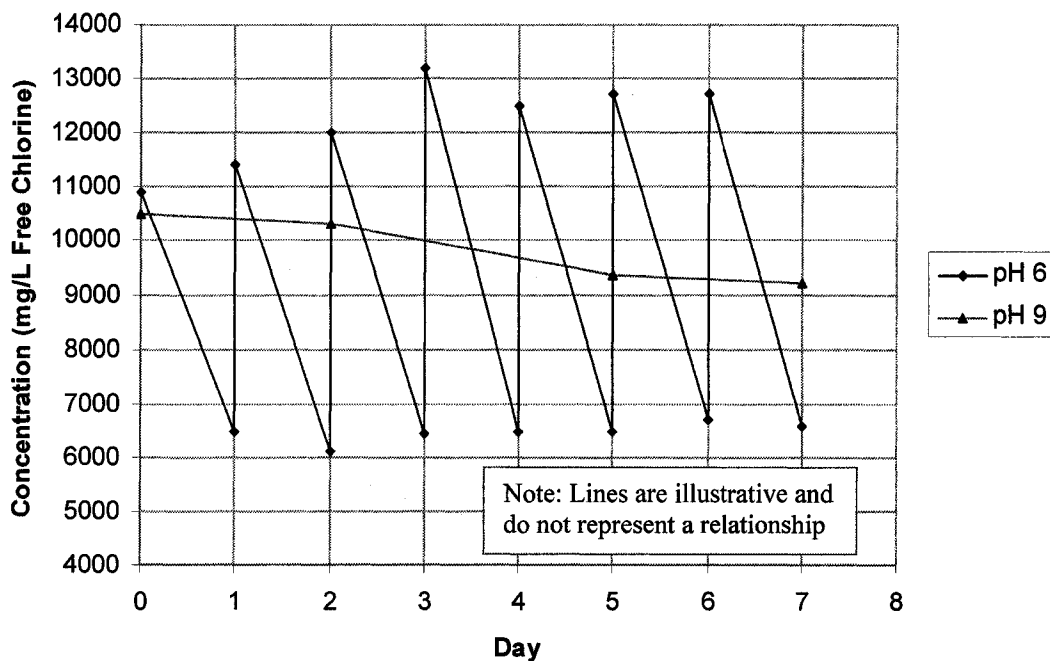


Figure 26: Cumulative exposure profile for 10,000 mg/L chlorine treatment (Run 2).

10.2 Hydrophobicity

Hydrophobicity analysis took place over several days for the first run, and in one day for the second. Advancing contact angle measurements are shown for both runs in Figure 27 and Figure 28. Concentrations are found along the x-axis with the pH and membrane type being represented by different bars. The confidence interval at 95% for each run are included as error bars on the figures. The first run shows an increase in contact angle with chlorine exposure, indicating an increase in hydrophobicity. The results of the second run are not as clear, as the 10,000 mg/L chlorine treatment appears to have a different impact than it did in Run 1. Receding angle measurements were also made, but were deemed unreliable and therefore not included.

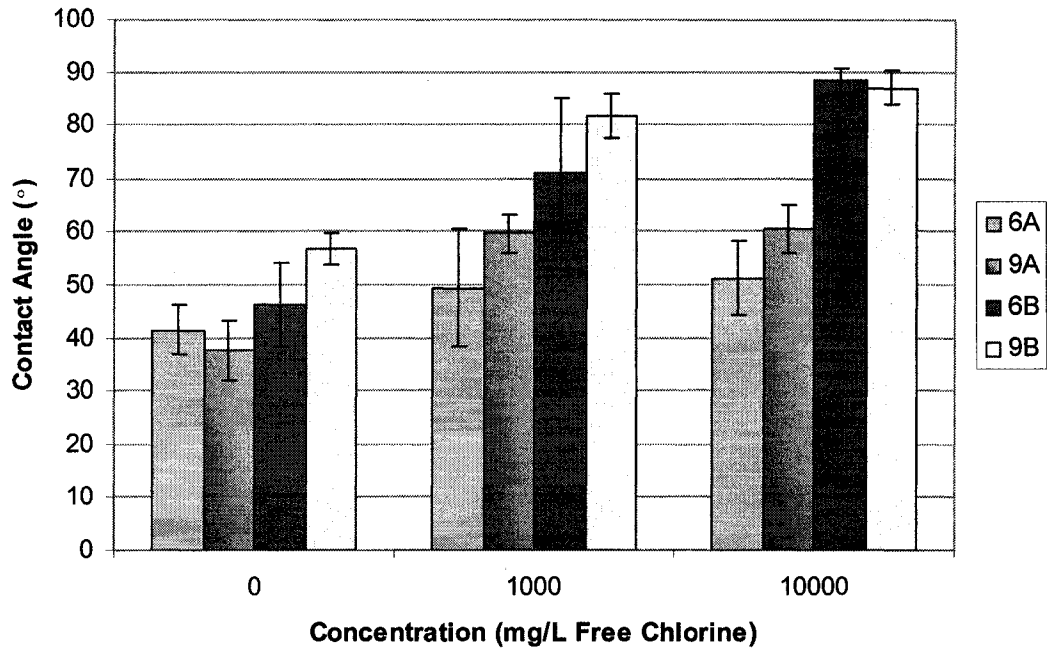


Figure 27: Advancing contact angle (Run 1)

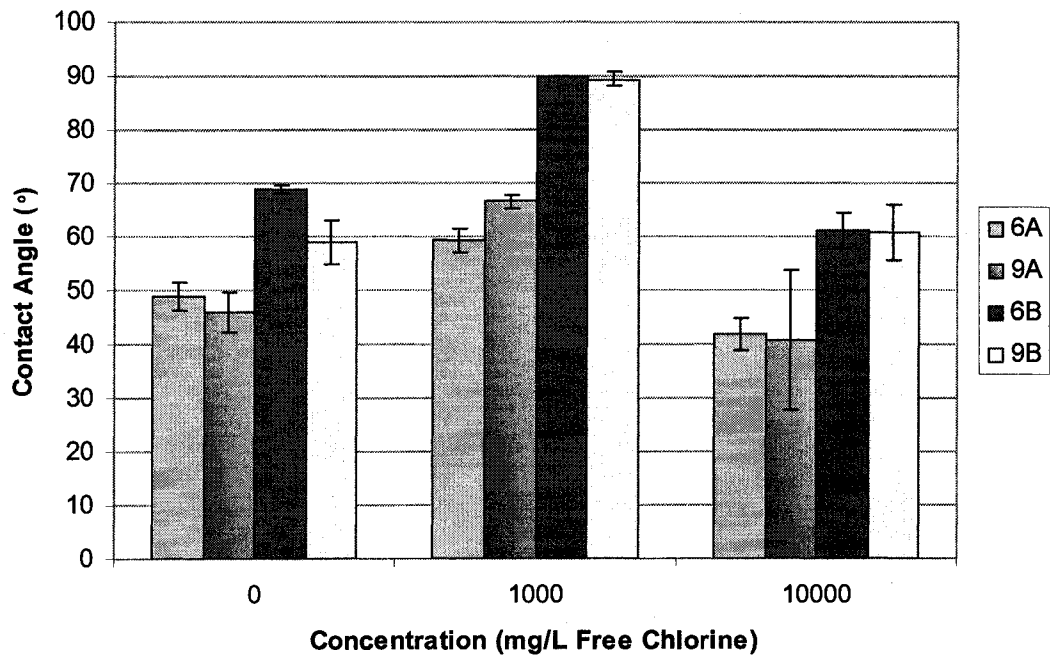


Figure 28: Advancing contact angle (Run 2)

The experimental results between Run 1 and 2 varied substantially and as a result, significance determined from the statistical analysis also varied. In Run 1, every main factor was found to be significant at a 95% confidence level, as well as all of the interactions with the exception of the pH-membrane and the pH-concentration two-way interactions. Similarly, Run 2 found all of the main effects significant at 95%, and all of the interactions with the exception of the pH-membrane two way interaction significant. Of the membrane type and pH combinations, only the pH 6, membrane B combination showed a significant increase in hydrophobicity with increasing concentration. No other trends were apparent. A summary of the determined significance is found in Table 20.

Table 20: Significance of treatments on advancing angle (at a 95% confidence level)

Treatment	Significance		p-Value	
	Run 1	Run 2	Run 1	Run 2
Membrane	Yes	Yes	< 0.0001	< 0.0001
pH	Yes	Yes	0.0318	0.0011
Concentration	Yes	Yes	< 0.0001	< 0.0001
Membrane-pH	No	No	0.2855	0.9494
pH-Concentration	No	Yes	0.0727	< 0.0001
Membrane-Concentration	Yes	Yes	0.0058	0.0002
Membrane-pH-Concentration	Yes	Yes	0.0014	< 0.0001

10.3 Strength

The parameters of displacement at ultimate yield, the modulus of elasticity, and force at ultimate yield were measured and shown for Run 2 in Figure 29, Figure 30, and Figure 31, respectively. A large difference between the two membrane types with respect to all three strength parameters was experienced. Clearly, the modification made to the fibre appears to have a larger effect on its mechanical characteristics than the treatments employed. Inconsistencies in the strength testing protocol in Run 1 made the data unreliable, and it was therefore not reported nor discussed. Although the results obtained were similar, there was substantially less confidence in the data.

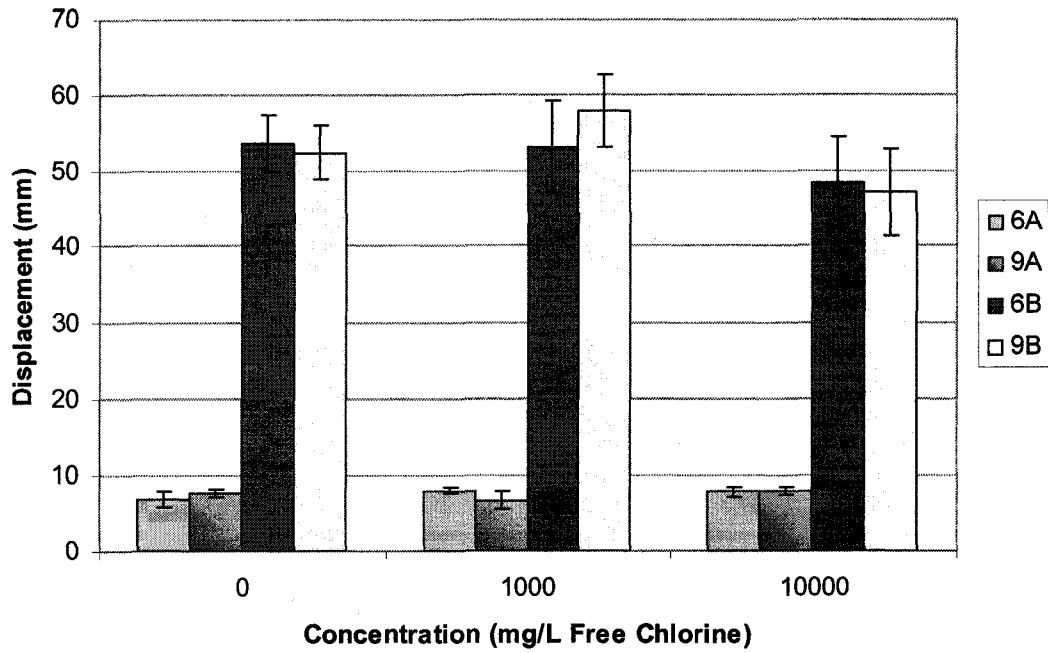


Figure 29: Displacement at ultimate yield

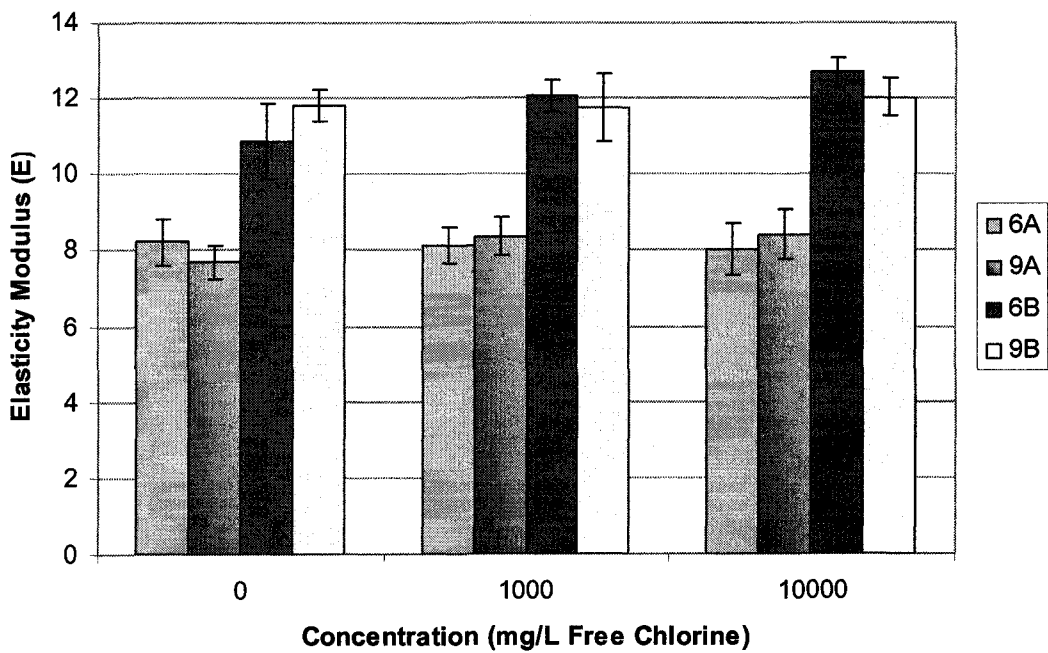


Figure 30: Modulus of elasticity

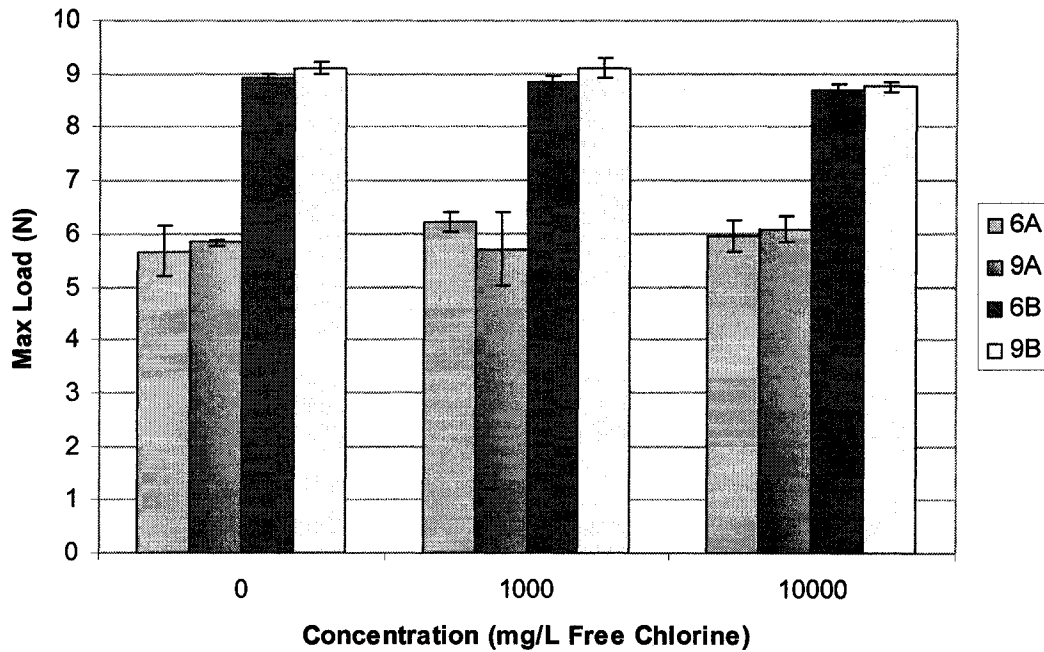


Figure 31: Tensile strength at ultimate yield

As summarized in Table 21, the membrane type was the only significant effect of every strength parameter at a 95% confidence level. Of the other main effects, concentration was found to be significant for the elasticity modulus and displacement at yield. Significance was also shown for the membrane-concentration interaction for displacement and the membrane-pH-concentration three-way interaction for the elasticity modulus.

Table 21: Significance of Run 2 strength parameters (at a 95% confidence level)

Treatment	Displacement		Ultimate Strength		Elasticity Modulus	
	Sig.	p-Value	Sig.	p-Value	Sig.	p-Value
Membrane	Yes	< 0.0001	Yes	< 0.0001	Yes	< 0.0001
pH	No	0.8010	No	0.5919	No	0.9648
Concentration	Yes	0.0300	No	0.6442	Yes	0.0184
Membrane-pH	No	0.6685	No	0.1666	No	0.9234
pH-Concentration	No	0.6429	No	0.3524	No	0.7513
Membrane-Conc.	Yes	0.0081	No	0.0520	No	0.2253
Membrane-pH-Conc.	No	0.2538	No	0.1076	Yes	0.0169

As can be seen in Figure 29, Figure 30, and Figure 31, there are very little two way comparisons that are significant outside of the membrane type. With respect to displacement, the pH plays a significant role in membrane B, but not in membrane A, and the concentration has more of an impact at a pH of 9. When looking at the modulus of elasticity for the pH 6 level, there is significance between the control and both concentrations, but not between the two concentrations. The paired comparisons demonstrate the lack of consistent trends within the results that are significant. For instance, although concentration was significant for the elasticity modulus, increasing concentration does not equate to an increasing elasticity modulus as the differences between the 1000 and 10,000 mg/L chlorine concentration exposures are not significant.

A comparison between the force at initial and ultimate yield is included in Figure 32. The yield and ultimate strengths in the modified membrane are almost identical whereas the yield strengths appear to be smaller than the ultimate strengths in the unmodified membrane. This would mean that after initial yield the unmodified membrane can withstand further application of force while the modified membrane cannot. The initial yield results were not statistically analysed and will be discussed in Section 11.2.2.

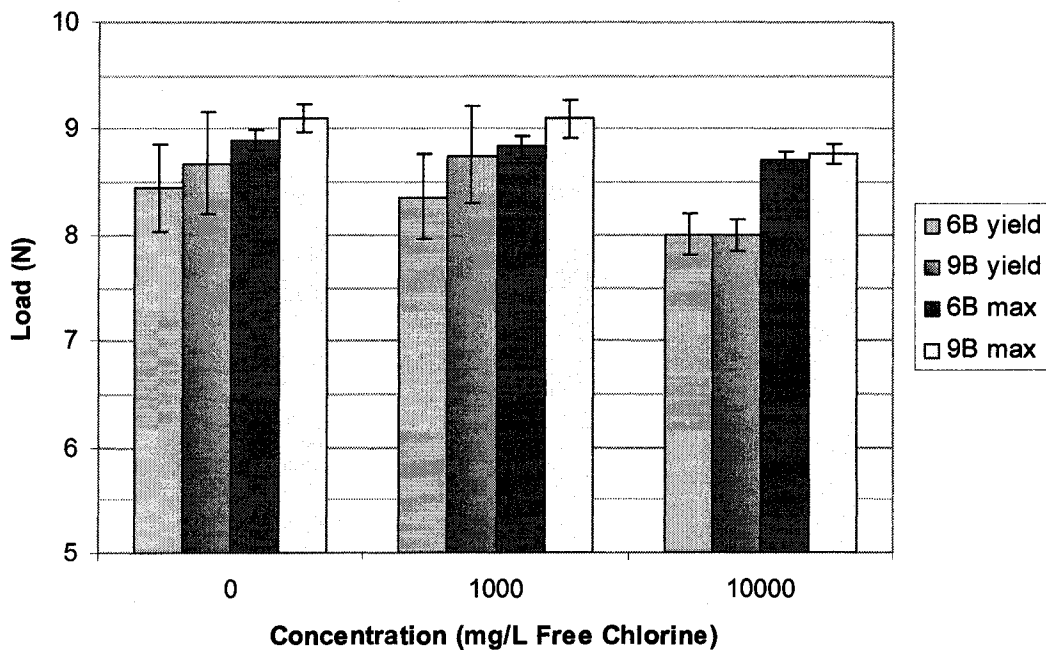


Figure 32: Yield and ultimate strength comparison

Residual analysis was performed using combinations of two level concentrations for the different strength parameters. In most cases, the data were found to be normal and randomly distributed with a few data points that were potentially outliers. The exception was the displacement at yield parameter, which was found to have non-constant variance between the two membrane types. The unmodified membrane (B) exhibited far greater variance than the modified membrane. As a result, ANOVA was subsequently carried out on the data for the two membrane types independently, resulting in a two factor factorial (pH and concentration) for each membrane type. Although displacement at yield was the only parameter that displayed non constant variance, the rest of the parameters were also included in order to see the entire picture of each membrane independent of the other. The results of this analysis are detailed in Table 22. A sample of the residual analysis including n-score plots, histograms, and residual plots is included in Appendix G using data from the significant concentration effect for the elasticity modulus between chlorine concentrations between 0 and 10,000 mg/L as well as 1000 mg/L and 10,000 mg/L of chlorine.

Table 22: Significance of Run 2 strength parameters with modified 2-level factorial for each membrane type (at a 95% confidence level)

Mem.	Treatment	Displacement		Ultimate Strength		Elasticity Modulus	
		Sig.	p-Value	Sig.	p-Value	Sig.	p-Value
A	Concentration	No	0.1674	No	0.4152	No	0.5875
	pH	No	0.5351	No	0.6551	No	0.9161
	pH-Concentration	Yes	0.0289	No	0.1938	No	0.2644
B	Concentration	Yes	0.0158	Yes	<0.0001	Yes	0.0145
	pH	No	0.7331	Yes	0.0018	No	0.9724
	pH-Concentration	No	0.4288	No	0.2374	No	0.0621

After separating the two membrane types, significance at 95% can be seen in the pH-concentration interaction for the displacement at yield parameter in the modified membrane (A). In the unmodified membrane (B), significance is shown (at 95%) for concentration in every parameter with pH significant for the ultimate strength parameter. Tukey paired comparisons were carried out on the split ANOVAs. Like the previous ANOVA, when looking at the paired comparisons there are no consistent trends where

one can say that an increase in concentration leads to an increase in ultimate yield, or an increase in pH results in greater displacement at yield. There was no significance in any of the two way comparisons for the modified membrane using Tukey comparisons.

Another way of indicating the impact of treatments on membrane characteristics is to show the relative values compared to the virgin condition. In this way, unitless comparisons can be made with a value of 1.0, or 100%, compared to the original state. For instance, a loss of strength would be indicated by a drop in relative percentage. One could look at the comparison and conclude that, due to a particular treatment, the membrane lost a certain percentage of its strength. Using this method, the relative tensile strength at ultimate yield with respect to chlorine concentration is shown in Figure 33.

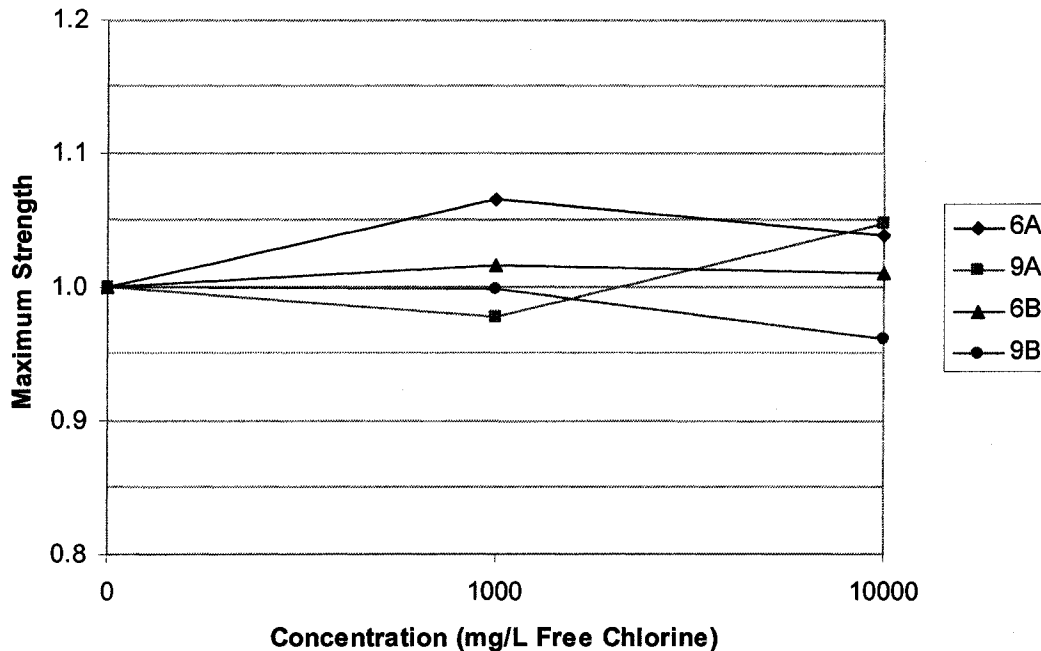


Figure 33: Relative tensile strength at ultimate yield

Because no significant change in tensile strength at ultimate yield were found for either membrane type, at either pH, and at the concentration conditions chosen, the variations from the virgin condition do not show a pattern nor significance. Similar figures for the other responding variables were not considered of value and were therefore not constructed.

10.4 Microscopy

SEM imaging was performed on hollow fibre membranes of numerous exposure conditions as well as hollow fibres that had been put in operation (pressurized and permeated from the outside to the inside) at different pressures and varying amounts of time. The results of the pressurized and unpressurized membrane investigation can be found in Section 10.5 and its discussion in Section 11.3.

The virgin, unmodified, untreated membrane is depicted in Figure 34 and Figure 35, the first displaying the (a) outside surface and (b) inside surface, and the latter showing the cross sectional areas at the (a) top surface and (b) inner surface. From the SEM images, the structure of the membrane becomes clear. There is a loose and tortuous pore structure throughout its depth with a tightening of pores at the surface. The difference between the pore sizes on the outside and inside surface is evident in the top and bottom view micrographs of Figure 34. The anisotropy is apparent in Figure 36, showing a more shallow surface layer of tighter pores over a more porous substructure. Figure 17 also shows the anisotropy of the membrane fibre. A weaker surface plane between the two layers became evident in membrane preparation. This was especially apparent in the samples that were frozen in liquid nitrogen, as the outside surface would peel off and crack in numerous locations.

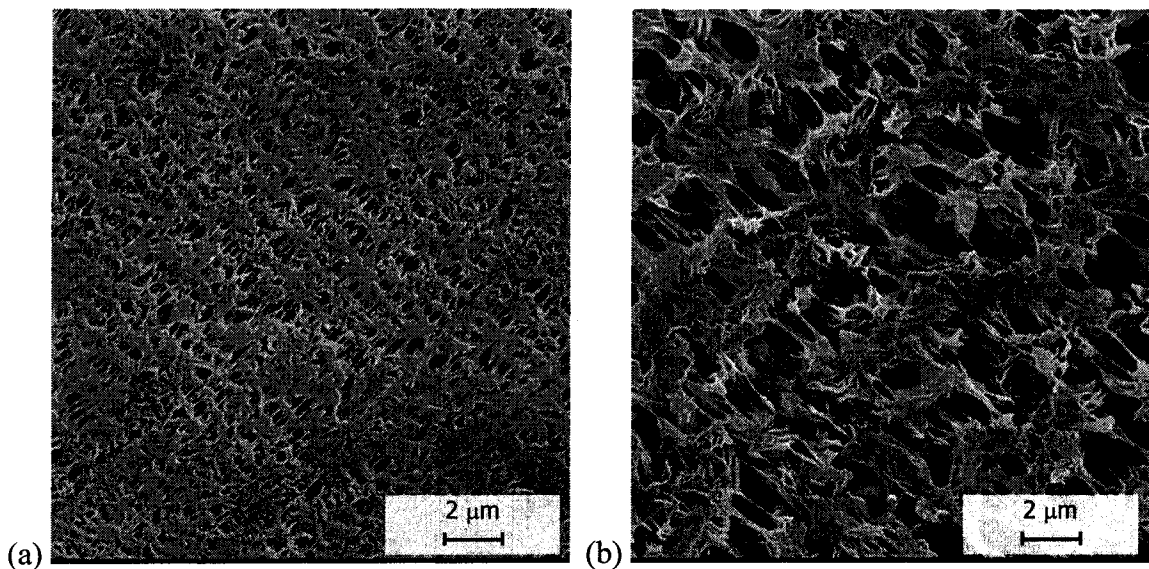


Figure 34: Virgin membrane micrograph of the (a) top surface, and (b) bottom surface

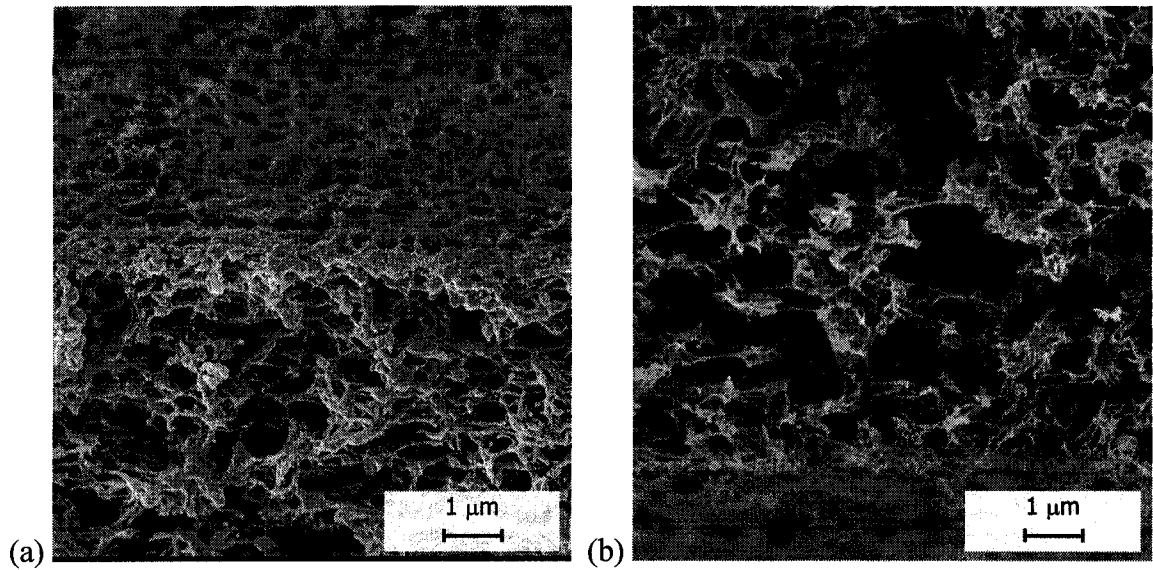


Figure 35: Virgin membrane micrograph of the (a) outer cross section (b) inner cross section

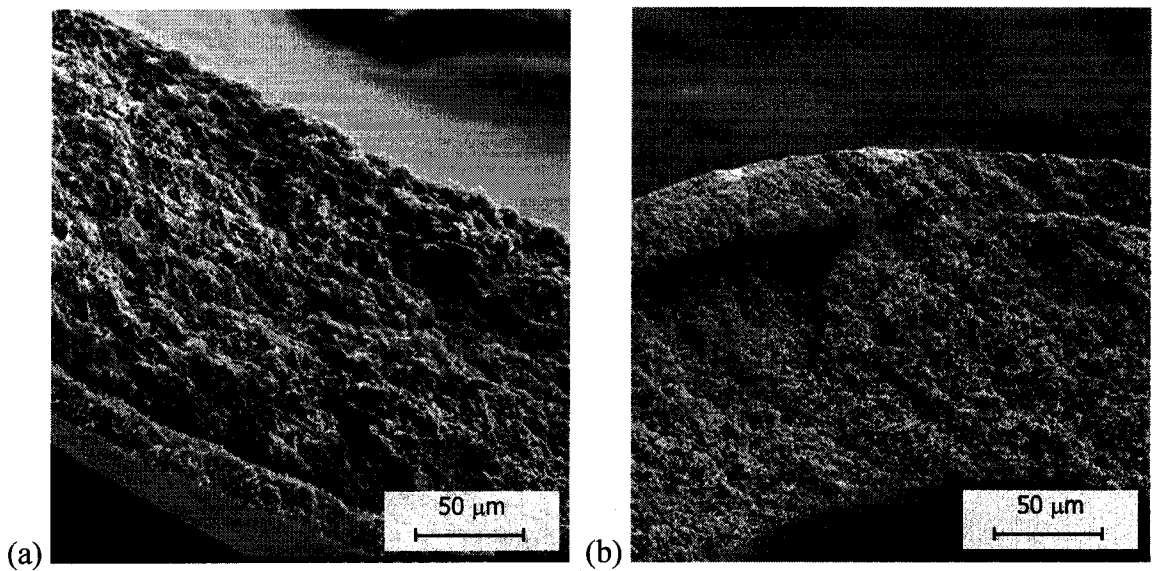


Figure 36: Anisotropic structure of membrane (a) peeled apart, and (b) dried in liquid nitrogen

SEM was unable to conclusively show any apparent differences between the two types of membranes or the exposure conditions as shown in Figure 37. Exposure to the modified membrane at different chlorine exposures is shown in Figure 37(a) and Figure 37(b) where the unmodified membrane is similarly shown in Figure 37(c) and Figure 37(d). The micrographs demonstrate exposures at a pH of 6 as it would be expected to

have a more severe effect on the polymer due to the increased oxidation potential. However, no obvious differences were found between the pH conditions and therefore the pH 9 treatment micrographs are not shown.

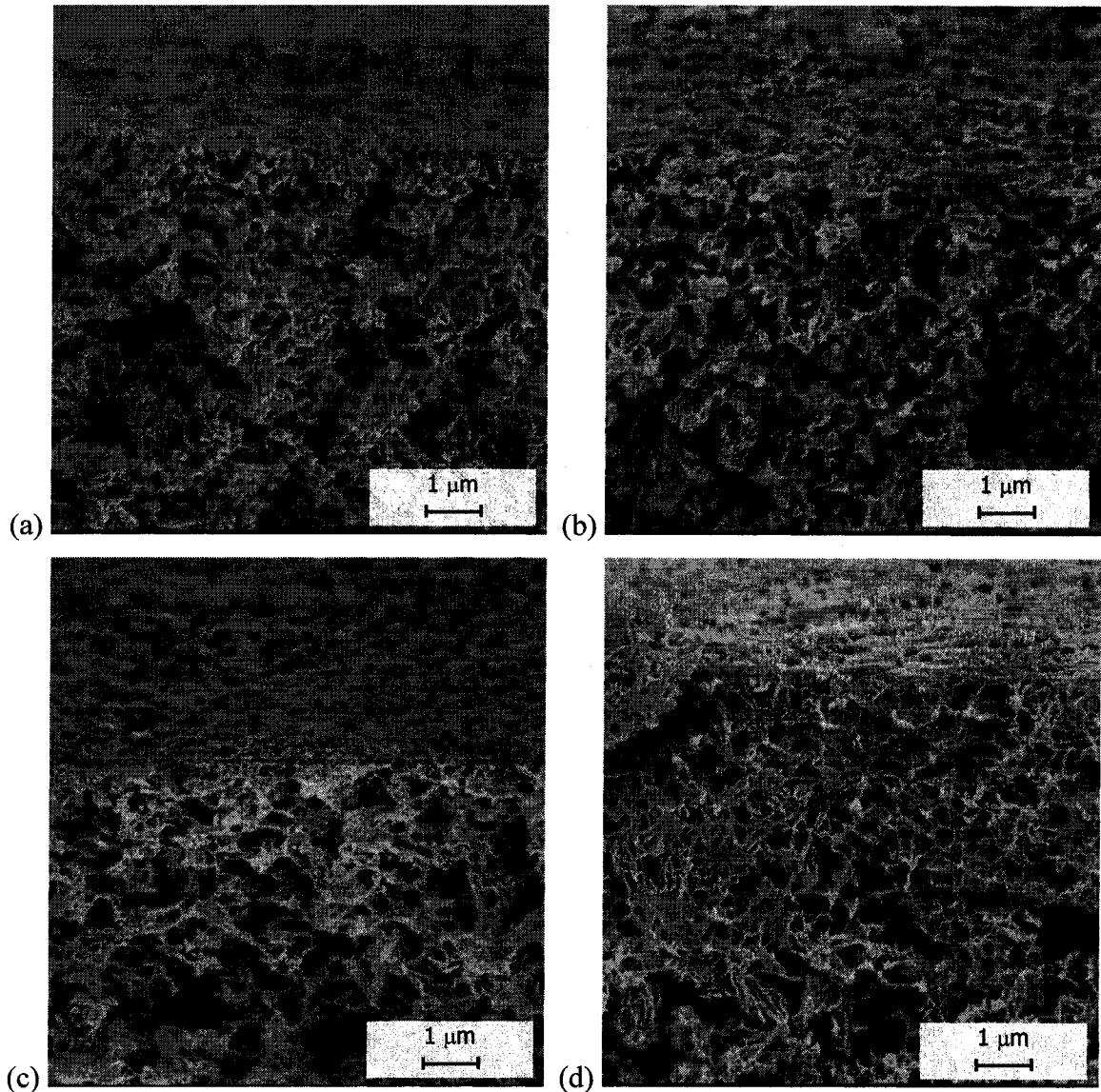


Figure 37: Outside cross section of a modified membrane exposed to a chlorine concentration of (a) 1000 mg/L, (b) 10000 mg/L, and an unmodified membrane at (c) 1000 mg/L, and (d) 10,000 mg/L, all at a pH of 6.

10.5 Membrane Problem Investigation

10.5.1 Structure

In order to explore the problems that were encountered with the membrane fibres after pressurizing, SEM analysis of the pressurized and non-pressurized fibres was performed and large differences were found. As can be seen in Figure 38 and Figure 39, the surface structure of the membrane after pressurization was dramatically altered. Both figures show the change in the outer surface structure, with Figure 38 providing a top view and Figure 39 a cross sectional view.

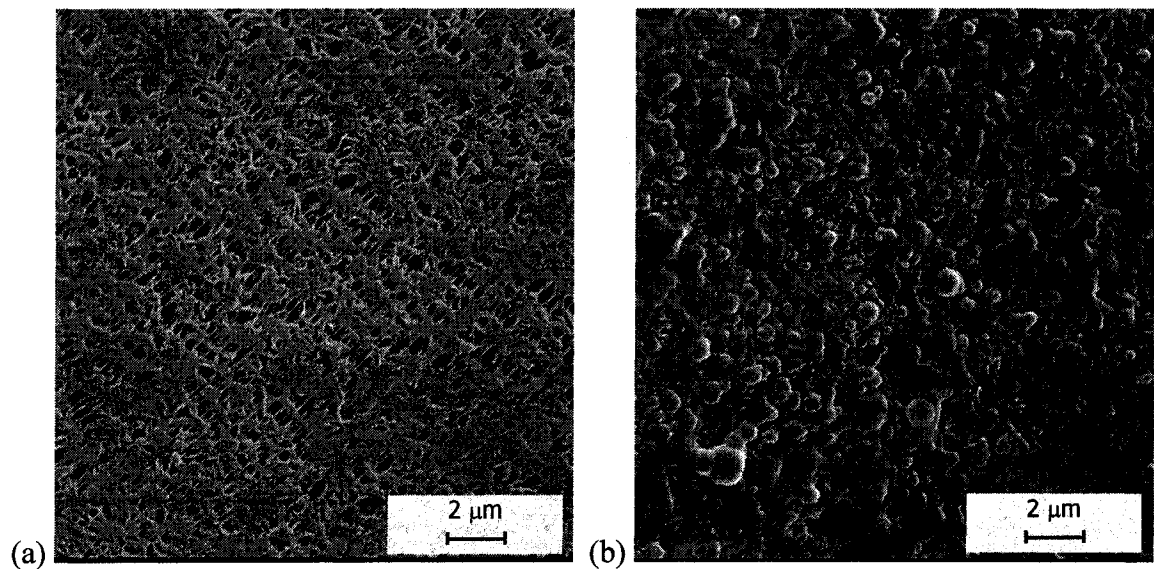


Figure 38: Top view of an unmodified (a) unpressurized membrane and (b) pressurized membrane

There appears to be a structural collapse of the pore structure or some sort of gelling effect. The surface porosity was reduced upon pressurization as pores seem to have been either covered or collapsed. Pore structure changes are especially clear on the cross sectional micrographs, although only the very top structure seems to be impacted.

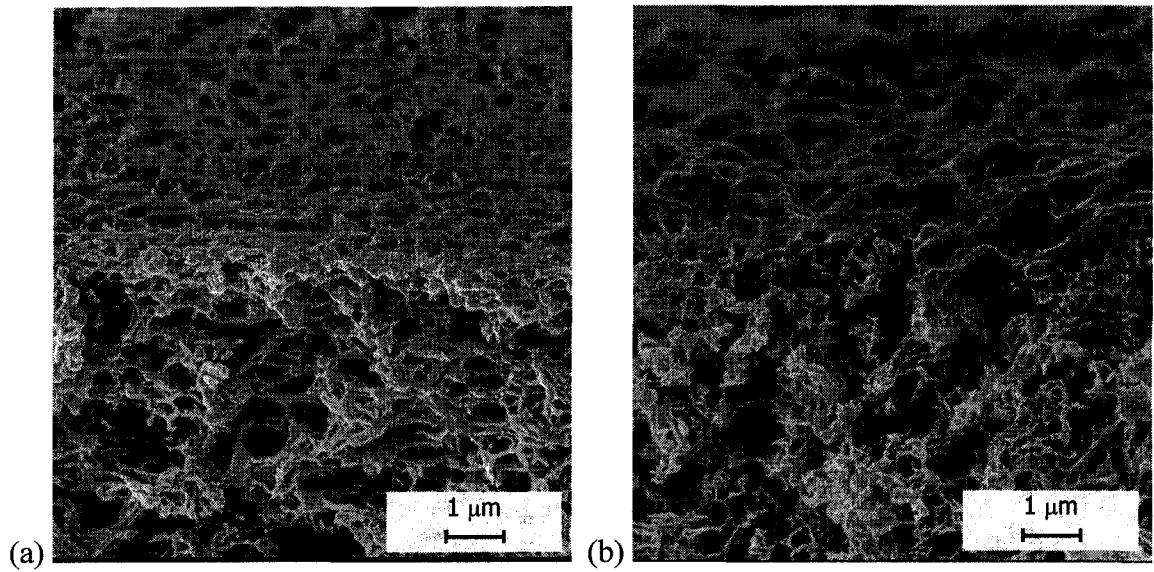


Figure 39: Cross sectional view of an unmodified (a) unpressurized membrane and (b) pressurized membrane

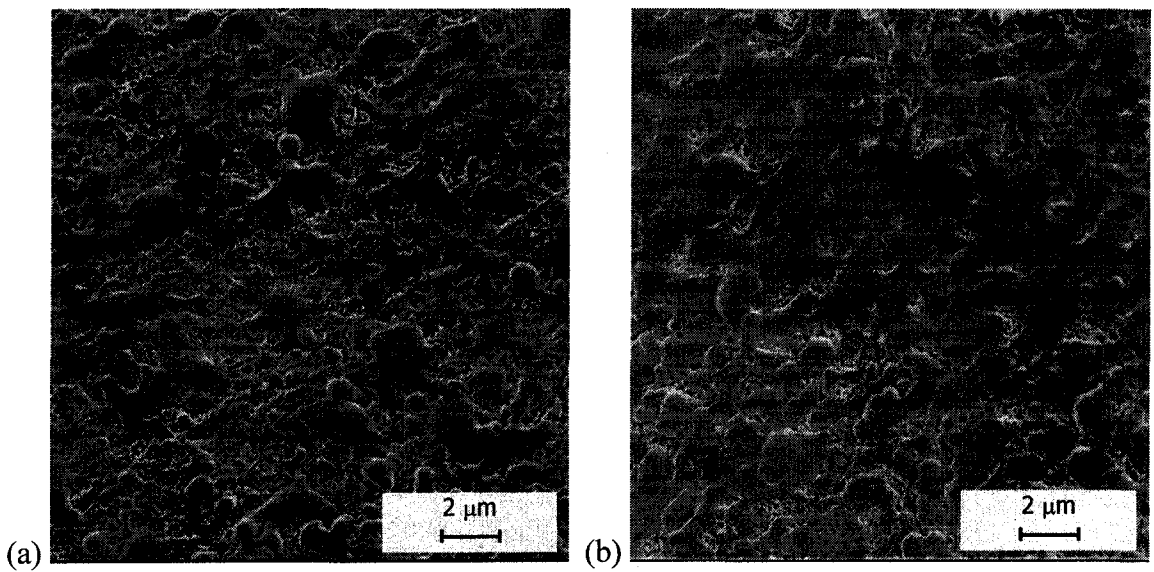


Figure 40: Top view of an unmodified progressively pressurized membrane at (a) 30 minutes and (b) 4 hours

The micrographs of Figure 40 show a progression of operational time equivalent to 30 minutes and four hours of operation at 50 kPa. In each of the pressurized cases, flux was reduced considerably over the time frame they were operated, similar to those demonstrated in Figure 41 of the preceding section. More of the pore structure that is

evident in Figure 34(a) is clear in the membrane that has been pressurized for a shorter time. The four hour pressurization appears to have almost completely covered the pore structure.

10.5.2 Hydrophobicity and Strength

Hydrophobicity and strength testing were performed after fibres were pressurized. Four untreated membranes were pressurized until flow stabilized or to a maximum of 4.5 hours. The flux loss, demonstrated by the reduction in permeation rate, is demonstrated in Figure 41. The relationships shown represent the average flux of each of the modified and unmodified membrane groups that were pressurized.

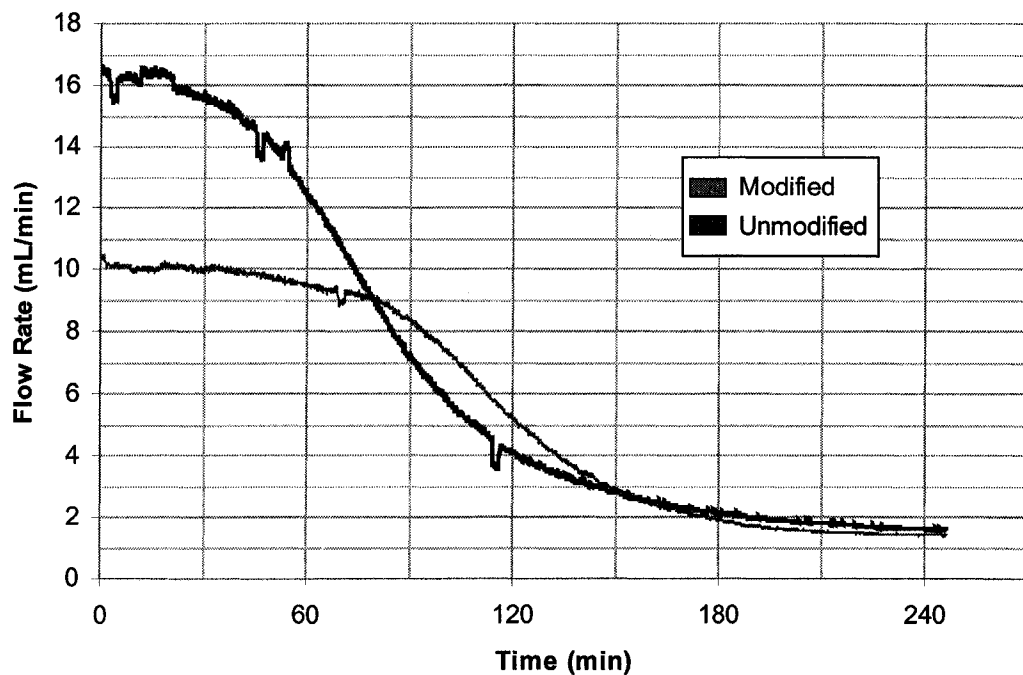


Figure 41: Flow rate reduction in pressurized modified and unmodified fibres

Although the modified membrane has a higher initial flux, it experiences flux loss more quickly and settles to approximately the same irreversible final flux as the unmodified fibre. In previous experiments and not indicated on the figure, backwashing separately with ethanol, pure water, and 500 mg/L free chlorine was unsuccessful in regaining flux. However, fluxes higher than what was achieved in the natural permeating

direction were obtained when backwashing from the inside to the outside of the fibre. This occurred even after all the flux had deteriorated to its minimum.

Of the membranes tested for hydrophobicity after pressurization, all exhibited contact angles of 90°. The hydrophobicity of the modified and unmodified controls in previous testing were variable, but all under 70°. Controls that were tested in conjunction with the pressurized membranes were found to have contact angles of approximately 20° for both membrane types. Any hydrophilicity that existed on the surface of the membrane fibres was stripped with pressurization.

Unlike hydrophobicity, strength testing on the same fibres showed no difference in any strength parameters relative to the previously tested unexposed membranes. Membranes from the Run 2 treatments were concurrently re-tested to ensure that consistency was being obtained in the experiment. All were found to be within the confidence limits of the previous testing.

11 Discussion of Results

The present research investigated the impact of free chlorine on modified (A) and unmodified (B) PVDF hollow fibre UF membranes within a Ct framework. Chlorine was chosen as a generic cleaning chemical so the potential long term impacts of cleaning in operation could be evaluated. Membrane fibres were characterized by strength and hydrophobicity testing, as well as by microscopic analysis. Initially, it was hoped to investigate the fouling potential and solute transport properties, but this was not possible due to issues that arose when pressurizing the membrane fibres. With this in mind, the objectives of the research were to:

1. identify a relationship between exposure to free chlorine and membrane performance,
2. characterize impacts of free chlorine exposure with regards to select water treatment properties as well as the difference between types of membranes, and
3. to review the existing and to develop methodologies to achieve the first two goals.

Regarding the first objective, it was clear that free chlorine had an impact on membrane characteristics, but no relationships were found. The hydrophobicity results were mixed, with repeatability proving to be challenging, but generally showed an increase in hydrophobicity with chlorine exposure. It has been well documented that increased hydrophobicity has a negative impact on fouling, particularly on fouling involving NOM. It could therefore be inferred that the increase in hydrophobicity may lead to increased fouling. Although chlorine exposure has shown to embrittle membrane fibres of other materials, the exposure to chlorine was found to have a mixed and inconclusive impact on strength properties, including brittleness. Although effective at identifying the consequence of pressurizing the membrane fibres, SEM images showed no visual differences between the treatments.

The two characterization techniques were effective at identifying the differences between the modified and unmodified fibres. As was expected, the hydrophobicity of the modified membrane was lower than that of the unmodified. Interestingly, the modified

membrane was found to be considerably more brittle and exhibit lower tensile strength and a smaller modulus of elasticity. Consequently, the modified membrane would be more susceptible to damage in operation. When looking solely at the impact of chlorine exposure, the experimental results show that long term exposure to chlorine at both exposure levels showed some impact on its hydrophobicity, but had little impact on strength characteristics demonstrating the fibre's resistance to 'aging' via oxidation.

The completion of the last objective is evidenced in Section 8 and by the protocols and worksheets on permeability, fouling propensity, and solute transport. The literature on the respective subjects was reviewed and the most appropriate methodologies were adapted for use with hollow fibre membranes. As the majority of the literature has traditionally focused on flat sheet membrane testing, the present research effectively applied the growing available research on hollow fibres and the existing information on flatsheets to assemble manageable strategies for testing. An experimental apparatus and construction techniques were developed that is capable of performing the necessary testing for the proposed methodologies in addition to being flexible so to suit other needs (vacuum filtration for example). The subsequent sections discuss the various aspects of the research program in more detail, including aspects that may have lead to experimental error.

11.1 Characterizations

Although operational characterization testing of solute transport and fouling propensity were not conducted due to the aforementioned problems experienced with the membranes, valuable information was still obtained through the hydrophobicity and strength characterization. The overall focus of the research shifted slightly as it became more of a material impact study as opposed to an overall characterization, though the material characteristics ultimately have consequences in operation.

Research that has been performed on other membrane materials, though not directly applicable to PVDF membranes, can be a starting point in both methodology development and in the understanding of the outcomes. Additionally, the present results and methods can assist in research on membranes of other materials. Most of the limited

work on the effect of chlorine on membranes in water treatment has been performed on either PS or PES membranes.

11.1.1 Hydrophobicity

The results of the hydrophobicity analysis clearly show that chlorine exposure has a large bearing on the hydrophobicity of this membrane, whether the chlorine concentration is 1000 mg/L or 10,000 mg/L. Significance at 95% is shown across both runs for all of the main effects and interactions with the exception of the membrane-pH interaction for both runs, and the pH-concentration interaction for the first run. However, the obtained significance and results in general need to be examined closer before conclusions can be made.

Although the presence of an impact of chlorine in the membrane fibres is strongly shown by the low p-values obtained in the ANOVA, the results were unclear with respect to the impact chlorine had on the membrane at the different concentrations. Chlorine exposure appeared to increase the hydrophobicity in most of the samples with the exception of the 10,000 mg/L exposure condition in the second run. The decrease in contact angle between this treatment from the controls is puzzling and likely indicates an inconsistency in either preparation or handling of the treatment condition. Differences were also demonstrated between the types of membrane fibre, where the modified membrane showed a consistently lower hydrophobicity than the unmodified membrane. This was expected as the purpose of the surface modification was to reduce the hydrophobicity of the membrane material.

The presence of two and three way interactions between most of the variables cannot be reliably determined based on the results. Rather, it appears that the nature of the measurements and the location of the variability skewed the results. There is relatively high precision within each particular treatment, but low precision between the same treatments of the two runs. It is likely that the experienced discrepancy is due to the exposure conditions across the same treatment between Run 1 and Run 2 and not to actual significance. In other words, there are large differences between similar treatment conditions that are not expressed within individual treatments. Because the individual

variance was so much lower than that between the treatments, significance is shown for virtual all main effects and interactions.

In trying to understand the discrepancies between the first and second run, it is beneficial to first examine the potential source of the variance discrepancies. These discrepancies seem to indicate that the hydrophobicity test is adequate in that it was able to identify hydrophobicity differences in a repeatable manner. But it also suggests that the membrane hydrophobicity is sensitive to conditions in addition to chlorine exposure. Other impacts could potentially include the preparation and wetting of the fibres or the handling of the fibres. For instance, the controls in the second exposure may have not been wetted to the same extent as those in the first round, resulting in higher apparent hydrophobicities. Similarly, air exposure during membrane handling could have had the same impact. The potential wetting issue is explored in Section 11.4. The large differences between the treatments and between the controls in particular could be partially attributed to these potential problems.

The receding angle was also measured and statistically analyzed. However, the receding angle determined by the capillary method with the FTA 200 was not found to be reliable. Small deviations in the speed of retraction, the location of the measurement, and the angle in which the fibre was dipped all had a substantial impact on the resulting angle. Moreover, the receding angle is far less reported in the literature and is not considered as important as the advancing angle.

There are a distinct number of conclusions that can be drawn from the experimental contact angle results. It is apparent that the hydrophobicity of the modified and unmodified membranes were significantly different. This was expected, as the purpose of the modification was to reduce its hydrophobicity and therefore improve its fouling characteristics. Secondly, it is clear that exposure to chlorine has a significant impact on hydrophobicity. However, the impact of the chlorine concentration at 1000 mg/L versus 10,000 mg/L is unclear, with the two runs showing conflicting results on which treatment has a greater impact. Very few authors have looked at the impact of oxidation on hydrophobicity. Combe et al. (1999) looked at short term oxidation of CA membranes and found a decrease in hydrophobicity.

The capillary method and the corresponding FTA 200 equipment was found to be partially successful in its contact angle application. However, there are a number of improvements and important considerations when using this methodology. The most important consideration being the consistency of measurement. The presence of surface films as well as contaminants in the immersion fluid, speed of immersion, and immersion depth all can affect the results. A depth of 3 mm was chosen because it was found through trial and error that the edge effects of the fibre no longer had an impact. Ultimately, these factors did not appear to affect results, but may have increased the variability of some of the treatments. As the capillary method of hollow fibre hydrophobicity has not been used in the literature, problems in its application are expected. Further exploration with the capillary method technique, including using fluids other than water, could identify how it could better be applied. Its ease and economy of use make it attractive as a characterization technique.

It is also useful to discuss the relationship that hydrophobicity has on fouling propensity. Hydrophobicity was chosen as a parameter of interest primarily due to its impact on fouling, and it was hoped that hydrophobicity work in addition to the fouling testing would provide a greater depth of knowledge and confirm their interrelationship, specifically in regards to NOM fouling. Although it was not possible to compare the two characteristics due to the encountered circumstances, one can still hypothesise the impact on fouling based solely on the hydrophobicity results. As the hydrophobicity increased with exposure to chlorine, it is expected that there would be an increase in fouling propensity.

11.1.2 Strength

It became apparent after characterization that the surface modification process had an influence on its strength characteristics, all of which were strongly significant at 95%. After the establishment of significance in the membrane type, each membrane type was evaluated independently of each other. This was performed after non-constant variance was discovered in the displacement data, rendering the ANOVA for that particular parameter potentially inapplicable. The other parameters were included to supplement the

original ANOVA on the full dataset. Tukey paired comparisons were used to refine the analysis on the split ANOVAs.

The modified membrane was more brittle, exhibited lower tensile strength, and had a lower modulus of elasticity. To understand what this means, it is useful to look at the approximate stress-strain relationships obtained for the two membranes, shown in Figure 42. Although not to scale, the figure shows the unitless relative differences consistently obtained between the two fibres. The stress strain curves displayed represent the relationship that was found in both the modified and unmodified membranes. Although the unmodified membrane was substantially less brittle than the modified membrane, it was found to be more rigid. The amount of elastic deformation that occurred was found to be less than that of the modified membrane, even though deformation after yield was far greater.

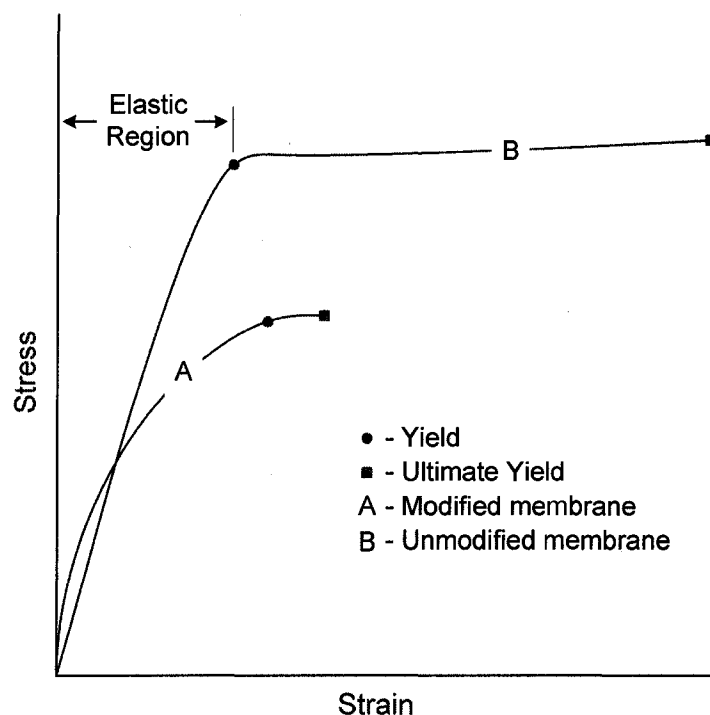


Figure 42: General stress strain relationship for the modified and unmodified membrane fibre

The actual break that occurs between the two membrane fibres is very distinct as well, evidenced in the micrographs shown in Figure 43 and Figure 44. As previously

discussed, the unmodified membrane undergoes a considerably greater deformation after yield and requires a greater force for rupture. However, it is also more rigid in the elastic region. Figure 43 shows the modified membrane fracturing across its diameter before rupture as it begins to fail as soon as stress is applied. The fracturing is also evidenced by the shape of the modified membrane curve in Figure 42. The unmodified membrane (B) has a well defined elastic region where the modified membrane (A) has more of a transitional elastic region. It has no effective rigidity or elastic deformation as there is no linear 'elastic' region indicated by a linear stress-strain relationship and from which the modulus of elasticity is calculated. The demonstrated rapid failure of the modified membrane could have substantial operational implications and merits further investigation.

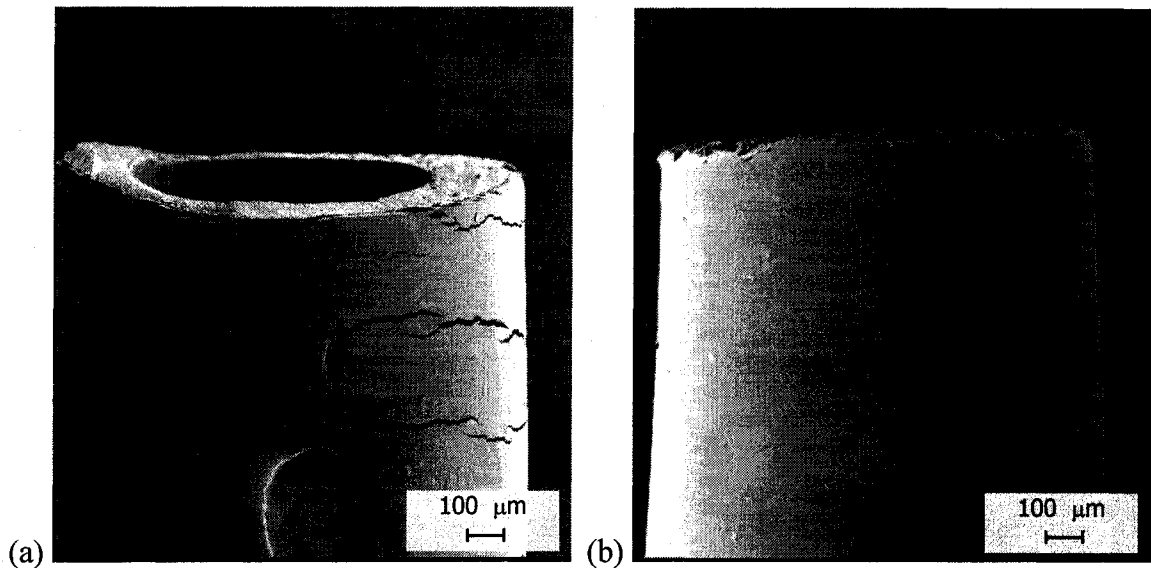


Figure 43: SEM micrographs of (a) modified, and (b) unmodified membrane rupture

A relatively clean break occurs at ultimate failure in the modified membrane when compared to the unmodified membrane. Figure 44 demonstrates the clean break with few shadows showing in the modified versus unmodified membrane. On the micrographs, the shadows represent depth and the unmodified membrane clearly demonstrates greater topographical variation across its cross section. In addition to describing the rigidity of

the modified membrane, the cracks also support the claim of greater brittleness as the membrane structure fails with the application of stress and cannot deform further.

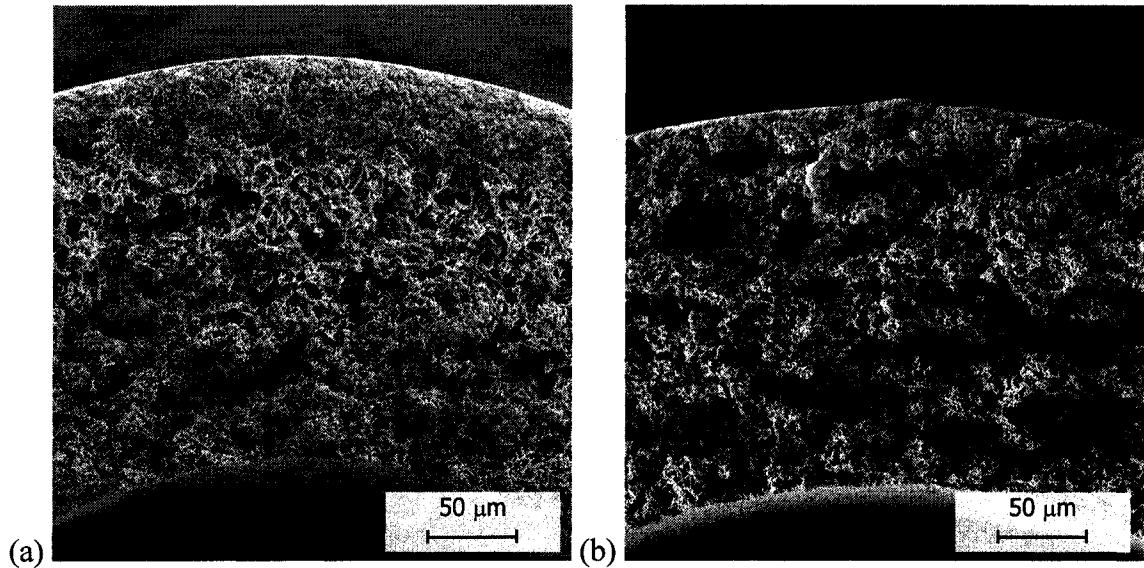


Figure 44: SEM micrographs of (a) modified, and (b) unmodified membrane rupture cross section

Although treatment significance is shown in a number of the parameters for each membrane type, most strongly for chlorine concentration, it is important not to overestimate their impacts. Looking at the paired comparisons, there are no relationships established outside of the obvious differences between the membrane types. This is especially true for the modified membrane. After the ANOVA was performed on the membrane types independently, no significance of any of the parameters was found outside of the pH-concentration interaction for the displacement at yield parameter. And when Tukey paired comparisons are made, nothing is significant at 95%. The Tukey comparisons are more strict than the paired *t*-test comparisons and were therefore employed for the strength data.

With respect to the unmodified membrane, it cannot be said that chlorine exposure embrittles, increases the modulus of elasticity, or weakens the membrane, even though there is significance at 95% in the effects. Looking at the bar graph in Figure 30 it can be seen that the only impact of either concentration or pH has is on the membrane B, pH 6

treatments. Strong significance was found between the treatments containing chlorine concentrations of 0 mg/L and 1000 mg/L, and 0 mg/L and 10,000 mg/L. Yet no relationship was found between the 1000 mg/L and 10,000 mg/L treatments. In physical terms, these results would indicate that at a pH of 6 a concentration effect was apparent for the unmodified membrane, but there was not a more severe effect at a higher concentration. With this in mind, it is difficult to come to any conclusions regarding the impact of concentration other than the fact that there was an impact, albeit a weak one. Moreover, the results also indicate that there was no Ct effect.

The results are contrary to the research published by Rouaix et al. (2006) and Gijsbertsen-Abrahamse et al. (2006), who found chlorine exposure embrittled PS membranes but did not impact its rigidity or yield strength. It is difficult to directly compare the present research to their findings because the membranes were made of a different material, and as a result, the oxidation would have a different effect. In the PS research, it was concluded that a polymer additive that was introduced in the construction process was leached out by the chlorine contact. The same additive was not present in the PVDF membranes used in the present research. Although the reported literature studied PS membranes, mechanical impacts of chlorine exposure is possible in other polymer materials (through other mechanisms) and may lead to performance concerns.

Tensile strength implications in membrane operation are intuitively not as important as those due to lateral stress because a scenario where a membrane would endure tensile stress would not occur. It therefore appears that shear stress testing would be more beneficial, as it would examine an operational reality. However, tensile testing was chosen and has been used in the literature for a number of reasons. Tensile methods are widely used resulting in existing techniques with easy replication and use equipment that is widespread and easily accessible. Moreover, tests have proven to be applicable to operational situations. Tensile tests are commonly used in material property characterization and the parameters they determine give a good indication of how a membrane material would respond to other types of stresses.

The load cell that was used has a capacity of 100 N. An ideal test has the ultimate yield occurring between 20% and 80% of the load cell's capacity. The measured ultimate yields of both types of membranes occurred below 20% capacity of the load cell, and

therefore out of the target range. Initially this was a concern, but the results were found to be adequately repeatable and were easily able to identify significance between the membrane materials. As the goal of the research was to simply identify the presence of relationships and not accurately determine the inherent membrane properties, the load cell was considered satisfactory. However, in hindsight it would appear that the greater resolution that may have been possible with a smaller load cell and may have shown greater treatment differences and provided clearer results.

11.1.3 Microscopy

Microscopy showed no visible differences between treatments, nor between the two types of membranes. At the highest magnification level used, the membrane structure of treated and non-treated membranes of both types showed no identifiable differences. Difficulty in discerning real effects from method artifacts were not possible, especially with the difficulty in obtaining similar viewing angles of the cross sections. The structure in Figure 37(d) appears to be slightly different, but this may be attributed to the angle in which the micrograph was taken or artifacts of sample preparation. Other micrographs taken, but not included, look similar to that of Figure 37(d) but were controls while other micrographs taken at the 10,000 mg/L chlorine concentration treatment level show the structure that is apparent in the other micrographs of Figure 37(a), (b), and (c). In spite of the difficulty experienced in deciphering differences (which may or may not have existed), the electron microscopy was very effective in identifying the structural changes that occurred on the membrane surface and the pore size differences between the top and bottom surfaces.

The membranes were prepared through a combination of cutting with a scalpel and liquid nitrogen freezing. The latter technique was found to improve the images over the scalpel method as the artifacts created from the physical force necessary to cut the polymer were not present. As the polymer material was soft, a sawing motion had to be used in order to cut it without collapsing the lumen. This introduced striations and compressed the pore structure along the cross section. Although largely effective in identifying the gross changes experienced, the negative impact of this technique can be clearly seen when compared to the liquid nitrogen treatment. In the nitrogen method, the

membranes are flash frozen before being shattered, allowing samples largely free of large artifacts to be obtained. It should be noted that in both methods, the membrane fibre had to be dried or partially dried first. This is not ideal, as the membrane are wet in operation and drying it may have an impact on the structure, although the fibres appeared to be unaffected by drying.

Another inherent problem with SEM analysis, is the size of the section being examined. Most of the micrographs examine an area 20 μm by 20 μm , which is hardly representative. Every effort was made to verify that what was seen in the sections produced in the micrograph were consistent with other sections of the same fibre piece. That being said, there is still a chance that a chosen section is not representative.

SEM is commonly used in characterization of membranes as indicated in the partial list included in Table 10. Research has been conducted for pore size characterization, but has been largely applied when variations in membrane manufacturing techniques are being studied. With the exception of the solute transport application and construction method characterizations, SEM often proves to be of little value. Therefore, the inability to gauge treatment differences from the micrographs was not unexpected. The impacts of surface oxidation are much smaller than those experienced in manufacturing and therefore are hard to detect. As the chemical and structural differences between the surface modified and non-surface modified membranes were unspecified by the supplier, it was unknown whether or not they would be visible.

11.2 Ct Relationship

In addition to determining whether or not there is, and what kind of impact accelerated aging using chlorine treatment has on hollow fibre membranes, an evaluation of its impact within a Ct framework was desired. More specifically, it was hoped to see if the level of chlorine exposure differs in its impact due to cumulative exposure differences. Demonstrating that chlorine does indeed have an impact on membrane characteristics is valuable, but not directly applicable to operational practice for two reasons. Chlorine has been used in membrane treatment since its inception and it has not shown to be enough of a concern for its use to be discontinued. Therefore, its impact on operational conditions is somewhat extraneous but interesting and helpful nonetheless.

Secondly, the conditions used in the research are far more severe than would normally be experienced and therefore the results are not directly applicable. However, by exploring the Ct relationship, the results can address the applicability of applying existing industry assumptions to chemical cleaning, namely the MCE values. Again, the results aren't directly applicable due to the high concentrations used, but can be used to allow for a fundamental understanding of 'shock' concentrations versus long term lower concentrations of chlorine.

Having two concentration values and a control only allows for a linear relationship to be determined. It would be advantageous to include another concentration to confirm or discard this assumption, but for the additional experimental effort involved it was not considered worthwhile and can easily be incorporated into future research. The simple identification of significant or non-significant differences in chlorine impact based on the construction of the Ct value would accomplish the goals of the present research.

An intuitive assumption regarding a potential Ct relationship is that a membrane's resistance changes based on its construction. It would be more resistance to longer term exposures at lower concentrations than short term high concentration exposures. This concept is demonstrated in Figure 7 showing an increasing Ct value resistance as the exposure time increases. Based on this premise, it would be expected that the characteristics would be more greatly effected at the higher exposure concentrations. However, there was the possibility that 1000 mg/L chlorine concentration was high enough to do damage that would not occur at lower concentrations. All this being said, little to no Ct relationship was demonstrated by the hydrophobicity or strength data and none could be detected using the SEM imagery. The results imply that free chlorine on its own does not impact membrane characteristics at the levels chosen and the types of membranes used. As the concentrations chosen were in line and higher than the cumulative exposure that membranes would be exposed to in operation, the present research suggests that higher concentrations could be used if it was thought it would improve membrane cleaning. However, chlorine was tested outside of an operational scenario and any other additional stresses.

11.3 Experienced Flux Loss

SEM analysis was effective in partially identifying the problems experienced when pressurizing the membranes when putting them into operation. Initially, the present research intended to operate the membranes and perform both the solute transport and fouling propensity methodologies described in Section 8, but this was not possible. Therefore, it was hoped the microscopy could identify some the problems experienced. As can be seen from the differences between Figure 38 and Figure 39, it was partially successful. There appears to be structural damage to the membrane surface of the pressurized membranes. From Figure 39, the change in the outside surface does not appear to be a deposit as it seems to be integrated with the polymer structure. Moreover, pure water was used in a clean module casing for a short amount of time making a deposit very unlikely. The progressive pressurization shown in Figure 40 clearly demonstrates the closing off of pores and disappearance of the underlying pore structure as the length of time increased. It is unclear how the structural change could have come about with the low pressures involved and that were well within the manufacturer's suggested range. It can only be concluded that either the membrane material was defective, or not properly structured for outside to inside operation.

The pressurization did not have an effect on strength properties, but impacted hydrophobicity. As the top surface of the membrane appeared to be affected, and only the top layer, it could be inferred that only surface properties would be effected. Looking at the micrographs showing damage incurred on the surface, such as in Figure 39(a), the damaged layer appears to be less than 0.5 μm in depth. It is reasonable to assume that only the surface property would be impacted. By making a surface less porous, its ability to absorb water would decrease thus making it more hydrophobic.

Ultimately, it is questionable whether the implications of the dramatic flux losses experienced are of value and if the reasons behind them were worth investigating. The membrane fibres appear to be defective in that they are unable to operate at the low end of their recommended pressure range in the manner in which they are intended to operate, and with pure water as a feed source. More troublesome than an inability to operate in filtration conditions that are approaching ideal, is the membrane's failure to recover flux. The microscopic work was necessary and valuable, as it provided evidence of structural

damage and eliminated the possibility, however remote, of fouling or air binding. Strength and hydrophobicity characterization held less value for the reasons just discussed, but did provide some insight into the amount of damage sustained. This could be useful in troubleshooting future membrane problems.

11.4 Experimental Error

In addition to the error associated with the hydrophobicity and strength testing already discussed, there were a number of issues that may have had a negative impact on the results. This potential problem is associated with wetting and storing the membranes, as well as that associated with the chlorine residual maintenance.

Perhaps the most considerable difficulty experienced was in the wetting of the membrane fibres. Initially, a 25% (V/V) solution of ethanol was ran through the membrane fibres from the inside to the outside in an open air container. When the membrane appeared fully saturated and after a minimum of 10 minutes, the membrane was considered wet. It was discovered after the experimental treatments, that not all of the membranes were completely wetted. This was especially true for the single fibres that were wetted in the multi-fibre element for the first run. Moreover, due to the physical contact between the membrane fibres and the pressure drops along some of the fibres, not all were wetted to the same degree. This was visually apparent and Figure 45 shows the appearance of dry spots on a fibre that had not been completely wetted. These problems first become apparent when conditioning the membranes of the second run. All of the fibres were subsequently examined and incomplete wetting was identified on a large number of the Run 1 membranes. To correct this problem, the multi-fibre elements for the second run were constructed with half the number of fibres, and consequently half the fibre density, and a 50% (V/V) ethanol solution was used. These modifications largely corrected the wetting problem experienced with the first run, but not entirely.

This problem, in addition to consistency issues with strength testing parameters such as crosshead speed, rendered the Run 1 strength data unusable. Fibres that were not entirely wet would be more brittle, more rigid, and likely take less force to yield. It also likely contributed to the inconsistencies in the hydrophobicity data. Due to the small samples used in the capillary method, a partially wet fibre would have very different and

substantially more hydrophobic results than a fully wetted fibre. That said, the hydrophobicities of the second run were generally higher than those of the first run with the exception of the treatment of 10,000 mg/L chlorine. Therefore, this may have been more of an issue in the 10,000 mg/L chlorine treatment of the first run, or some other unidentified factor played a larger role in the hydrophobicity discrepancies.

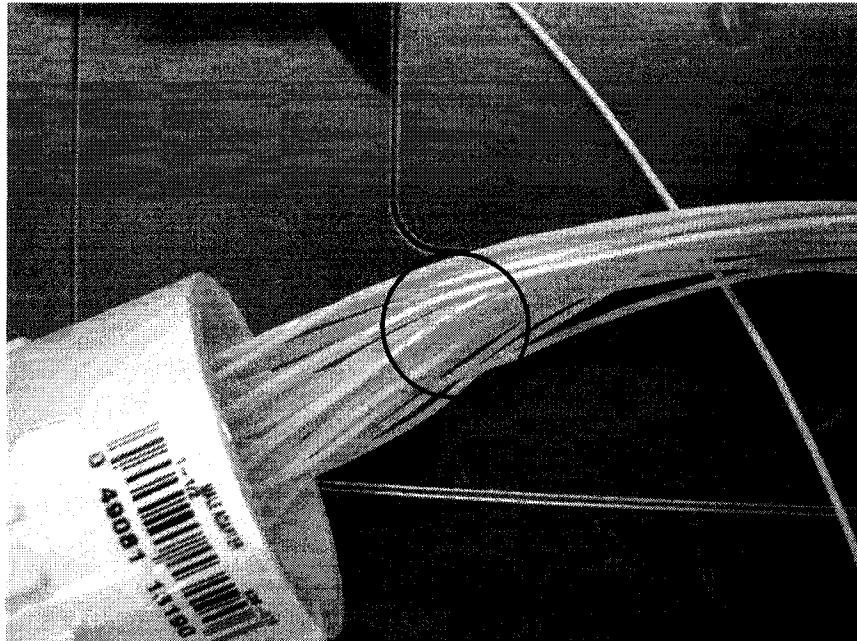


Figure 45: Appearance of an incompletely wetted membrane fibre

Membrane fibres were exposed for up to approximately two months, and in that time chlorine concentrations in the treatments had to be monitored and adjusted as necessary to maintain the proper concentration. As previously described, the concentrations were adjusted by an injection of bleach into the normally sealed treatment baths. Near the end of the second treatment run, a problem was encountered when the chlorine residual was measured not in just in one location, but in six locations in one bath and three locations in another for treatments containing a chlorine concentration of 1000 mg/L at a pH of 6. It was initially thought that adjusting the concentration in this manner would be adequate and that the baths would quickly equilibrate to create an even exposure. However, it was evident when testing the different locations one full day following an adjustment that this

was not the case. Figure 46 shows the treatment baths where the residual was measured in multiple locations.

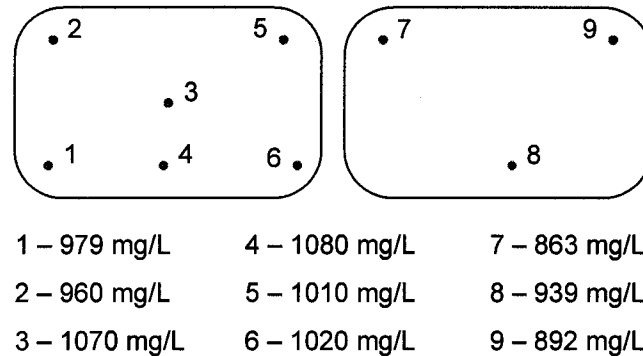


Figure 46: Distribution of chlorine residual sampling in treatments containing a concentration of 1000 mg/L at a pH of 6

The concentrations at the various spots were found to vary substantially over a fairly small localized area. In the bath on the left of Figure 46, it appears that the adjustment dose was injected close to sample location #4 and in the direction of sample location #6. As the issue was discovered near the end of the second treatment, only one sample had been taken when measuring the chlorine residual of these baths up until that point, possibly resulting in misrepresentative residuals and inaccurate Ct values. It became apparent that the chlorine solution was not equilibrating as it was assumed to be.

Fortunately, the presented problem only had a major impact on the treatment condition tested, and perhaps a smaller impact on the pH 9, 1000 mg/L chlorine concentration treatments. The pH 6 treatments of 10,000 mg/L chlorine were emptied and replenished daily and were therefore not ‘injected’ with chlorine like the pH 9 treatments of the same concentration. The concentration in the 1000 mg/L, pH 9 treatments was much more stable than the pH 6 treatments, and therefore were not adjusted as frequently and the impact would be smaller. The pH 9, 10,000 mg/L chlorine treatments were not adjusted at all. In a worst case scenario, where a concentration of 850 mg/L is considered for one section of the affected treatment bath for the entire treatment, a cumulative Ct value of approximately 1,300,000 mg·hr/L would have been obtained, 15% lower than the target. When looking at the obtained strength and hydrophobicity data for these

treatments, they do not have any greater variability than those of other treatments with the exception of the 1000 mg/L, pH 6, membrane B hydrophobicity treatment for Run 1. The Ct variability may have had an impact on this treatment, but does not look like it impacted any other treatment. Future experimentation should explore other approaches to adjustment of the chlorine residual.

Another potential problem with the experimental program, was the breakdown of the 24-hour epoxy that was used. Pre-testing was performed on the various epoxies to determine if they would withstand the chlorine concentrations used. As the buffer compositions had yet to be determined, they were tested in pure water at a natural pH but for a longer period of time than the treatments called for. Although no degradation of the polymer was experienced in the pre-tests, substantial deterioration occurred in both chlorine level exposures at a pH of 6. As a result, the membranes were partially coated in epoxy residue. However, it was apparent after characterization occurred that there was little to no detrimental affect on the samples evidenced by no difference between the pH 6 and pH 9 treatments at the 10,000 mg/L chlorine concentration where there was, and was not epoxy degradation. Nevertheless, the presence of the epoxy may have an impact on other characterization techniques and more suitable slow cure epoxy should be used.

11.5 Statistics

As previously discussed, two independent and internally replicated runs were carried out. The intent was to assess the repeatability of the procedure. Having two separate runs would also identify variable contributions such as discrepancies in chlorine concentration, pH, or other exposure conditions in addition to the variability of the membrane fibre's response to a particular treatment. Due to the large differences between the first and the second run, in part attributed to the sources of error already discussed, the two runs were treated independently and general conclusions were made based on each run separately. Any conclusions that have been drawn are mindful of the errors that were made as discussed in the previous sections.

A factorial design and the subsequent ANOVA analysis was considered the most appropriate experimental design for the chosen objectives. Not only was the experimental program simple and comprehensive, it provided a considerable amount of information for

the experimental effort that was undertaken. Within the ANOVA framework, *t*-tests were used to compare the treatments and the *p* value was used to determine significance. The Tukey multiple *t*-test was used in the split ANOVAs for the strength analysis. Its application allows paired comparisons of the different treatments using the overall error of the treatment whereas paired *t*-test comparisons only consider the two means independently (Berthouex and Brown, 2002). Where ANOVA identifies whether or not there is significance in particular factors, it does not identify between which treatments the significant difference in variance occurs. Although paired *t*-tests were employed for some of the analysis, the more strict Tukey analysis was used for the split strength ANOVAs to clarify the relationships between the various relationships.

Residual analysis was performed on selected results to check the assumptions of the ANOVA analysis. The residuals were found to be normally distributed, or close to normally distributed in all cases. From the residual plots, the variance appeared to be constant for all of the analysis with the exception of the hydrophobicity testing at the higher contact angles and the displacement at yield parameter between the two membrane types. As can be seen in Figure 27 and Figure 28, the variance was smaller at the higher contact angles. This was especially the case when the values were close to 90°. This can be largely attributed to the fact that the contact angles are only measurable up to 90° with the method used and not above. Even if the actual contact angle was 95° or 105° (where the fibre would depress the water below the surround water level), it would be recorded as 90°. This contributed to the problems experienced with the hydrophobicity testing and affirm the need for more precision at the lower contact angles. It was felt that ANOVA could handle the deviations from constant variance for the hydrophobicity testing. However, this was not the case for the displacement at yield parameter between the two membrane types. To overcome the non-constant variance and as previously discussed, ANOVAs were conducted for each membrane type independently.

11.5.1 Variance Determination

When dealing with material impacts such as those explored in the present study, the variance involved with experimentation may be comparable to that of the treatment outcomes. In other words, the variance intrinsic to the membrane and/or the methods may

envelop that of the treatments, thus taking away the ability to detect a significant impact. For instance, the impact of what section of membrane fibre or the presence of defects may have more of an effect on the experimental result than the level of chlorine that it was exposed to. Although the purpose of ANOVA is to determine whether or not there is significance, it is only as effective as its inputs and an improved experimental program would improve its output. Variance component analysis (VCA) is a technique used to identify the contributions of different experimental parameters to the overall variance.

VCA explores different levels variance and of potential replication. In the case of membrane fibre testing, variation may be introduced from three different sources: the batch of fibres that the bulk fibre is taken from, the length of fibre from which a section is cut, and from the analytical methods used. It is possible that there is substantially more variation in one of the three areas, but whether or not there is and if so, where it exists is unknown. As experimental effort is finite, choices must be made as to where replication should occur (thereby reducing the variation), and VCA can assist in these decisions. As an example, Mosqueda- Jimenez (2004) wanted to determine whether or not the variance in the findings were due to the variance from sample to sample, or from test unit to test unit. A higher variance was attributed to the membrane material, allowing for a better understanding of how to set up future experiments.

In the experimental plan carried out in the present research, it was not possible to perform this analysis based on the objectives and the available materials. This amounted to somewhat 'blind' testing, but as mentioned, the research was primarily comparative and as such, batch to batch variance was not a concern. It was infeasible to do the statistical analysis necessary to identify the variance components with the experimental effort available for the present research. Ideally, the statistical design would be carried out in two phases, the first would explore the variance implications where the second would use the information from phase 1 to design the replication schedule. In this manner, the experimental design could be optimized to reduce encountered variance. VCA analysis may have led to a better experimental design and potentially better results.

11.6 Research Significance

Any research in the area of membrane treatment, including that offered in the present research, contributes to the expanding body of knowledge on the subject. In particular, investigations into the impact of chemical cleaning on long term membrane performance better equip manufacturers and water treatment operators in their decision making. The findings of the present research, specifically the conclusions on strength and, to a lesser extent, hydrophobicity, can be widely applied to membranes of the same constitution. The methods developed for investigating select water treatment characteristics, including microscopy and those not actually experimentally employed, can be applied to future research of various membrane types. At the very least, the summary and review of many of the methods that exist in the literature is constructive.

11.6.1 Direct Implications

The results of the strength testing found no strongly significant impact of chlorine on the rigidity, brittleness, or overall strength of the membrane material tested under the exposures investigated. As the Ct value chosen represents lifetime exposure, the indifference of the membrane material demonstrates its structural resiliency to chlorine and can potentially impact the predicted lifetime of the membrane material as well as accompanying warranties.

Conversely, the demonstrated impact of chlorine on membrane hydrophobicity was largely significant. However, further study is necessary to confirm its impact due to conflicting results at the highest concentration level. If the significance is confirmed, it may show how chlorine exposure adversely affects the life time performance of the membrane material. As the concentrations experienced are far higher than those experienced in actual operation, it may not be as crucial a concern as the results indicate. Also, without collaborative and concurrent fouling studies, it is difficult to assess the impact of increased hydrophobicity. That said, the potential increase in hydrophobicity is cause for concern.

The issue encountered when pressurizing the membranes indicate substantial concern for the commercialization of the membranes in their present form. Moreover, the impact

the pressurization on hydrophobicity indicates potential operational problems if any level of similar membrane damage occurs.

The effectiveness of strength, and microscopy analysis in characterizing membrane fibres was proven or confirmed with the present research. The applicability of the capillary method of hydrophobicity determination is promising, but more work needs to be done to identify and reduce the experienced variability. SEM analysis was found to be useful, in spite of the fact that they did not provide as much information as was hoped. Similar techniques can be applied to other research in the field.

11.7 Future Research

Ultimately, it was hoped that a better understanding of long term chlorine exposure will improve how PVDF membrane systems are operated over their lifetime by a more appropriate use of chlorine, whether it be in applied concentrations or cleaning frequency. Although, for the most part, the chemical cleaning concentrations chosen to test far exceeded those that would be experienced in operation, the fibre response provided valuable information on gross impacts of chlorine on the PVDF membrane material. The results of the study are preliminary in regards to the conditions chosen, and at best offer general conclusions on the impact of long term membrane cleaning using chlorine. However, this preliminary work can be used to further develop methodologies to expand research in the area of membrane degradation in water treatment and to provide avenues for further research. Some of these avenues are discussed below.

11.7.1 Source Water and Fouling Conditions

The present study developed methods using the simplest source water and one of the simplest fouling condition. Introducing more factors may have obscured the basic information that was deemed important and skipped the fundamental first steps necessary in the development of methodologies. Once confidence in characterization methods are achieved, more complicated water matrices and fouling scenarios can be investigated as changes due to chlorine exposure will likely impact every situation differently.

11.7.2 Cleaning Regimes

Similar to increasing experimental complexity with fouling matrices, so to exists the potential to understand the impact of various cleaning regimes using the discussed methodology framed in the Ct concept. It is understood that sodium hypochlorite is not simply used on its own at the pH values of 6 and 9, but it is used in conjunction with other chemicals and at a particular pH. Researchers can use whatever combination of chemicals and pH that a particular membrane installation uses and examine the impact of that cleaning regime has on its long term membrane properties.

11.7.3 Temperature

Cold water conditions exist throughout Canada, impacting the temperature of the water entering water treatment plants. It is not feasible to adjust the temperature of the water to standard laboratory conditions and water treatment plants have to adjust accordingly. As water temperature is related to chlorine reactivity, water viscosity, and osmotic effects, it can have a significant contribution to the impact of chemical cleaning and operational characterization. It would be of value to study the impact of temperature, particularly lower temperatures have on chlorine cleaning implications.

11.7.4 Hollow Fibre Vs. Flatsheet

There has been, until recently, limited available literature and methodologies regarding hollow fibre membranes. Reasons for this were previously discussed. The ease in which flatsheet membranes can be tested give merits to their use and make them a useful surrogate for hollow fibre membranes. This has been done, and the pertinent research papers are referenced earlier. Also discussed, was the potential limitations of applying flatsheet studies to hollow fibres. There is a potential research opportunity to compare the laboratory response of flatsheet to hollow fibre membranes. Particularly suited characterization techniques could be chosen and experimentation could be run concurrently for flatsheet and hollow fibre membranes of the same material to assess the transferability of the obtained results.

11.7.5 Mechanical Stresses

Through regular operation, membranes are exposed to varying pressures, agitation, stretching, and movement. As a result, the membrane material may be physically damaged or fatigued so to impact its performance and/or its integrity over its lifetime. Currently, there is little published information in the literature exploring the consequences of these stresses. In addition to the isolated chemical impacts studied in the present research, isolated physical impacts could be explored as well as the combined impact of mechanical and chemical stresses. Examples of potential research projects include lifetime on/off pressure changes, or repetitive lateral movement or stretching. For instance, a hydrostatic head could easily be developed and an actuated valves could be opened and closed continuously to pressurize and depressurize the membrane. The fibre could be subsequently characterized in a similar manner to the membranes in the present study.

11.7.6 Characterization

In addition to SEM analysis, other characterization techniques can be used to identify structural and operational changes in treated membrane fibres. In particular, surface roughness and chemical composition can be investigated. AFM has been successfully used for surface roughness and pore property characterization. ATR-FTIR and XPS have been effectively used to characterize changes in membrane composition. Lastly, streaming potential and surface charge have been investigated in the literature. All of these techniques can be applied to membrane characterization studies and would provide additional insight into the impacts of chemical cleaning than the limited techniques applied in the present research.

12 Conclusions and Recommendations

12.1 Conclusions

The results of the present research have provided information on the impact that chlorine exposure has on PVDF hollow fibre UF membrane strength, hydrophobicity, and structure. In addition, the literature on membrane characterization techniques and cleaning was reviewed and methodologies were subsequently developed for solute transport and fouling propensity investigations. The most significant findings of the research project separated into the study areas are:

Strength

1. no Ct relationship was found using a value of 1,500,000 mg·hr/L with a maximum chlorine exposure of 10,000 mg/L for tensile strength,
2. there was little to no impact of chlorine concentration on the strength of either the surface modified or unmodified membrane,
3. the modified membrane began to fail soon after stress was applied having little to no elastic deformation,

Hydrophobicity

4. it was unclear whether or not a Ct relationship existed between chlorine exposure and hydrophobicity,
5. chlorine concentration increased the hydrophobicity of both membranes tested with the exception of the highest concentration level in the second run, likely increasing its propensity to foul,
6. the hydrophobicity of the modified membrane was found to be lower than that of the unmodified membrane,

Membrane type and structure

7. there was a distinct difference between the two types of membranes with regards to strength and hydrophobicity, but no differences between the membrane types were evident through electron microscopy under the conditions used,

8. no Ct relationship or chlorine impact on membrane structure could be conclusively discerned under the microscopy conditions used,
9. pressurizing the membrane fibres of both type and operating from the outside to inside had a major impact on their ability to operate, causing irreversible structural changes that impeded permeation, and
10. this structural change had no significant impact on their tensile strength properties, but dramatically increased their hydrophobicity.

The methodologies and equipment design show potential in this area as they have the capability to perform substantive research in an efficient and cost effective manner. Ultimately, although unable to fulfil the objectives explicitly, fundamental information about PVDF membranes was produced and groundwork was laid for future research in the hollow fibre low pressure field of membrane research in water treatment.

12.2 Recommendations

While there are numerous avenues on which to continue the present research, many of them discussed in the previous section, the following areas in particular warrant additional investigation:

1. further analysis of the failure of the modified membrane soon after the application of stress,
2. further characterization studies using the Ct framework to confirm the results of the present research, including the investigation of a non-linear relationship,
3. the implementation of the research program on membranes of varied material make-up as well as fibres that have been commercialized, and
4. a comparison between flatsheet and hollow fibre materials of the same material and pore structure using the methods described in the present research.

References

- Adham, S., K. Chiu, C. Mysore and Z. Do-Quang. Current status of worldwide MF/UF full-scale plants. 2005 Membrane Technology Conference, Phoenix, AZ.
- Aimar, P., M. Meireles and V. Sanchez. 1990. A contribution to the translation of retention curves into pore size distributions for sieving membranes. *Journal of Membrane Science*, **54**(3): 321.
- Avlonitis, S., W. T. Hanbury and T. Hodgkiess. 1992. Chlorine degradation of aromatic polyamides. *Desalination*, **85**(3): 321-334.
- AWWA. 2005. Microfiltration and ultrafiltration of membranes for drinking water - M53. American Water Works Association, Denver, CO.
- Barzin, J., C. Feng, K. C. Khulbe, T. Matsuura, C. C. Madaeni and H. Mirzadeh. 2004. Characterization of polyethersulfone hemodialysis membrane by ultrafiltration and atomic force microscopy. *Journal of Membrane Science*, **237**: 77-85.
- Batsch, A., D. Tyszler, A. Brugger, S. Panglisch and T. Melin. 2005. Foulant analysis of modified and unmodified membranes for water and wastewater treatment with LC-OCD. *Desalination*, **178**(1-3): 63-72.
- Belfort, G., R. H. Davis and A. L. Zydney. 1994. The behaviour of suspensions and macromolecular solutions in crossflow microfiltration. *Journal of Membrane Science*, **96**(1-2): 1.
- Berthouex, P. M. and L. C. Brown. 2002. Statistics for environmental engineers. CRC Press LLC, Boca Raton, FL.
- Berube, P. R. and E. Lei. 2006. The effect of hydrodynamic conditions and system configurations on the permeate flux in a submerged hollow fiber membrane system. *Journal of Membrane Science*, **271**(1-2): 29.
- Bottino, A., G. Capannelli, O. Monticelli and P. Piaggio. 2000. Poly(vinylidene fluoride) with improved functionalization for membrane production. *Journal Of Membrane Science*, **166**(1): 23-29.
- Bowen, W. R. and F. Jenner. 1995. Theoretical descriptions of membrane filtration of colloids and fine particles - an assessment and review. *Advances In Colloid And Interface Science*, **56**: 141-200.
- Boyd, R. F. and A. L. Zydney. 1997. Sieving characteristics of multilayer ultrafiltration membranes. *Journal of Membrane Science*, **131**(1-2): 155.

- Carroll, T. 2001. The effect of cake and fibre properties on flux declines in hollow-fibre microfiltration membranes. *Journal of Membrane Science*, **189**(2): 167.
- Causserand, C., P. Aimar, C. Vilani and T. Zambelli. 2002. Study of the effects of defects in ultrafiltration membranes on the water flux and the molecular weight cut-off. *Desalination*, **149**(1-3): 485-491.
- Causserand, C., S. Rouaix, A. Akbari and P. Aimar. 2004. Improvement of a method for the characterization of ultrafiltration membranes by measurements of tracers retention. *Journal of Membrane Science*, **238**(1-2): 177.
- Cha, B. J. and J. M. Yang. 2007. Preparation of poly(vinylidene fluoride) hollow fiber membranes for microfiltration using modified TIPS process. *Journal of Membrane Science*, **291**(1-2): 191.
- Chan, R. and V. Chen. 2004. Characterization of protein fouling on membranes: opportunities and challenges. *Journal of Membrane Science*, **242**(1-2): 169.
- Chang, S., A. G. Fane and T. D. Waite. 2006. Analysis of constant permeate flow filtration using dead-end hollow fiber membranes. *Journal of Membrane Science*, **268**(2): 132.
- Chen, J. P., S. L. Kim and Y. P. Ting. 2003. Optimization of membrane physical and chemical cleaning by a statistically designed approach. *Journal of Membrane Science*, **219**(1-2): 27.
- Cheryan, M. 1998. Ultrafiltration and microfiltration handbook. Technomic Pub. Co., Lancaster, PA.
- Cho, J., G. Amy and J. Pellegrino. 2000. Membrane filtration of natural organic matter: factors and mechanisms affecting rejection and flux decline with charged ultrafiltration (UF) membrane. *Journal of Membrane Science*, **164**(1-2): 89.
- Clarke, A. R. and C. N. Eberhardt. 2002. Microscopy techniques for materials science. CRC Press, Boca Raton, FL.
- Cleveland, C. T., T. F. Seacord and A. K. Zander. 2002. Standardized membrane pore size characterization by polyethylene glycol rejection. *Journal of Environmental Engineering*, **128**(5): 399-407.
- Combe, C., E. Molis, P. Lucas, R. Riley and M. M. Clark. 1999. The effect of CA membrane properties on adsorptive fouling by humic acid. *Journal of Membrane Science*, **154**(1): 73.
- Connel, G. F. 1996. The chlorination/chloramination handbook. AWWA, Denver, CO.

- Cornelissen, E. R., T. van den Boomgaard and H. Strathmann. 1998. Physicochemical aspects of polymer selection for ultrafiltration and microfiltration membranes. *Colloids and Surfaces A: Physicochemical and Engineering Aspects*, **138**(2-3): 283.
- Costa, A. R., M. N. de Pinho and M. Elimelech. 2006. Mechanisms of colloidal natural organic matter fouling in ultrafiltration. *Journal of Membrane Science*, **281**(1-2): 716.
- Cote, P., D. Mourato, C. Gungerich, J. Russell and E. Houghton. 1998. Immersed membrane filtration for the production of drinking water: Case studies. *Desalination*, **117**: 181-188.
- Dal-Cin, M. M., F. McLellan, C. N. Striez, C. M. Tam, T. A. Tweddle and A. Kumar. 1996. Membrane performance with a pulp mill effluent: Relative contributions of fouling mechanisms. *Journal of Membrane Science*, **120**(2): 273.
- Derjani-Bayeh, S. and V. G. J. Rodgers. 2002. Sieving variations due to the choice in pore size distribution model. *Journal of Membrane Science*, **209**(1): 1.
- Eaton, A. D., L. S. Clesceri and A. E. Greenberg, Eds. 2000. Standard methods for the examination of water and wastewater. Washington, APHA.
- Elimelech, M., Z. Xiaohua, A. E. Childress and H. Seungkwan. 1997. Role of membrane surface morphology in colloidal fouling of cellulose acetate and composite aromatic polyamide reverse osmosis membranes. *Journal of Membrane Science*, **127**(1): 101.
- Fan, L., J. L. Harris, F. A. Roddick and N. A. Booker. 2001. Influence of the characteristics of natural organic matter on the fouling of microfiltration membranes. *Water Research*, **35**(18): 4455.
- Fane, A. G. 2005. Module design and operation. Nanofiltration: Principles and applications. A. I. Schafer, A. G. Fane and T. D. Waite. Elsevier Advanced Technology, Oxford, UK: 68-88.
- Farahbakhsh, K., S. Adham and D. W. Smith. 2003. Monitoring the integrity of low pressure membranes. *Journal American Water Works Association*, **95**(6): 95-107.
- Farahbakhsh, K., C. Svrcek, R. K. Guest and D. W. Smith. 2004. A review of the impact of chemical pre-treatment on low pressure water treatment membranes. *Journal of Environmental Engineering and Science*, **3**(4): 237-253.
- Fiksdal, L. and T. Leiknes. 2006. The effect of coagulation with MF/UF membrane filtration for the removal of virus in drinking water. *Journal of Membrane Science*, **279**(1-2): 364.

- Fontyn, M., B. H. Bijsterbosch and K. Riet. 1987. Chemical characterization of ultrafiltration membranes by spectroscopic techniques. *Journal of Membrane Science*, **36**: 141-145.
- Fritzsche, A. K., A. R. Arevalo, A. F. Connolly, M. D. Moore, V. B. Elings and C. M. Wu. 1992a. The structure and morphology of the skin of polyethersulfone ultrafiltration membranes: A comparative atomic force microscope and scanning electron microscope study. *Journal of Applied Polymer Science*, **45**: 1945-1956.
- Fritzsche, A. K., A. R. Arevalo, M. D. Moore, V. B. Elings, K. Kjoller and C. M. Wu. 1992b. The surface structure and morphology of polyvinylidene fluoride microfiltration membranes by atomic force microscopy. *Journal of Membrane Science*, **68**(1-2): 65.
- Gabelich, C. J., J. C. Frankin, F. W. Gerringer, K. P. Ishida and I. H. Suffet. 2005. Enhanced oxidation of polyamide membranes using monochloramine and ferrous iron. *Journal of Membrane Science*, **258**(1-2): 64.
- Garcia-Aleman, J. and J. Lozier. Managing fibre breakage: LRV operations and design issues under the LT2 framework. 2005 Journal American Water Works Association Membrane Tech. Conference, Phoenix, AZ.
- Gaudichet-Maurin, E. and F. ThomINETTE. 2006. Ageing of polysulfone ultrafiltration membranes in contact with bleach solutions. *Journal of Membrane Science*, **282**(1-2): 198-204.
- Genkin, G., T. D. Waite, A. G. Fane and S. Chang. 2006. The effect of vibration and coagulant addition on the filtration performance of submerged hollow fibre membranes. *Journal of Membrane Science*, **281**(1-2): 726.
- Ghosh, R. 2006. Enhancement of membrane permeability by gas-sparging in submerged hollow fibre ultrafiltration of macromolecular solutions: Role of module design. *Journal of Membrane Science*, **274**(1-2): 73.
- Gijsbertsen-Abrahamse, A. J., E. R. Cornelissen and J. A. M. H. Hofman. 2006. Fiber failure frequency and causes of hollow fiber integrity loss. *Desalination*, **194**(1-3): 251.
- Glater, J., S.-K. Hong and M. Elimelech. 1994. The search for a chlorine-resistant reverse osmosis membrane. *Desalination*, **95**(3): 325-345.
- Gu, Y., D. Li and P. Cheng. 1997. A novel contact angle measurement technique by analysis of capillary rise profile around a cylinder (ACRPAC). *Colloids and Surfaces A: Physicochemical and Engineering Aspects*, **122**(1-3): 135.

- Howe, K. J. (2001). Effect of coagulation pretreatment on membrane filtration performance. PhD Thesis. University of Illinois, Urbana-Champaign.
- Howe, K. J. and M. M. Clark. 2002. Fouling of microfiltration and ultrafiltration membranes by natural waters. *Environmental Science and Technology*, **36**: 3571-3576.
- Iritani, E., Y. Mukai and E. Hagihara. 2002. Measurements and evaluation of concentration distributions in filter cake formed in dead-end ultrafiltration of protein solutions. *Chemical Engineering Science*, **57**(1): 53.
- Johnson, W. 2003. Automatic monitoring of membrane integrity in microfiltration systems. *Desalination*, **113**: 303-307.
- Jonsson, C. and A.-S. Jonsson. 1995. Influence of the membrane material on the adsorptive fouling of ultrafiltration membranes. *Journal of Membrane Science*, **108**(1-2): 79.
- Jucker, C. and M. M. Clark. 1994. Adsorption of aquatic humic substances on hydrophobic ultrafiltration membranes. *Journal of Membrane Science*, **97**: 37-52.
- Kaiya, Y., Y. Itoh, K. Fujita and S. Takizawa. 1996. Study on fouling materials in the membrane treatment process for potable water. *Desalination*, **106**(1-3): 71.
- Katsoufidou, K., S. G. Yiantsios and A. J. Karabelas. 2005. A study of ultrafiltration membrane fouling by humic acids and flux recovery by backwashing: Experiments and modeling. *Journal of Membrane Science*, **266**(1-2): 40.
- Khayet, M., C. Y. Feng, K. C. Khulbe and T. Matsuura. 2002a. Preparation and characterization of polyvinylidene fluoride hollow fiber membranes for ultrafiltration. *Polymer*, **43**(14): 3879.
- Khayet, M., C. Y. Feng, K. C. Khulbe and T. Matsuura. 2002b. Study on the effect of a non-solvent additive on the morphology and performance of ultrafiltration hollow-fiber membranes. *Desalination*, **148**(1-3): 321.
- Khulbe, K. C. and T. Matsuura. 2000. Characterization of synthetic membranes by Raman spectroscopy, electron spin resonance, and atomic force microscopy; a review. *Polymer*, **41**(5): 1917.
- Kilduff, J. E., S. Mattaraj, M. Y. Zhou and G. Belfort. 2005. Kinetics of membrane flux decline: The role of natural colloids and mitigation via membrane surface modification. *Journal Of Nanoparticle Research*, **7**(4-5): 525-544.
- Kim, J. and F. A. DiGiano. 2006a. Defining critical flux in submerged membranes: Influence of length-distributed flux. *Journal of Membrane Science*, **280**(1-2): 752.

- Kim, J. and F. A. DiGiano. 2006b. A two-fiber, bench-scale test of ultrafiltration (UF) for investigation of fouling rate and characteristics. *Journal of Membrane Science*, **271**(1-2): 196.
- Kim, K.-J., P. Sun, V. Chen, D. E. Wiley and A. G. Fane. 1993. The cleaning of ultrafiltration membranes fouled by protein. *Journal of Membrane Science*, **80**(1): 241.
- Kim, K. J., A. G. Fane, R. Ben Aim, M. G. Liu, G. Jonsson, I. C. Tessaro, A. P. Broek and D. Bargeman. 1994. A comparative study of techniques used for porous membrane characterization: pore characterization. *Journal of Membrane Science*, **87**(1-2): 35.
- Kim, K. J., A. G. Fane, C. J. D. Fell, T. Suzuki and M. R. Dickson. 1990. Quantitative microscopic study of surface characteristics of ultrafiltration membranes. *Journal of Membrane Science*, **54**(1-2): 89.
- Kimura, K., Y. Hane, Y. Watanabe, G. Amy and N. Ohkuma. 2004. Irreversible membrane fouling during ultrafiltration of surface water. *Water Research*, **38**: 3431-3441.
- Ko, M. K. and J. J. Pellegrino. 1992. Determination of osmotic pressure and fouling resistances and their effects on performance of ultrafiltration membranes. *Journal of Membrane Science*, **74**(1-2): 141-157.
- Koh, M., M. M. Clark and K. J. Howe. 2005. Filtration of lake natural organic matter: Adsorption capacity of a polypropylene microfilter. *Journal of Membrane Science*, **256**(1-2): 169.
- Kong, J. and K. Li. 2001. An improved gas permeation method for characterising and predicting the performance of microporous asymmetric hollow fibre membranes used in gas absorption. *Journal of Membrane Science*, **182**(1-2): 271.
- Kuzmenko, D., E. Arkhangelsky, S. Belfer, V. Freger and V. Gitis. 2005. Chemical cleaning of UF membranes fouled by BSA. *Desalination*, **179**(1-3): 323.
- Kwon, Y.-N. and J. O. Leckie. 2006. Hypochlorite degradation of crosslinked polyamide membranes: I. Changes in chemical/morphological properties. *Journal of Membrane Science*, **283**(1-2): 21.
- Laine, J. M., C. Campose, I. Baudin and M. L. Janex. 2003. Understanding membrane fouling: A review of over a decade of research. *Water Science and Technology*, **3**(5-6): 155-164.
- Laine, J. M., D. Vial and P. Moulart. 2000. Status after 10 years of operation -- overview of UF technology today. *Desalination*, **131**(1-3): 17.

- Latt, K. K. and T. Kobayashi. 2006. Ultrasound-membrane hybrid processes for enhancement of filtration properties. *Ultrasonics Sonochemistry*, **13**(4): 321.
- Lee, N., G. Amy, J.-P. Croue and H. Buisson. 2004. Identification and understanding of fouling in low-pressure membrane (MF/UF) filtration by natural organic matter (NOM). *Water Research*, **38**(20): 4511.
- Lee, N., G. Amy and J. Lozier. 2005. Understanding natural organic matter fouling in low-pressure membrane filtration. *Desalination*, **178**(1-3): 85.
- Li, Q. and M. Elimelech. 2004. Organic Fouling and Chemical Cleaning of Nanofiltration Membranes: Measurements and Mechanisms. *Environmental Science and Technology*, **38**(17): 4683-4693.
- Liikanen, R., J. Yli-Kuivila and R. Laukkanen. 2002. Efficiency of various chemical cleanings for nanofiltration membrane fouled by conventionally-treated surface water. *Journal of Membrane Science*, **195**(2): 265.
- Lin, C. F., C. H. Wu and S. W. Kuo. 2005. Temporal evolution of resistances in the ultrafiltration of humic substances. *Desalination*, **172**(2): 99-106.
- Lindau, J. and A. S. Jonsson. 1999. Adsorptive fouling of modified and unmodified commercial polymeric ultrafiltration membranes. *Journal of Membrane Science*, **160**(1): 65.
- Liu, C., S. Caothien, J. Hayes and T. Caothuy (2004). Membrane chemical cleaning: From art to science. Pall Corporation.
- Liu, T., S. Xu, D. Zhang, S. Sourirajan and T. Matsuura. 1991. Pore size and pore size distribution on the surface of polyethersulfone hollow fiber membranes. *Desalination*, **85**(1): 1.
- Martinez, J. 2005. Advantages of pressure MF systems over vacuum systems. *Membrane Technology (not peer reviewed)*, **2**(1).
- Meireles, M., A. Bessieres, I. Rogissart, P. Aimar and V. Sanchez. 1995. An appropriate molecular size parameter for porous membranes calibration. *Journal of Membrane Science*, **103**(1-2): 105.
- Metcalf and Eddy. 2003. Wastewater engineering: Treatment and reuse. McGraw Hill, Toronto, ON.
- Mohammadi, T. and A. Esmaelifar. 2004. Wastewater treatment using ultrafiltration at a vegetable oil factory. *Desalination*, **166**: 329.

- Mosqueda-Jimenez, D. B., R. M. Narbaitz and T. Matsuura. 2004. Membrane fouling test: Apparatus evaluation. *Journal of Environmental Engineering*, **130**(1): 90-99.
- Munoz-Aguado, M. J., D. E. Wiley and A. G. Fane. 1996. Enzymatic and detergent cleaning of a polysulfone ultrafiltration membrane fouled with BSA and whey. *Journal of Membrane Science*, **117**(1-2): 175.
- Nabetani, H., M. Nakajima, A. Watanabe, S. Nakao and S. Kimura. 1990. Effects of osmotic pressure and adsorption on ultrafiltration of ovalbumin. *AIChE Journal*, **36**(6): 907-915.
- Nakao, S. 1994. Determination of pore size and pore size distribution: 3. Filtration membranes. *Journal of Membrane Science*, **96**(1-2): 131.
- Nakao, S. and S. Kimura. 1981. Analysis of solutes rejection in ultrafiltration. *Journal of Chemical Engineering of Japan*, **14**(1).
- Nghiem, L. D. and A. I. Schafer. 2006. Fouling autopsy of hollow-fibre MF membranes in wastewater reclamation. *Desalination*, **188**(1-3): 113.
- Nobrega, R., H. De Balmann, P. Aimar and V. Sanchez. 1989. Transfer of dextran through ultrafiltration membranes: a study of rejection data analysed by gel permeation chromatography. *Journal of Membrane Science*, **45**(1-2): 17.
- Oldani, M. and G. Schock. 1989. Characterization of ultrafiltration membranes by infrared spectroscopy, ESCA, and contact angle measurements. *Journal of Membrane Science*, **43**(2-3): 243.
- Oschmann, N., L. D. Nghiem and A. I. Schafer. 2005. Fouling mechanisms of submerged ultrafiltration membranes in greywater recycling. *Desalination*, **179**(1-3): 215.
- Park, N., B. Kwon, M. Sun, H. Ahn, C. Kim, C. Kwoak, D. Lee, S. Chae, H. Hyung and J. Cho. 2005. Application of various membranes to remove NOM typically occurring in Korea with respect to DBP, AOC and transport parameters. *Desalination*, **178**(1-3): 161.
- Peng, W., I. C. Escobar and D. B. White. 2004. Effects of water chemistries and properties of membrane on the performance and fouling--a model development study. *Journal of Membrane Science*, **238**(1-2): 33-46.
- Platt, S., M. Mauramo, S. Butylina and M. Nystrom. 2002. Retention of PEGs in cross-flow ultrafiltration through membranes. *Desalination*, **149**(1-3): 417.
- Pontie, M., L. Durand-Bourlier, D. Lemordant and J. M. Laine. 1998. Control fouling and cleaning procedures of UF membranes by a streaming potential method. *Separation and Purification Technology*, **14**(1-3): 1.

- Pradanos, P., J. I. Arribas and A. Hernandez. 1995. Mass transfer coefficient and retention of PEGs in low pressure cross-flow ultrafiltration through asymmetric membranes. *Journal of Membrane Science*, **99**(1): 1.
- Qin, J.-J., Y.-M. Cao and Y. Li. 2005. Effect of hypochlorite concentration on properties of posttreated outer-skin ultrafiltration membranes spun from cellulose acetate/poly(vinyl pyrrolidone) blends. *Journal of Applied Polymer Science*, **97**(1): 227-231.
- Qin, J. and T.-S. Chung. 1999. Effect of dope flow rate on the morphology, separation performance, thermal and mechanical properties of ultrafiltration hollow fibre membranes. *Journal of Membrane Science*, **157**(1): 35.
- Rana, D., T. Matsuura, R. M. Narbaitz and C. Feng. 2005. Development and characterization of novel hydrophilic surface modifying macromolecule for polymeric membranes. *Journal of Membrane Science*, **249**(1-2): 103.
- Ren, J., Z. Li and F.-S. Wong. 2006. A new method for the prediction of pore size distribution and MWCO of ultrafiltration membranes. *Journal of Membrane Science*, **279**(1-2): 558.
- Rouaix, S., C. Causserand and P. Aimar. 2006. Experimental study of the effects of hypochlorite on polysulfone membrane properties. *Journal of Membrane Science*, **277**(1-2): 137.
- Sablani, S. S., M. F. A. Goosen, R. Al-Belushi and M. Wilf. 2001. Concentration polarization in ultrafiltration and reverse osmosis: a critical review. *Desalination*, **141**(3): 269.
- Saravia, F., C. Zwiener and F. H. Frimmel. 2006. Interactions between membrane surface, dissolved organic substances and ions in submerged membrane filtration. *Desalination*, **192**(1-3): 280.
- Schafer, A. I., N. Andritsos, A. J. Karabelas, E. Hoek, R. Schneider and M. Nystrom. 2005. Fouling in nanofiltration. In *Nanofiltration: Principles and applications*. A. I. Schafer, A. G. Fane and T. D. Waite. Elsevier Advanced Technology, Oxford, UK.
- Schafer, A. I., U. Schwicker, M. M. Fischer, A. G. Fane and T. D. Waite. 2000. Microfiltration of colloids and natural organic matter. *Journal of Membrane Science*, **171**(2): 151.
- Schlichter, B., V. Mavrov and H. Chmiel. 2000. Comparative characterisation of different commercial UF membranes for drinking water production. *Journal of Water Supply: Research and Technology*, **49**(6): 321-328.

- Sheldon, J. M. 1991. The fine-structure of ultrafiltration membranes. I. Clean membranes. *Journal of Membrane Science*, **62**(1): 75-86.
- Shon, H. K., S. Vigneswaran, I. S. Kim, J. W. Cho and H. H. Ngo. 2004. Effect of pretreatment on the fouling of membranes: application in biologically treated sewage effluent. *Journal of Membrane Science*, **234**: 111-120.
- Singh, S., K. C. Khulbe, T. Matsuura and P. Ramamurthy. 1998. Membrane characterization by solute transport and atomic force microscopy. *Journal of Membrane Science*, **142**(1): 111.
- Smith, S. R., R. W. Field and Z. F. Cui. 2006. Predicting the performance of gas-sparged and non-gas-sparged ultrafiltration. *Desalination*, **191**(1-3): 376.
- Smolders, C. A. and E. Vugteveen. 1985. New characterization methods for asymmetric ultrafiltration membranes. *Materials Science of Synthetic Membranes*: 327-338.
- Song, W., V. Ravindran, B. E. Koel and M. Pirbazari. 2004. Nanofiltration of natural organic matter with H₂O₂/UV pretreatment: fouling mitigation and membrane surface characterization. *Journal of Membrane Science*, **241**(1): 143.
- Sundaramoorthy, K., A. Brugger, S. Panglisch, A. Lerch and R. Gimbel. 2005. Studies on the minimisation of NOM fouling of MF/UF membranes with the help of a submerged "single" capillary membrane apparatus. *Desalination*, **179**(1-3): 355-367.
- Tam, C. M. and A. Y. Tremblay. 1991. Membrane pore characterization--comparison between single and multicomponent solute probe techniques. *Journal of Membrane Science*, **57**(2-3): 271.
- Tan, X., S. P. Tan, W. K. Teo and K. Li. 2006. Polyvinylidene fluoride (PVDF) hollow fibre membranes for ammonia removal from water. *Journal of Membrane Science*, **271**(1-2): 59.
- Tarabara, V., R. Hovinga and M. R. Wiesner. 2002. Constant transmembrane pressure vs. constant permeate flux: effect of particle size on crossflow membrane filtration. *Environmental Engineering Science*, **19**(6): 343-355.
- Thominette, F., O. Farnault, E. Gaudichet-Maurin, C. Machinal and J.-C. Schrotter. 2006. Ageing of polyethersulfone ultrafiltration membranes in hypochlorite treatment. *Desalination*, **200**(1-3): 7.
- Tiller, C. L. and C. R. O'Melia. 1993. Natural organic matter and colloidal stability: Models and measurements. *Colloids and Surfaces A: Physicochemical and Engineering Aspects*, **73**: 89.

- Tu, S.-C., V. Ravindran and M. Pirbazari. 2005. A pore diffusion transport model for forecasting the performance of membrane processes. *Journal of Membrane Science*, **265**(1-2): 29.
- USEPA (2005). Membrane filtration guidance manual. Office of Ground Water and Drinking Water. United States Environmental Protection Agency, Washington, DC.
- Vaisanen, P., M. R. Bird and M. Nystrom. 2002. Treatment of UF membranes with simple and formulated cleaning agents. *Food and Bioproducts Processing*, **80**(C2): 98-108.
- Vickers, J. C., M. A. Thompson and U. G. Kelkar. 1995. The use of membrane filtration in conjunction with coagulation processes for improved NOM removal. *Desalination*, **102**(1-3): 57-61.
- Vos, K. D., I. Nusbaum, A. P. Hatcher and F. O. Burris. 1968. Storage, disinfection, and life of cellulose acetate reverse osmosis membranes. *Desalination*, **5**: 157-166.
- Wang, D., K. Li and W. K. Teo. 1999. Preparation and characterization of polyvinylidene fluoride (PVDF) hollow fiber membranes. *Journal of Membrane Science*, **163**(2): 211.
- Weis, A., M. R. Bird and M. Nystrom. 2003. The chemical cleaning of polymeric UF membranes fouled with spent sulphite liquor over multiple operational cycles. *Journal of Membrane Science*, **216**(1-2): 67.
- Wicaksana, F., A. G. Fane and V. Chen. 2006. Fibre movement induced by bubbling using submerged hollow fibre membranes. *Journal of Membrane Science*, **271**(1-2): 186.
- Wienk, I. M., E. E. B. Meuleman, Z. Borneman, V. D. B. T. and C. A. Smolders. 1995. Chemical treatment of membranes of a polymer blend: Mechanism of the reaction of hypochlorite with poly(vinyl pyrrolidone). *Journal of Polymer Science: Part A: Polymer Chemistry*, **33**: 49-54.
- Wiesner, M. R. and P. Aptel. 1996. Mass transport and permeate flux and fouling in pressure-driven processes. Water treatment: Membrane processes. J. Mallevalle. American Water Works Association, Denver, CO.
- Wolff, S. H. and A. L. Zydney. 2004. Effect of bleach on the transport characteristics of polysulfone hemodialyzers. *Journal of Membrane Science*, **243**(1-2): 389.

- Xu, Z.-L., T.-S. Chung and Y. Huang. 1999. Effect of polyvinylpyrrolidone molecular weights on morphology, oil/water separation, mechanical and thermal properties of polyetherimide/polyvinylpyrrolidone hollow fiber membranes. *Journal of Applied Polymer Science*, **74**(9): 2220-2233.
- Yeh, H.-H. and W.-H. Wang. 2004. A study on the fouling phenomena of microfiltration membrane. *Water Science and Technology: Water Supply*, **4**(5-6): 223-231.
- Ying, L., G. Zhai, A. Y. Winata, E. T. Kang and K. G. Neoh. 2003. pH effect of coagulation bath on the characteristics of poly(acrylic acid)-grafted and poly(4-vinylpyridine)-grafted poly(vinylidene fluoride) microfiltration membranes. *Journal of Colloid and Interface Science*, **265**(2): 396.
- Youm, K. H. and W. S. Kim. 1991. Prediction of intrinsic pore properties of ultrafiltration membrane by solute rejection curves: Effects of operating conditions on pore properties. *Journal of Chemical Engineering of Japan*, **24**(1): 1-7.
- Yu, H.-Y., Y.-J. Xie, M.-X. Hu, J.-L. Wang, S.-Y. Wang and Z.-K. Xu. 2005. Surface modification of polypropylene microporous membrane to improve its antifouling property in MBR: CO₂ plasma treatment. *Journal of Membrane Science*, **254**(1-2): 219.
- Yu, H.-Y., Z.-K. Xu, Q. Yang, M.-X. Hu and S.-Y. Wang. 2006. Improvement of the antifouling characteristics for polypropylene microporous membranes by the sequential photoinduced graft polymerization of acrylic acid. *Journal of Membrane Science*, **281**(1-2): 658.
- Yuan, W. and A. L. Zydney. 1999. Humic acid fouling during microfiltration. *Journal of Membrane Science*, **157**(1): 1.
- Yuan, W. and A. L. Zydney. 2000. Humic Acid Fouling during Ultrafiltration. *Environmental Science and Technology*, **34**(23): 5043-5050.
- Zemen, L., G. Tkacik and P. Le Parlouer. 1985. Pore volume distribution in UF membranes. *Materials Science of Synthetic Membranes*: 339.
- Zhang, W. and B. Hallstrom. 1990. Membrane characterization using the contact angle technique I. Methodology of the captive bubble technique. *Desalination*, **79**: 1-12.
- Zhang, W., M. Wahlgren and B. Sivik. 1989. Membrane characterization by the contact angle technique II. Characterization of UF-membranes and comparison between the captive bubble and sessile drop as methods to obtain water contact angle. *Desalination*, **72**: 263-273.

- Zhao, C., X. Zhou and Y. Yue. 2000. Determination of pore size and pore size distribution on the surface of hollow-fiber filtration membranes: a review of methods. *Desalination*, **129**(2): 107.
- Zhu, H. and M. Nystrom. 1998. Cleaning results characterized by flux, streaming potential and FTIR measurements. *Colloids and Surfaces A: Physicochemical and Engineering Aspects*, **138**(2-3): 309.
- Zularisam, A. W., A. F. Ismail and R. Salim. 2006. Behaviours of natural organic matter in membrane filtration for surface water treatment - a review. *Desalination*, **194**(1-3): 211.
- Zydney, A. L. 1997. Stagnant film model for concentration polarization in membrane systems. *Journal of Membrane Science*, **130**(1-2): 275.
- Zydney, A. L., P. Aimar, M. Meireles, J. M. Pimbley and G. Belfort. 1994. Use of the log-normal probability density function to analyze membrane pore size distributions: functional forms and discrepancies. *Journal of Membrane Science*, **91**(3): 293.
- Zydney, A. L. and A. Xenopoulos. 2007. Improving dextran tests for ultrafiltration membranes: Effect of device format. *Journal of Membrane Science*, **292**(1-2): 180.

Appendix A: Procedure for Membrane Element Construction

Single Fibre Element

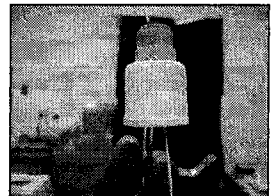
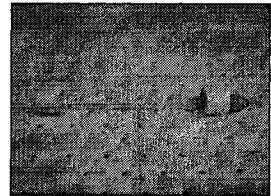
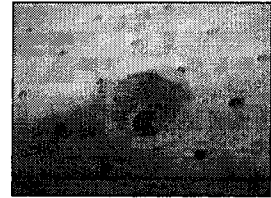
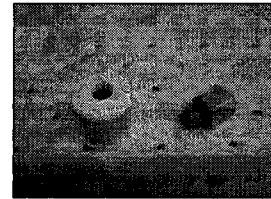
The membrane element can be incorporated into a casing with an inlet and outlet structure to make-up the membrane module. The element is made up of a single fibre of approximately 16 mm that can be operated inside-to-out or outside-to-in depending on the set-up of the inlet and outlet structures. The procedure for construction is detailed below.

Materials

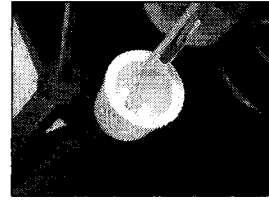
- 1 – 25 mm dry membrane fibre
- 2 – 19 mm diameter PVC threadless pipe caps
- 1 – 6.35 mm NPT (m) push connect fitting
- 1 – 20 mm glass rod
- Flexible 6.35 mm diameter tubing
- Hot glue with glue gun
- 24 hr setting epoxy (Nu-Luster-55)
- Viscous quick setting epoxy (Holdtite Macrolex 15 min)

Procedure

1. Drill a 6.35 mm hole in one of the PVC caps, thread the hole, and screw in the 6.35 mm NPT(M) push connect fitting using Teflon tape.
2. Cut off a 10 mm piece of the flexible 6.35 mm diameter tubing and hot glue it into the centre of the remaining cap.
3. Place the glass rod inside both bottom and top caps and glue them in place with the viscous epoxy.
4. After setting, place the element shell in clamps with the fitting side up and thread the membrane fibre into the push connect fitting until it protrudes while placing the bottom of the fibre into the plastic tubing hot glued to the bottom cap. This will keep the fibre centered.



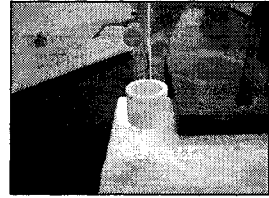
5. Using the viscous epoxy, glue the fibre into the tubing in the bottom cap.



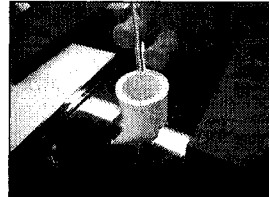
6. After setting, mix the 24 hr epoxy according to the manufacturers directions and pour into the bottom cap until it is flush with the top edge, ensuring that no epoxy touches the future active surface area of the membrane fibre.



7. Blow on the surface of the epoxy with a straw to pop air bubbles that may have formed.

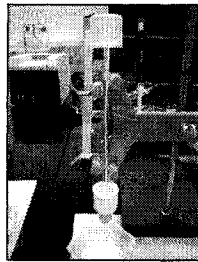


8. After setting, invert the partially constructed element and tape the protruding fibre to the outside of the element so that the fibre stands straight and almost (not quite) taught in the element shell. Taping can be performed before step 6 to center the fibre if necessary.

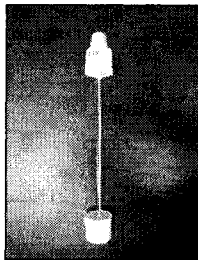


9. Cover the inside of the 6.35 mm NPT(M) with the viscous epoxy so to seal off the membrane from the outside of the top cap ensuring that no epoxy drips through. It is very important to ensure a complete seal, so once dry, visually inspect and apply more epoxy if necessary

10. After setting, fill the remaining volume of the top cap with 24 hr setting epoxy.



11. After setting, take out the element from the clamps and pull the protruding fibre out of the top of the element – it should pull off flush to the inside level of epoxy. If it does not, use tweezers to gently remove the remaining fibre, taking care not to deposit any pieces into the fibre lumen.

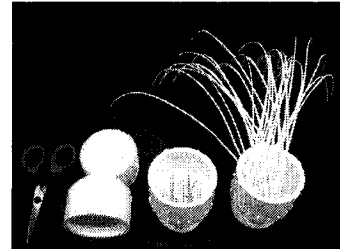


Multi-Fibre Element

The multi-fibre membrane element can be incorporated into a large casing with an inlet and outlet structure (making the membrane module). The element is made up of 30 fibres (recommended) of approximately 15 to 20mm in effective length and can be operated inside-to-out or outside-to-in depending on the set-up of the inlet and outlet structures. The procedure for construction is detailed below.

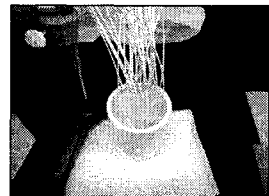
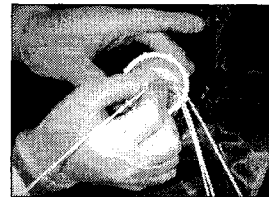
Materials

- 30 – 25 mm dry membrane fibres
- 1 – 38 mm diameter PVC threadless pipe set
- 1 – 6.35 mm NPT(M) push connect fitting
- 1 – cross-stitch material with stitching approx. the same size as fibre
- 1 – toothpick
- Viscous quick setting epoxy (Holdtite Macrolex)
- 24 hr setting epoxy (Nu-Luster-55)

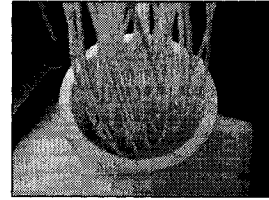


Procedure

1. Drill a 6.35 mm hole in the PVC cap, thread the hole, and screw in the 6.35 mm NPT(M) push connect fitting using Teflon tape.
2. Cut out a section of cross-stitch material that fits into the cross section of the male threaded PVC cap and glue it in with the viscous epoxy. Tamp down the edges so to obtain a good seal.
3. Using the toothpick, widen the spaces within the cross-stitch and thread a membrane fibre through the material until it touches the lab bench. Continue to do this in evenly spaced intervals until the desired number of fibres are in place.
4. Using a clamp, carefully suspend the fibres so that they are in a direction close to vertical.

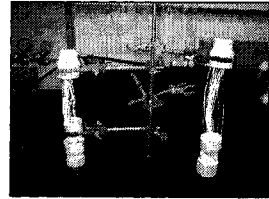


5. Place viscous epoxy on top of the cross-stitch material and around the membrane fibres so to seal off the remaining openings in the material. Check to see if any epoxy leaked through the material while its setting. If some has leaked through, remove it before it completely sets.

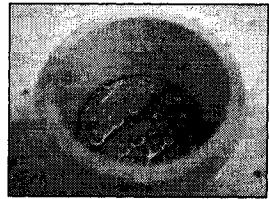


6. Fill the remaining volume in the cap with the 24 hr setting epoxy and let set.

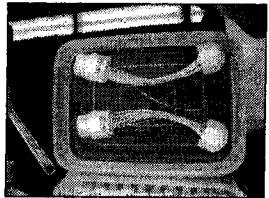
7. After setting, flip the partially completed element and dip the open end of the fibres into a threadless cap filled with 24hr setting epoxy. Carefully suspend the already set cap so that the fibres sit vertical and somewhat spaced out in the setting cap. Ensure that the fibres are not in tension.



8. Fill the other side of cap with the cross-stitch material $\frac{1}{2}$ way so that some of the fibres still protrude from the epoxy.



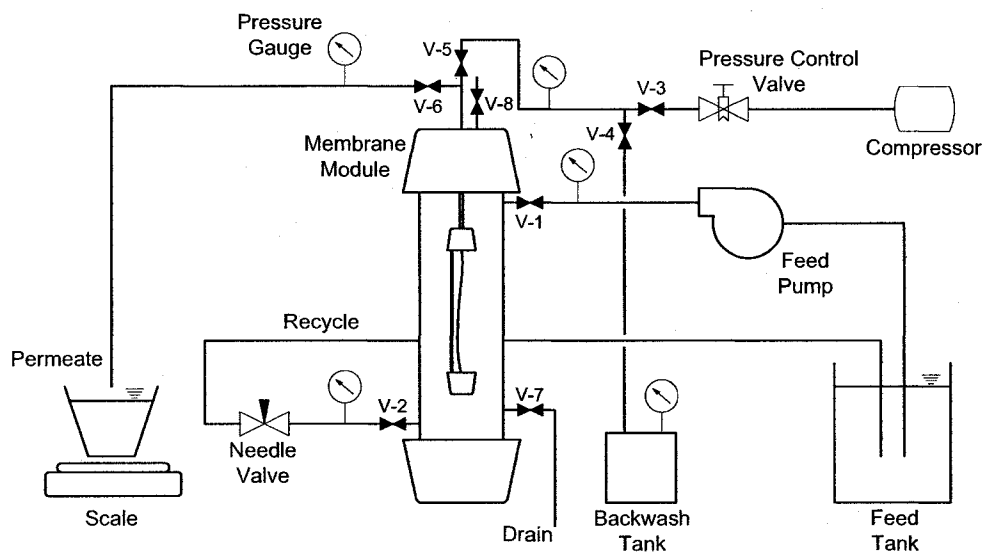
9. After setting pull off the protruding ends of the fibres so that there is a flush surface with the set epoxy. Screw on the cap with the push connect fitting and the element is complete.



Appendix B: Permeability Protocol and Worksheet

Permeability Protocol

Activity	Notes
1 Rinse vessel with 4 L DI water	<ul style="list-style-type: none"> If the module hasn't been used for a long period, shock with 500 mg/L chlorine and thoroughly rinse with DI water Have V-8 open when rinsing and filling Needle valve should be fully open
2 Insert membrane element	<ul style="list-style-type: none"> Screw off the top cap of the module and push connect the top of the element into the connected tubing Screw on the cap (by hand) tightly using Teflon tape
3 Turn on LabView program	<ul style="list-style-type: none"> Initiate the LabView program Press 'Run' and save the file with an '.xls' extension into a data folder Press 'Start' to begin logging data
4 Prepare module and condition membrane	<ul style="list-style-type: none"> Rinse module with 1 L of DI water Permeate at 35 kPa for 1 hr V-1, V-2, and V-6 are open, V-5, V-7, and V-8 are closed
5 Pressurize to 25 kPa	<ul style="list-style-type: none"> Adjust the pressure by opening or closing the needle valve Let run for 10 minutes while data logging on LabView
6 Pressurize to 50 kPa	<ul style="list-style-type: none"> Increase the pressure by closing needle valve Let run for 10 minutes while data logging on LabView
7 Pressurize to 75 kPa	<ul style="list-style-type: none"> Increase the pressure by closing the needle valve Let run for 10 minutes while data logging on LabView
8 Shutdown	<ul style="list-style-type: none"> Press 'Stop' on the LabView program Turn off the pump and open up the pump head half way
Notes <ul style="list-style-type: none"> DI water used must be greater than 15 MΩ-cm and a cross flow rate of 2 L/min is used for all testing 	



Permeability Worksheet
Hypothetical Data

	Protected Cell
	Data Entry

Data

Membrane Resistance

Avg Pres kPa	Flow Rt mL/min	Flux x 10 ⁻⁵ m/s
21.4	1.20	2.04
28.3	1.65	2.81
35.2	2.14	3.63
42.1	2.58	4.38
49.0	3.05	5.18

Temperature (°C)	20
Viscosity	1.007
Length (mm)	160
Diameter (mm)	1.95
Area (m ²)	0.00098

Eq:	1.03E-06
μ (mN·s/m ²):	1.007
R _m (m ⁻¹):	9.60E+11

Viscosity Table

Temp °C	Viscosity mN·s/m ²
0	1.792
5	1.519
10	1.308
15	1.141
20	1.007

Step 1

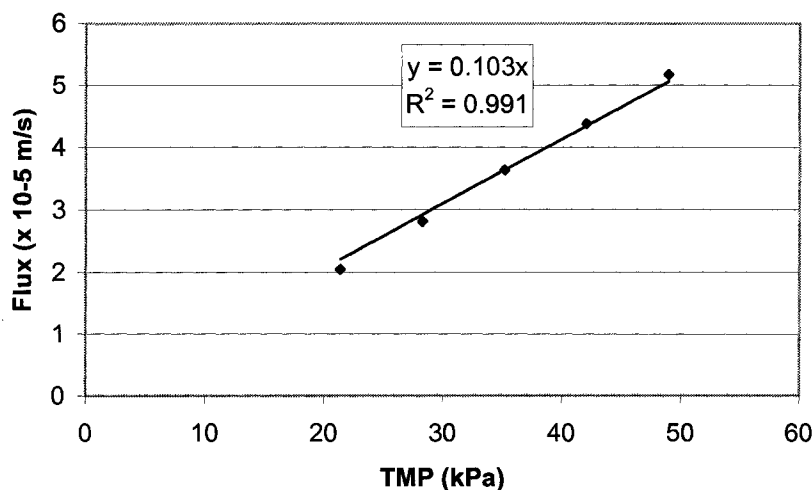
The first step in both the solute and fouling studies involves measuring the membranes intrinsic resistance as defined in the relationship below:

$$J = \frac{\Delta P}{\mu R_m}$$

Flow rates are measured at different pressures and then the corresponding fluxes are calculated using physical membrane information

Results

Membrane Resistance



Step 2

Using the viscosity table, the viscosity is extrapolated using the water temperature and the membrane resistance curve is graphed. The intrinsic membrane resistance is calculated from linear regression and displayed in the equation on the Membrane Resistance graph.

Appendix C: Solute Transport Protocol and Worksheets

Solute Retention Protocol

	Activity	Notes
1	Rinse vessel with 4 L DI water	<ul style="list-style-type: none"> • If the module hasn't been used for a long period, shock with 500 mg/L chlorine and thoroughly rinse with DI water • Have V-8 open when rinsing and filling • Needle valve should be fully open
2	Insert membrane element	<ul style="list-style-type: none"> • Screw off the top cap of the module and push connect the top of the element into the connected tubing • Screw on the cap tightly using Teflon tape
3	Turn on LabView program	<ul style="list-style-type: none"> • Initiate the LabView program • Press 'Run' and save the file with an '.xls' extension into a data folder and press 'Start' to begin logging data
4	Check membrane integrity	<ul style="list-style-type: none"> • See Integrity Protocol
5	Prepare module and condition membrane	<ul style="list-style-type: none"> • Rinse module with 1 L of DI water • Permeate at 35 kPa • Take sample blanks by obtaining 30 mL of sample of the permeate and concentrate • V-1, V-2, and V-6 are open, V-5, V-7, and V-8 are closed
6	Measure permeability	<ul style="list-style-type: none"> • See Permeability Protocol
7	Run PEG solution through membrane module	<ul style="list-style-type: none"> • Run for at least ½ hour or until the permeate flow rate stabilizes at 25 kPa • Use the largest PEG solution
8	Take PEG sample	<ul style="list-style-type: none"> • Obtain 30 mL of sample of permeate and concentrate while logging data
9	Repeat for other pressures	<ul style="list-style-type: none"> • Repeat steps 7 and 8 for 50 kPa and 75 kPa
10	Rinse membrane	<ul style="list-style-type: none"> • Drain the module and rinse with 5 L of DI water • Run DI water through membrane for 15 minutes • Take a blank sample of 30 mL at the end of the rinse
11	Repeat for other PEG sizes	<ul style="list-style-type: none"> • Repeat steps 7 through 10 for the other PEG sizes • Use successively smaller PEG sizes
12	Analyze data	<ul style="list-style-type: none"> • Perform TOC analysis on samples • See the Solute Worksheet
<p data-bbox="342 1688 407 1718"><u>Notes</u></p> <ul style="list-style-type: none"> • DI water used must be greater than 15 MΩ-cm and a cross flow rate of 2 L/min is used for all testing • Pressures have to be chosen so that a common flux is bracketed for all the different solute sizes, allowing R_m to be calculated for each solute size using a common flux. • Record the air and water temperature to compensate for viscosity effects 		

Solute Retention

Data from Causserand et al. (2004)

	Protected Cell
	Data Entry

Flux Data

Condition	Pressure kPa	Flow Rt mL/min	Flux $\times 10^{-5}$ m/s
PEG 1	25	2.04	3.46
	50	1.67	2.84
	75	1.72	2.92
PEG 2	25	2.03	3.45
	50	2.03	3.45
	75	2.03	3.45
PEG 3	25	2.03	3.45
	50	2.03	3.45
	75	2.03	3.45

Parameters

Length (mm):	160
Diameter (mm):	1.95
Area (m ²):	9.80E-04

Step 1

For each of the PEM size, filtration occurs at three different pressures until the flux stabilizes. The flux is measured and samples of the feed and permeate are taken.

TOC Data

Condition	Concentration		R_{obs}	Flux $\times 10^{-5}$ m/s	$\ln \left(\frac{1 - R_{obs}}{R_{obs}} \right)$
	Permeate	Feed			
PEG 1 (4.6)	3.00	3.20	0.32	1.55	0.75
	5.00	5.20	0.21	2.55	1.32
	7.00	7.20	0.11	3.65	2.09
PEG 2 (20)	3.00	3.20	0.88	1.20	-1.99
	5.00	5.20	0.70	1.90	-0.85
	7.00	7.20	0.40	2.90	0.41
PEG 3 (100)	3.00	3.20	0.96	1.35	-3.18
	5.00	5.20	0.92	1.80	-2.44
	7.00	7.20	0.89	2.15	-2.09

Step 2

Concentrations of the feed and permeate are analyzed using total organic carbon (TOC) analysis. R_{obs} is calculated from:

$$R_{obs} = 1 - \frac{C_p}{C_f}$$

Step 3

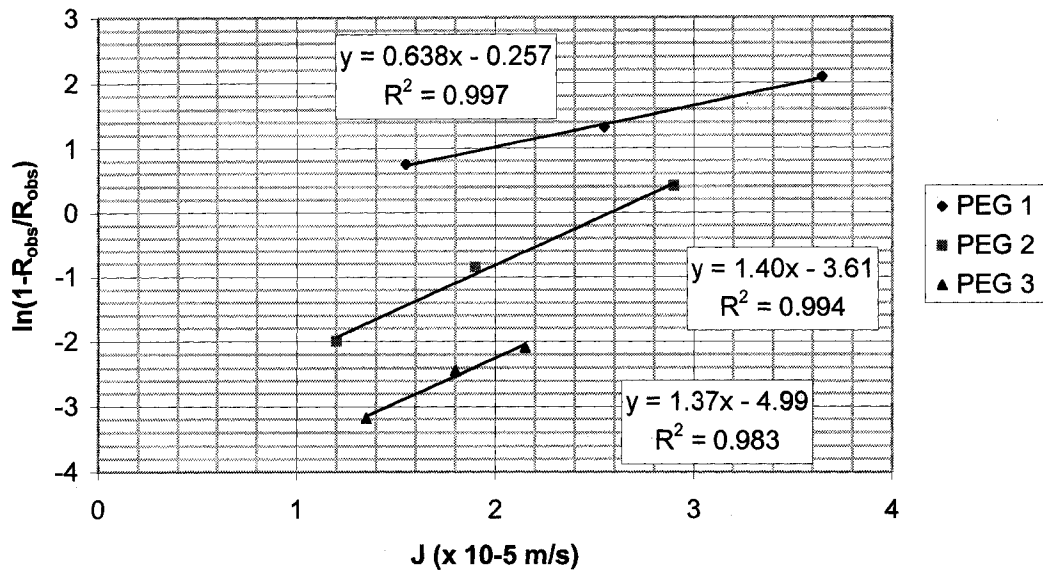
The natural log term in the highlighted column is determined from the R_{obs} and flux values. The graphical relationship from thin film theory when the flux is controlled by mass transport is used to calculate the concentration of the solute at the membrane surface. The relationship is:

$$\ln \left(\frac{1 - R_{obs}}{R_{obs}} \right) = \left(\frac{J}{k} \right) + \ln \left(\frac{1 - R_m}{R_m} \right)$$

equivalent to $y = mx + b$. The relationship is graphed and the mass transport coefficient is determined from the slope and the concentration at the membrane surface determined from the intercept. It should be noted that pressures are chosen so that all the different flux ranges overlap at some point. This allows the rejection at a particular flux to be evaluated.

Results

Thin Film Characterization Curves



Step 4

The slopes and intercepts are tabulated as below and the rejection at the membrane and the mass transport constant (under this particular set of conditions) are calculated. Although the mass transport constant is not used in the subsequent analysis, it may be useful in membrane comparisons in understanding the boundary layer condition

R_m Tabulation

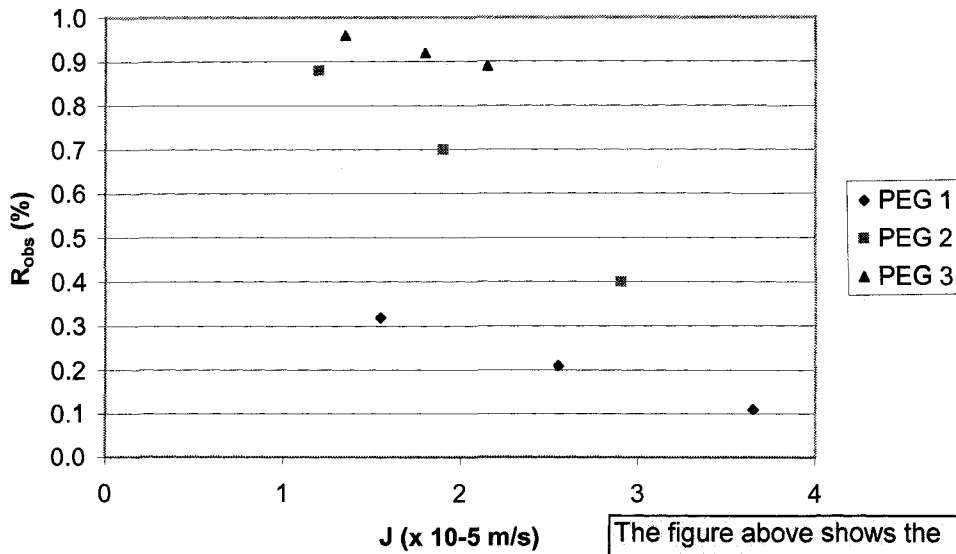
	<i>m</i>	<i>b</i>	R _m	<i>k</i>
PEG 1	0.638	-0.257	0.564	1.57E-05
PEG 2	1.40	-3.61	0.974	7.14E-06
PEG 3	1.37	-4.99	0.993	7.29E-06

Note

The present analysis treats mass transport very simply and makes a number of assumptions. It is assumed that mass transport governs rejection in the conditions tested, that the mass transport coefficient is constant for a particular sized solute, and that the solute size represents an equivalent pore size.

Results

Observed Rejection Relationships

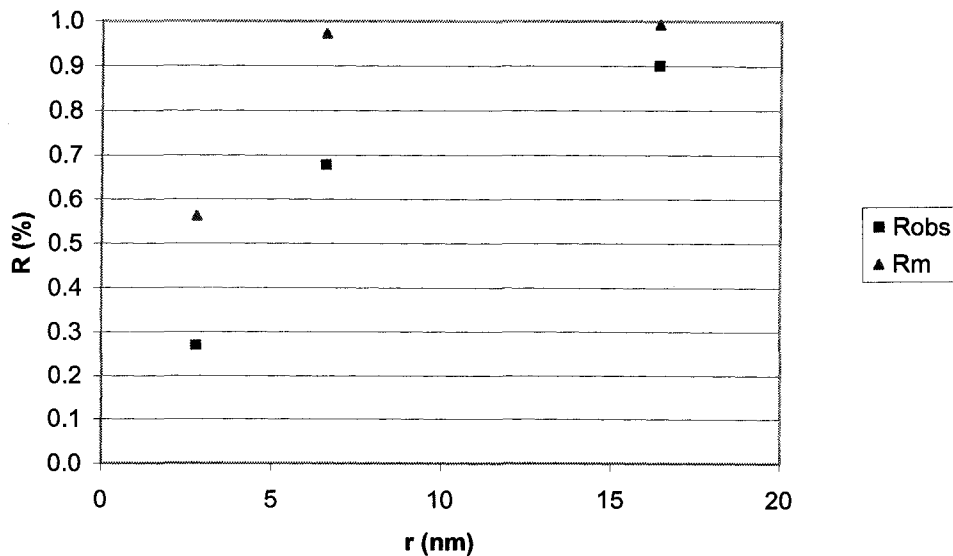


R_{obs} @ flux of 2.0 x 10⁻⁵

	R _{obs}	R _m	r
PEG 1	0.27	0.56	2.8
PEG 2	0.68	0.97	6.6
PEG 3	0.90	0.99	16.4

The figure above shows the observed rejection measured in the 'experimental run', whereas the figure below demonstrates the observed and actual rejection curves based on the Stokes' diameter of the solutes. It can be easily seen for this example, that the actual rejection is higher.

Observed Rejection Relationships



Appendix D: Solute Transport Research using PEMs

Author	Paper Title	Solutes Used	Notes
Zydney and Xenopolous (2007)	Improving dextran tests for ultrafiltration membranes: Effect of device format	Dextran: 1 to 2000 kDa	<ul style="list-style-type: none"> • PES and regenerated cellulose (RC) membranes were used • Millipore flat sheet test cell used
Rana et al. (2005)	Development and characterization of novel hydrophilic surface modifying macromolecule for polymeric membranes	PEG: 1.5 to 35 kDa PEO: 100 to 300 kDa	<ul style="list-style-type: none"> • PES membranes used • Pressure of 300 kPa
Causserand et al. (2004)	Improvement of a method for the characterization of UF membranes by measurements of tracers retention	PEG: 1 to 100 kDa Dextran: 9.3 kDa	<ul style="list-style-type: none"> • PS hollow fibre membranes used • Pressures between 30-80 kPa
Khayet et al. (2002)	Preparation and characterization of polyvinylidene fluoride hollow fiber membranes for ultrafiltration	PEG: 35 kDa PEO: 100 to 400 kDa	<ul style="list-style-type: none"> • PVDF membranes used • SEM and AFM also used
Causserand et al. (2002)	Study of the effects of defects in ultrafiltration membranes on the water flux and the molecular weight cut-off	Dextran: 9 to 200 kDa	<ul style="list-style-type: none"> • Showed that MWCO was not sensitive to pinholes (50 and 150 μm) • Work demonstrated difficulties in using a mixture of dextrans as opposed to isolated solutes
Platt et al. (2002)	Retention of PEGs in cross-flow UF through membranes	PEG: 1.5 to 10 kDa	<ul style="list-style-type: none"> • CA and PES membrane materials • Cross flow velocity of 2 m/s and flux of 40 l/h/m² to achieve reasonable mass transfer
Cleveland et al. (2002)	Standardized membrane pore size characterization by PEG rejection	PEG: 0.6 to 35 kDa	<ul style="list-style-type: none"> • PS, CA materials used • Velocity variation method using velocities of 0.06 to 0.25 m/s at constant pressure
Derjani-Bayeh and Roger (2002)	Sieving variations due to the choice in pore size distribution model	n/a	<ul style="list-style-type: none"> • Mathematical study • PS, CA membrane materials
Schlichter et al. (2000)	Comparative characterization of different commercial UF membranes for drinking water production	Dextran: 8 to 2000 kDa	<ul style="list-style-type: none"> • PA, PAN, CA, PS, PES all used • Hollow fibre and flatsheet used
Combe et al. (1999)	The effect of CA membrane properties on adsorptive fouling by humic acid	PEG: 3 to 10 kDa	<ul style="list-style-type: none"> • CA membranes used • TMPs between 100 kPa and 350 kPa • Oxidation was concurrently explored
Wang et al. (1999)	Preparation and characterization of PVDF hollow fiber membranes	Dextran: 110 to 500 kDa	<ul style="list-style-type: none"> • PVDF membrane materials • Crossflow velocity of 2.5 m/min • TOC analysis used
Singh et al. (1998)	Membrane characterization by solute transport and AFM	PEG: Up to 35 kDa PEO: Up to 200 kDa	<ul style="list-style-type: none"> • PES membrane material • Compaction pressure of 551 kPa

Author	Paper Title	Solutes Used	Notes
			<ul style="list-style-type: none"> • 345 kPa
Meireles et al. (1995)	An appropriate molecular size parameter for porous membrane calibration	PEG: 3 to 100 kDa Dextran: 9.3 to 66.3 kDa Protein: 1 to 156 kDa	<ul style="list-style-type: none"> • PVDF, PS materials tested • 10 to 50 kPa
Pradanos et al. (1995)	Mass transfer coefficient and retention of PEGs in low pressure cross-flow UF	PEG: 0.3 to 12 kDa	<ul style="list-style-type: none"> • PS/PA membrane material • Compaction pressure of 650 kPa • Up to 650 kPa
Kim et al. (1994)	A comparative study of techniques used for porous membrane characterization: pore characterization	PEG: n/a Dextran: n/a	<ul style="list-style-type: none"> • PS and RC membrane material • Compared solute transport with permoperometry and thermoporometry
Tam and Tremblay (1991)	Membrane pore characterization – comparisons between single and multi-component solute probe techniques	PEG: 0.6 to 12 kDa	<ul style="list-style-type: none"> • Asserts that using mixtures underestimates the MWCO as characterization technique is relative • PEG solutions of 200 ppm • TOC analysis used • 345 kPa
Youm and Kim (1991)	Prediction of intrinsic pore properties of UF membrane by solute rejection curves: effects of operating conditions	PEG: 1.5 to 6 kDa Dextran: 20 to 110 kDa	<ul style="list-style-type: none"> • Also varied crossflow velocity (0.2, 0.3, 0.4, 0.5, 0.6 m/s) and feed concentration (3.53, 6.57, 10.35, 13.56 g/L) as well • 50 to 400 kPa
Liu et al. (1991)	Pore size and pore size distribution on the surface of polyethersulfone hollow fiber membranes	PEG: 1 to 9 kDa	<ul style="list-style-type: none"> • PES membrane material • PEG concentrations of 200 ppm used • Pressure of 138 kPa
Aimar et al. {, 1990 #205}	A contribution to the translation of retention curves into pore size distributions for sieving membranes	n/a	<ul style="list-style-type: none"> • Describes the application of pore size distributions to experimental dextran data
Nobrega et al. (1989)	Transfer of dextran through UF membranes: a study of rejection data analysed by gel permeation chromatography	Dextran: 10 to 100 kDa	<ul style="list-style-type: none"> • PS membrane material
Nakao and Kiumura (1981)	Analysis of solutes rejection in UF	PEG: 3 kDa Other: <1.5 kDa	<ul style="list-style-type: none"> • CA membranes • Used velocity variation method to determine mass transfer coefficients • Developed solute permeability and reflection coefficient parameters

Appendix E: Flux Loss Ratio Protocol and Worksheets

Fouling Propensity Protocol

Activity		Notes
1	Rinse vessel with 4 L DI water	<ul style="list-style-type: none"> • If the module hasn't been used for a long period, shock with 500 mg/L chlorine and thoroughly rinse with DI water • Have V-8 open when rinsing and filling
2	Insert membrane element	<ul style="list-style-type: none"> • Screw off the top cap of the module and push connect the top of the element into the connected tubing • Screw on the cap (by hand) tightly using Teflon tape
3	Turn on LabView program	<ul style="list-style-type: none"> • Initiate the LabView program • Press 'Run' and save the file with an '.xls' extension into a data folder • Press 'Start' to begin logging data
4	Check membrane integrity	<ul style="list-style-type: none"> • See Integrity Protocol
5	Prepare module and condition membrane	<ul style="list-style-type: none"> • Rinse module with 1 L of DI water • Permeate at 35 kPa • V-1, V-2, and V-6 are open, V-5, V-7, and V-8 are closed
6	Measure permeability	<ul style="list-style-type: none"> • See Permeability Protocol
7	Foul membrane	<ul style="list-style-type: none"> • Use 10 mg/L humic acid solution described in Section -- • Permeate at 35 kPa for ½ hour • Recycle cross flow back into the feed tank • Record the permeate flow rate at the end of the ½ hour
8	Rinse membrane	<ul style="list-style-type: none"> • Drain the module • Rinse with 5 L of DI water
9	Measure DI permeability through fouled membrane	<ul style="list-style-type: none"> • Filter DI water at 35 kPa for ½ hour • Record the permeate flow rate at the end of the ½ hour
10	Backwash membrane	<ul style="list-style-type: none"> • Fill the BW tank with 500 mg/L hypochlorite solution • Pressurize BW tank to 70 kPa • Open valve to the BW tank while leaving the vessel valve open to clear out lumen • Slowly close the needle valve to pressurize the lumen • After about 10 s, open the bleed valve on the vessel • Record the BW flow after ½ hour
11	Rinse membrane	<ul style="list-style-type: none"> • Drain the module • Rinse with 3 L of DI water
12	Measure DI permeability through BWed membrane	<ul style="list-style-type: none"> • Filter DI water at 35 kPa for ½ hour • Record the permeate flow rate at the end of the ½ hour
13	Calculate flux loss ratios	<ul style="list-style-type: none"> • See the Flux Loss Ratio Worksheet
Notes <ul style="list-style-type: none"> • DI water used must be greater than 15 MΩ-cm and a cross flow rate of 2 L/min is used for all testing 		

Fouling Protocol Run Through
Hypothetical Data

	Protected Cell
	Data Entry

Data

Measured Fluxes

Condition	Avg Pres kPa	Flow Rt mL/min	Flux x 10 ⁻⁵ m/s
J _{pwv}	35.2	1.47	2.50
J _{fs}	35.2	1.18	1.60
J _{pwf}	35.2	1.01	1.72
J _{pwb}	35.2	1.28	2.17

Step 1
Fluxes are taken for pure water virgin, fouled, backwashed, and fouling solution through a fouled membrane.

Temperature (°C)	20
Viscosity	1.007
Length (mm):	160
Diameter (mm):	1.95
Area (m ²):	0.00098
Eq:	1.03E-06
μ (mN·s/m ²):	1.007
R _m (m ⁻¹):	9.60E+11

Step 2
The viscosity is extrapolated from the water parameters and the intrinsic membrane resistance show in the permeability worksheet.

Step 3
The resistance terms a calculated, R_f and R_T from the formula:

$$\frac{J_{pwv}}{J_{fs}} = \frac{R_m + R_f}{R_m} = 1 + \frac{R_f}{R_m}$$

Results

Resistance Values

R _m	9.60E+11
R _f	5.39E+11
R _T	1.50E+12

FLR

D _m	64.1%
D _{rf}	22.9%
D _{if}	13.0%
sum	100%

FLR (ext.)

D _m	64.1%
D _{rf}	18.1%
D _{if}	13.0%
D _{cp}	4.8%
sum	100%

Resistances (w/CP)

R _m	9.60E+11	64.1%
R _{rf}	2.90E+11	19.3%
R _{if}	1.44E+11	9.6%
R _{cp}	1.05E+11	7.0%
R _T	1.50E+12	100.0%

Comparing the reversible fouling resistance and FLR, it can be seen that the resistance in series method finds irreversible fouling to be relatively less important than the FLR methodology.

Step 4
The flux loss ratios are subsequently calculated from the flux and resistance values using the formulas (not all included):

$$D_{if} = R_f \times \frac{J_{pwv} - J_{pwb}}{J_{pwv} - J_{pwf}}$$

$$D_{rf} = R_f \times \frac{J_{pwb} - J_{pwf}}{J_{pwv} - J_{pwf}}$$

Appendix F: Chlorine Residual Protocol and Data

Chlorine Residual Protocol

Standard Curve

	Activity	Notes
1	Turn on Spectrophotometer	<ul style="list-style-type: none"> Needs about 10 minutes to warm up Set 'Absorbance' to 515 nm
2	Transfer 25 mL of DI water, 1, 2, 3, and 4 mg/L standards to vials	<ul style="list-style-type: none"> Use only ODF (oxidant demand free) glassware indicated by the presence of foil over openings Start with DI, then 1, 2, 3, and 4 mg/L solutions (go up in concentration) Do not blow out pipette tip when draining fluid but do so into a waste container before taking the next sample Make sure NOT to suck fluid into the pipetter by overshooting the fill line
3	Empty DPD pouch into sample and measure absorbance	<ul style="list-style-type: none"> Cut off top of pouch with scissors and carefully pore in powder Invert vial slowly 10 times and then wait until a minute has passed from DPD addition Fill cuvette to line at 1 minute and measure absorbance Ensure that the outside of the cuvette is clean by cleaning surface with lint free KimWipes Only handle cuvette on frosted sides
4	Repeat step 3 for every sample	<ul style="list-style-type: none"> Ensure testing conditions are the same for every sample Rinse out cuvette with DI water and drain/dry upside down between measurements
5	Graph Standard Curve	<ul style="list-style-type: none"> Check Std Curve suitability by graphing Concentration vs Absorbance on Excel (on the computer in the lab) Add a 'best fit linear line' and check the equation of the line and R^2 value If the standard curve looks good, continue with other measurements

Chlorine Residual

Activity		Notes
1	Dilute solution to the 0 to 4 mg/L range	<ul style="list-style-type: none">• For 30 mg/L solutions, sample 1 mL from solutions and place in 25 mL volumetric flask• For 10,000 mg/L solutions, sample 10 mL and dilute in 1000 mL volumetric flask, invert 10 times slowly, dilute 10 mL into 500 mL volumetric flask, invert 10 times slowly
2	Fill vial	<ul style="list-style-type: none">• Sample 25 mL from diluted solution
3	Measure absorbance	<ul style="list-style-type: none">• Measure absorbance as above
4	Repeat step 1 to 3	<ul style="list-style-type: none">• For 30 mg/L solutions, repeat for other reactor and then whole steps 1 to 4 for duplicate analysis• For 10,000 mg/L, repeat measurements at 15 minutes, 30 minutes, 45 minutes, and 1 hr before repeating steps 1 to 4 for duplicate analysis
	Glassware maintenance	<ul style="list-style-type: none">• Use ODF glassware to start with and then between samples, rinse, empty, and cover with an appropriate amount of foil

Chlorine Residual Data

Residual concentrations were maintained by periodic chlorine adjustments. This was performed by complete replenishment and by the injection of a diluted free chlorine solution. Figures F1 and F2 detail the residual chlorine concentrations for the first and second round of 10,000 mg/L free chlorine treatment baths, respectively. Figure F1 has two different residuals for each pH as the treatments were carried out in four separate baths, whereas the membrane types were combined in the second round and only two treatment baths were used.

Figures F3 and F4 detail the residual concentrations in the 1000 mg/L free chlorine treatment baths, of which there were 4 baths for each round of treatment. The goal was to achieve a cumulative exposure condition of 1,500,000 mg-hr/L while maintaining an average free chlorine concentration of either 10,000 mg/L or 1000 mg/L.

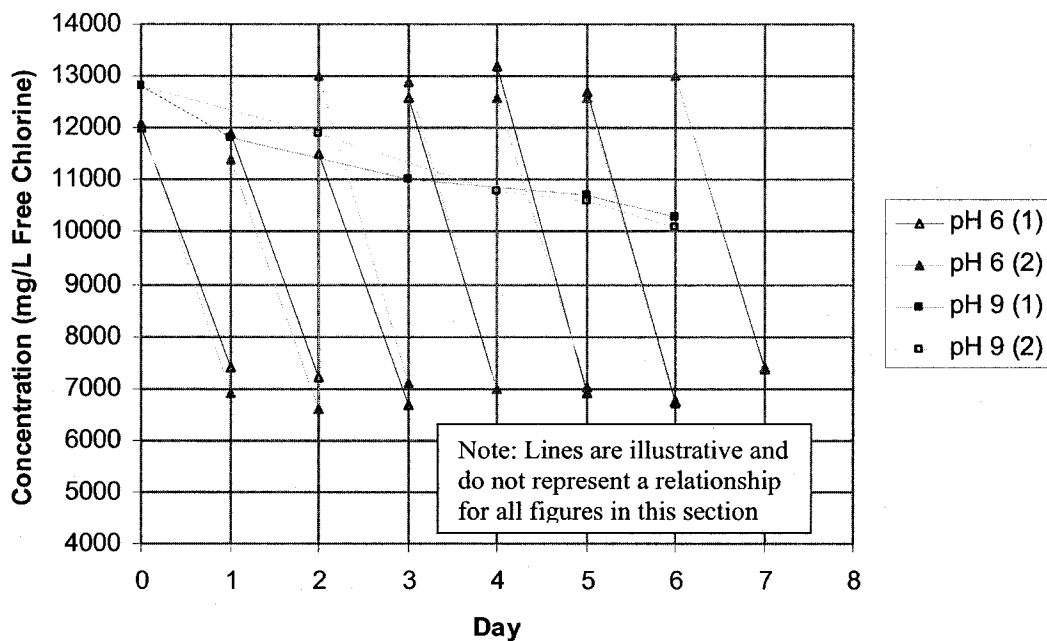


Figure F1: Residual free chlorine concentration for 10,000 mg/L treatments (Run 1)

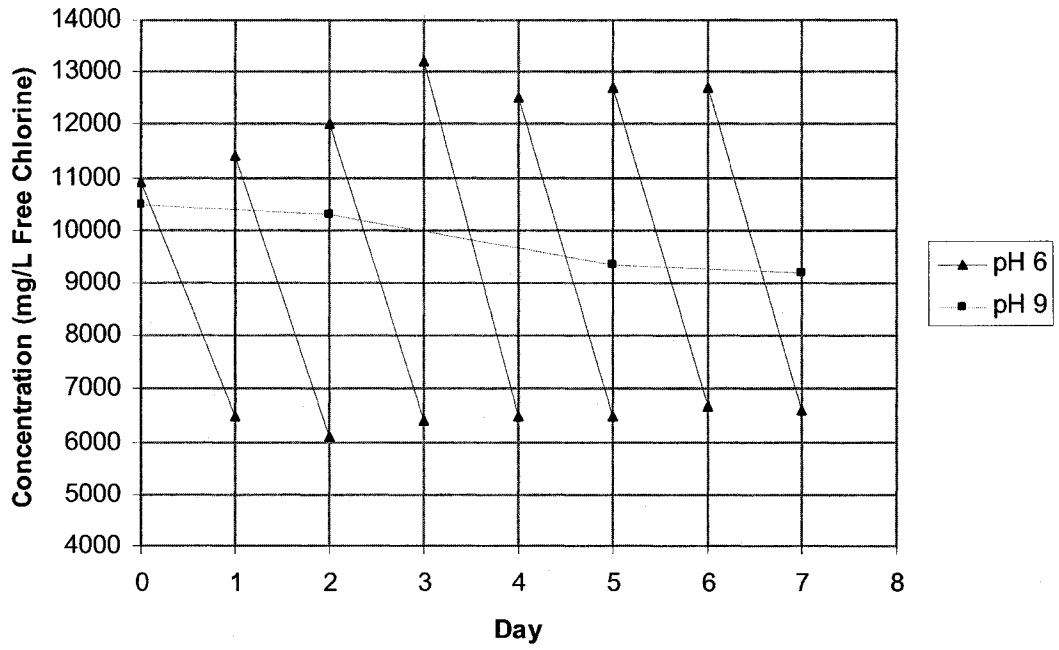


Figure F2: Residual free chlorine concentration for 10,000 mg/L treatments (Run 2)

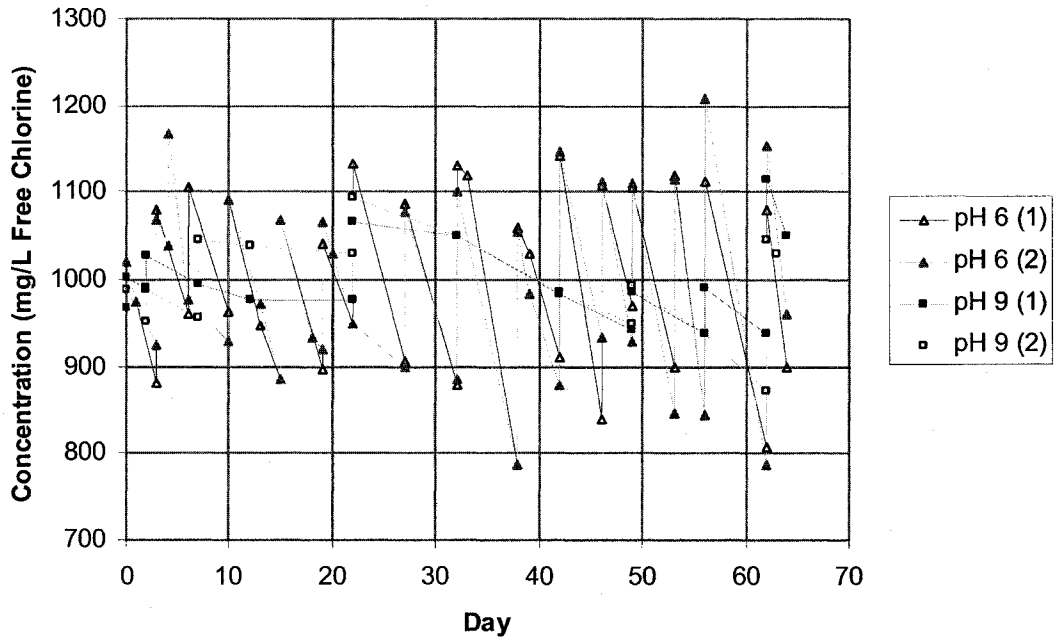


Figure F3: Residual free chlorine concentration for 1000 mg/L treatments (Run 1)

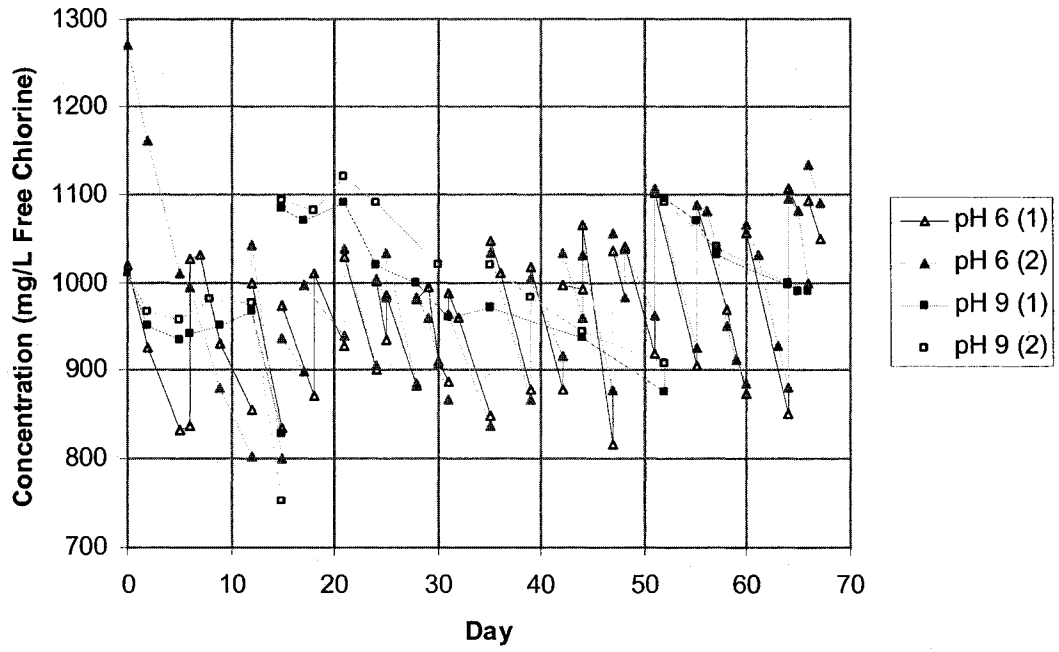


Figure F4: Residual free chlorine concentration for 1000 mg/L treatments (Run 2)

Appendix G: Statistical Analysis Data

Statistical Data

There are a number of assumptions inherent in ANOVA analysis and therefore the treatment of data. The data must be normally distributed, independent, and random. In order to check these assumptions, residual analysis was performed on some of the ANOVA results and a sample of that analysis is included below. For the residual analysis performed, the data satisfied both the normality and independence assumptions for the data with the exception of the displacement at yield parameter. Non constant variance was encountered between the two membrane samples the ANOVA was therefore split into two, 2 factor factorials so that the membrane types could be analyzed separately. Experimentation was carried out in a way that introduced randomization as much as possible.

Result of the residual analysis for the modulus of elasticity parameter are shown in Figures G1, G2, and G3. Analysis for two separate 2^3 ANOVAs are included, one with chlorine concentration levels of 0 and 10,000 mg/L and another with 1000 mg/L and 10,000 mg/L. Both include pH values of 6 and 9 and both membrane types. Separate ANOVAs were looked at as they were more simple to analyze with the software available.

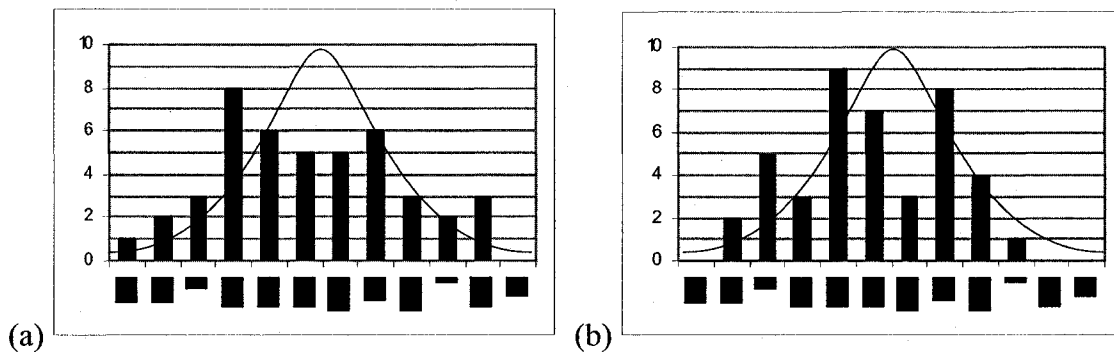


Figure G1: Histograms of the residual distribution for the two-level modulus comparison between (a) 0 and 10,000 mg/L chlorine, and (b) 1000 mg/L and 10,000 mg/L chlorine

Figure G1 shows histograms depicting where the residuals were found. Normality is demonstrated by the normal curve overlaying the charts. Although the results were not ideally normal and looks bimodal, ANOVA is robust and can tolerate small deviations.

Figure G2 shows the N-score plots, another test for normality. Data should be linear and centered around zero, as the figure demonstrates.

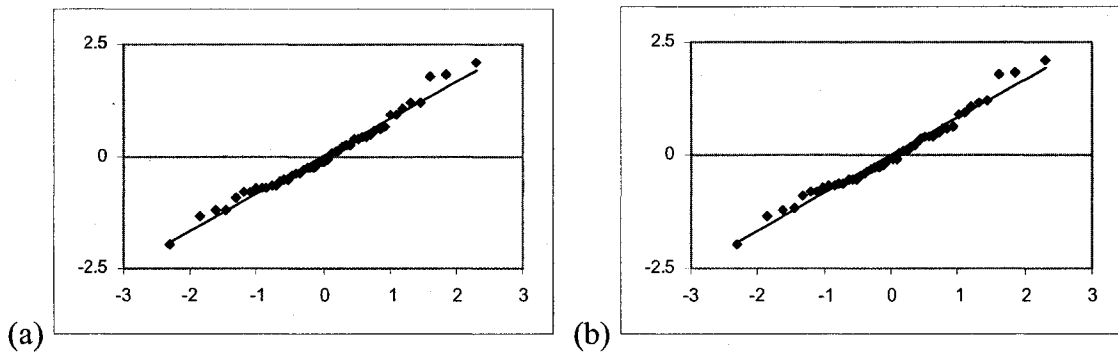


Figure G2: N-score plots for the two-level modulus comparison between (a) 0 and 10,000 mg/L chlorine, and (b) 1000 mg/L and 10,000 mg/L chlorine

The last test for ANOVA suitability was residual plots to investigate whether or not constant variance was experienced. A comparison between the modulus of elasticity and the estimates obtained through the statistical treatment are shown in Figure G3. There do not appear to be any trends as the estimate increases. In other words, there seems to be constant variance between estimates. As was previously mentioned, this was not the case for the displacement at yield parameter where the variance was much higher for membrane B than it was for membrane A. For this reason, the two membrane types response to chlorine and pH were analyzed independently of each other.

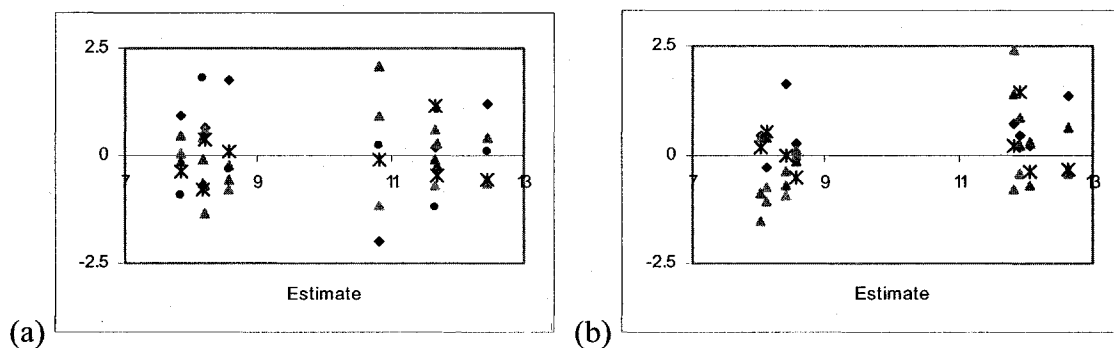


Figure G3: Residual plots (residual vs. estimate) for the two-level modulus comparison between (a) 0 and 10,000 mg/L chlorine, and (b) 1000 mg/L and 10,000 mg/L chlorine